DIPLOMARBEIT

Master Thesis

Derivation of the first-order theory for thin spherical shells, based on the principle of virtual power

ausgeführt zum Zwecke der Erlangung des akademischen Grades
eines Diplom-Ingenieurs

unter der Leitung von

Associate Prof. Priv.-Doz Dipl.-Ing. Dr. techn.
Bernhard PICHLER

E202

Institut für Mechanik der Werkstoffe und Strukturen

eingereicht an der Technischen Universität Wien
Fakultät für Bauingenieurwesen

von

Naim AJVAZI

1029701

Wien am 14.11.2016

eigenhändige Unterschrift

Vorwort des Betreuers der vorliegenden Masterarbeit

Die Grundgleichungen der Kugelschalentheorie I. Ordnung gelten als wohlbekannt. Daher stellt sich bereits vorab die sehr grundsätzliche Frage nach der Notwendigkeit bzw. der Sinnhaftigkeit der vorliegenden Masterarbeit.

Obwohl die Grundgleichungen von Schalentheorien in zahlreichen Lehrbücher und Skripten angegeben werden, bieten die meisten Standardwerke keine zufriedenstellend detaillierten sowie mathematisch und mechanisch einwandfreien Herleitungen dieser Grundgleichungen. Somit sind auch die den Theorien zu Grunde liegenden Annahmen oft nicht ausreichend klar dargestellt. Daher werden die aus den Annahmen folgenden Anwendungsgrenzen oft nur taxativ aufgezählt und von vielen Studierenden auswendig gelernt. Diese Situation galt es bereits etliche Jahre vor der Vergabe der vorliegenden Masterarbeit zu verbessern.

Es stellte sich insbesondere in Hinblick auf die akademische Lehre der Bedarf nach einer Methode für die Herleitung von Strukturtheorien für verschiedenste Tragwerkstypen, jeweils ausgehend von der Beschreibung der untersuchten Tragwerke als dreidimensionale kontinuierliche Körper. Das von P. Germain 1973 publizierte Prinzip der virtuellen Leistungen erlaubt genau diesen Übergang von der dreidimensionalen Kontinuumsmechanik auf entsprechende Strukturtheorien. Bei der Anwendung des Prinzips müssen die getroffenen kinematischen und materiellen Annahmen sehr deutlich beschrieben werden. Dadurch werden sie für Lernende sehr einfach erfassbar.

Daher ist das Prinzip der virtuellen Leistungen zu einer wichtigen Säule in den konstruktiv ausgerichteten Lehrveranstaltungen des Instituts für Mechanik der Werkstoffe und Strukturen der Fakultät für Bauingenieurwesen der Technischen Universität Wien geworden. Es wird in der Bachelorvorlesung aus Festigkeitslehre vorgestellt und auf gerade Stäbe angewendet, um Stabtheorien I. und II. Ordnung herzuleiten. Sie dienen als Grundlage für die Masterlehrveranstaltung aus Flächentragewerke, in der die Grundgleichungen der Plattentheorien I. und II. Ordnung hergeleitet werden, d.h. die Kirchhoffsche bzw. die von Karmansche Plattentheorie. Diese Anordnung der Lehrinhalte macht es Studierenden so einfach wie möglich, den konzeptionellen Übergang von eindimensionalen Stabtheorien auf zweidimensionale Plattentheorien zu erfassen. Im Anschluss wird in der Lehrveranstaltung aus Flächentragwerke auch noch die Zylinderschalentheorie I. Ordnung hergeleitet. Dieser zweidimensionalen Theorie war bisher das eindimensionale Pendant, nämlich die Kreisbogentheorie I. Ordnung, allerdings noch nicht vorangestellt.

Diese Ausgangssituation war die Motivation, eine Projektarbeit kombiniert mit einer Masterarbeit zu vergeben, um zuerst im Rahmen der Projektarbeit die Kreisbogentheorie I. Ordnung herzuleiten und sie anschließend im Rahmen der vorliegenden Masterarbeit auf die Kugelschalentheorie I. Ordnung zu erweitern. Im Interesse der Vollständigkeit wurde die Projektarbeit der vorliegenden Masterarbeit angehängt, siehe Anhang B. Auf

Basis der vorliegenden Masterarbeit wird in Zukunft das Prinzip der virtuellen Leistungen im Rahmen der Flächentragwerkslehre verwendet werden, um zuerst eine eindimensionale Kreisbogentheorie herzuleiten und sie anschließend auf zweidimensionale Theorien für Zylinder- und Kugelschalen zu erweitern. Die vorliegende Masterarbeit stellt somit einen wertvollen konzeptionellen Lückenschluss und eine interessante Ergänzung für die Lehre des konstruktiven Ingenieurbaus an der Technischen Universität Wien dar.

Wien, am 2. November 2016 Assoc.-Prof. Dr. Bernhard Pichler

Erweitere Kurzfassung in deutscher Sprache

Eine schubstarre Theorie erster Ordnung für dünne Kugelschalen wird mit Hilfe des Prinzips der virtuellen Leistungen hergeleitet. Es werden dünne Schalen mit konstanter Dicke analysiert, wobei die Dicke der Schale viel kleiner als der Radius der Schalenmittelfläche ist. Es wird ein Kugelkoordinatensystem mit einer Radialkoordinate r, einem Polarwinkel θ, und einem Azimutwinkel φ gewählt (Abbildung 1). Diese Diplomarbeit hat das Ziel, die geometrischen Beziehungen, konstitutiven Beziehungen und Gleichgewichtsbedingungen herzuleiten.

Zu Beginn der Anwendung des Prinzips der virtuellen Leistungen werden kinematischen Annahmen getroffen, das heißt wir beschränken uns auf Verschiebungsmöglichkeiten, die für eine Kugelschale charakteristisch sind, statt die sehr viel allgemeineren Verschiebungsmöglichkeiten eines dreidimensionalen Kontinuums zu untersuchen. Diese Annahmen erlauben das Entwickeln eines zweidimensionalen Rechenmodells, in dem ausschließlich die Mittelfläche untersucht wird, der Steifigkeitseigenschaften zugewiesen werden. Im Zuge der kinematischen Beschreibung beschränken wir uns auf kleine Erzeugendenverdrehungen und vernachlässigen die durch Belastung hervorgerufenen Änderungen der Schalendicke. Weiteres folgt die Annahme vom Geradebleiben der Schalenerzeugenden. Die Verschiebungsmöglichkeiten der Schalenerzeugenden sind somit auf fünf Starrkörperverschiebungsmoden eingeschränkt, nämlich auf drei translatorische Verschiebungen (in radialer, polarer und azimutaler Richtung) sowie auf zwei Verdrehungen (um die Tangenten an die Parameterlinien in polarer und azimutaler Richtung). Es folgt die Annahme, dass die Verschiebungen wesentlich kleiner als die Schalendicke sind. Infolgedessen sind die Koordinaten mit Bezug auf die unverformte Lage näherungsweise gleich den Koordinaten mit Bezug auf die verformte Lage. Zuletzt kann der linearisierte Verzerrungstensor verwendet werden, da kleine Verdrehungen zu kleinen Verschiebungsableitungen führen.

Durch Formulierung der virtuellen Leistung der äußeren Kräfte werden leistungsmotivierte Spannungsresultanten, konstitutive Gesetze sowie Beziehungen zwischen Schnittgrößen und Membranspannungen hergeleitet. Das dazu erforderliche virtuelle Geschwindigkeitsfeld wird analog zum eingeschränkten realen Verschiebungsfeld gewählt. Im Zuge der mathematischen Formulierung der virtuellen Leistung der äußeren Kräfte identifizieren wir leistungsmotivierte Spannungsresultanten einer Kugelschale, die an den charakteristischen Verschiebungsmöglichkeiten einer Schalenerzeugenden Arbeit leisten. Es wird ein Unterschied zwischen Einwirkungsresultanten und Schnittgrößen gemacht. Äußere Lasten werden zu Einwirkungsresultanten zusammengefasst. Die Flächenlasten leisten an virtuellen Verschiebungsraten der Plattenmittelfläche Arbeit. Die Flächenmomente leisten an den virtuellen Erzeugendenrotationen der Schalenmittelfläche Arbeit. Spannungen in der Schale werden zur Schnittgrößen zusammengefasst. Die transversalen Schubspannungsresultanten und die Membrankräfte leisten an den virtuellen Verschiebungsraten an den Schalenrändern Arbeit, und die Krempel- und

Drillmomente leisten an den virtuellen Erzeugendenrotationen an den Schalenrändern Arbeit. Zur Herleitung konstitutiver Beziehungen werden die Schalenmembranspannungen mit Hilfe des Hooke'schen Gesetzes durch isotrope Elastizitätskonstanten und durch die Freiheitsgrade der Schalenerzeugenden ausgedrückt. Die so erhaltenen Spannungsausdrücke werden in die Schnittgrößendefinitionen eingesetzt, um die konstitutiven Beziehungen zu erhalten. Durch Rückeinsetzen werden schließlich die Membranspannungen durch die Membranspannungsresultanten ausgedrückt.

Im Rahmen der Formulierung der virtuellen Leistung der inneren Kräfte erbringen reale Spannungen virtuelle Leistung entlang von virtuellen Verzerrungsraten. Dazu wird ein Feld von virtuellen Verzerrungsraten benötigt, die ausgehend vom virtuellen Geschwindigkeitszustand berechnet werden. Die Formulierung der virtuellen Arbeit der inneren Kräfte vervollständigt die Anwendung des Prinzips der virtuellen Leistungen und führt zu den fünf Gleichgewichtsbedingungen der beschriebenen Kugelschalentheorie.

Abstract

The purpose of this thesis is to derive a first-order theory for thin spherical shells based on the three-dimensional linear elasticity theory, using the principle of virtual power as a tool for the derivation. By "thin" we mean that the thickness-to-radius ratio is small compared to 1. In order to carry out the transition from a three-dimensional continuum to a shell structure, we focus our analysis to characteristic displacement and rotation possibilities of the shell generator. As a result, kinematic assumptions of spherical shells are made: (i) small shell generator rotations, (ii) shell generator remains straight and orthogonal to the deformed midsurface, and (iii) small displacements of the shell generator compared with the shell thickness. This leads to the identification of five types of rigid body motions representing five degrees of freedom of the shell generator, including three displacements (in radial, polar, and azimuthal direction) and two rotations (around the tangents of the parameter lines in polar and azimuthal direction).

In the course of formulating the virtual power of the external forces, stress resultants are identified. Applying Hooke's law allows for expressing membrane stresses by means of isotropic elastic constants and of shell generator degrees of freedom. Introducing the thus obtained expressions for membrane stresses into the expressions for stress resultants results in constitutive equations. In addition, introducing stress resultants into membrane stresses results in the relations between membrane stresses and stress resultants.

Furthermore, we calculate the virtual power of internal forces, where membrane stresses perform power along the virtual strain rates. The latter are chosen by analogy to the real strains. Specifying the expression for the virtual power of internal forces for the virtual strain rates and making use of the stress resultants leads to the identification of the virtual power of internal forces.

Finally, equating the mathematical formulations of the virtual power of the external forces and of the internal forces to zero delivers the equilibrium equations for thin spherical shells. Additionally, after specifying equilibrium equations only for membrane forces, we identify the conditions for membrane behaviour.

As a conclusion, the principal of virtual power is a very elegant approach for the derivation of structural theories, since it clearly shows the simplifying assumptions and represents a rigorous way of derivation.

Acknowledgements

This Master Thesis would not have come to existence without the help and support of several people. I would like to acknowledge and thank all those people who contributed to the work of this thesis.

First and foremost, I would like to express my deepest gratitude to my supervisor Assoc. Prof. Dipl.-Ing. Dr. techn. Bernhard Pichler, who provided valuable academic and scientific guidance throughout the entire process of writing this thesis. His extraordinary patience and constructive criticism did not only facilitate the completion of this master thesis but also gave me a stronger confidence in my skills and academic interest.

I would also like to thank Mr. Jiao Long Zhang for his great support. Mr. Zhang, checked patiently every single formula of this thesis and assisted my thesis with his valuable comments.

My very special thanks go to Raffaela for standing beside me throughout the entire years of my studies. She has been my inspiration and motivation for continuing to improve my knowledge and move my career forward. I also want to thank fellow colleagues and friends for stimulating discussions, encouragement during difficult times and their general support throughout the years of study.

Being able to study at the Technical University in Vienna was everything but a matter of course for me. The obstacles that I had to overcome to being able to pursue this highly valued place of study would not have been feasible without the constant support of my family. I cannot thank them enough for the tremendous personal and financial sacrifices they made. This accomplishment would not have been possible without you. Thank you.

List of Figures

List of symbols and abbreviations

C	shell extensional stiffness
C^*	center of the circular parameter line φ of the particular cut
C_1	integration constant
E	Young's modulus
$\mathbf{e}_r$, $\mathbf{e}_\theta$, $\mathbf{e}_\varphi$	base vectors of moving spherical coordinate system (with coordinates r, θ and φ)
$\mathbf{f}$	body forces vector
f_r, f_θ, f_φ	components of body forces vector in spherical coordinate system (with coordinates r, θ and φ)
g	gravitational acceleration
h	thickness of spherical shell
K	shell bending stiffness
$\mathcal{L}^{int}$	virtual power of internal forces
$\mathcal{L}^{ext}$	virtual power of external forces
$m_{\theta\theta}$, $m_{\varphi\varphi}$	bending moments
$m_{\theta\varphi}$	twisting moments
$\mathbf{n}$	surface normal vector
$n_{\theta\theta}$, $n_{\varphi\varphi}$, $n_{\theta\varphi}$	membrane forces
O	center of the spherical shell
q_r	transverse shear forces in radial direction
q_θ	transverse shear forces in polar direction
q_φ	transverse shear forces in azimuthal direction
r, θ, φ	spherical coordinate system referring to the deformed configuration
R	radius of the midsurface of the spherical shell
t	time
$\mathbf{T}$	surface traction vector
T_r, T_θ, T_φ	components of surface traction vector in spherical coordinate system (with coordinates r, θ and φ)
$\mathbf{u}$	displacement vector
u, v, w	displacement vector components in spherical coordinate system (with coordinates r, θ and φ)

u_m, v_m, w_m	displacement vector components of the midsurface of the shell in spherical coordinate system
$\breve{\mathbf{u}}$	virtual displacement vector
$\breve{u}$, $\breve{v}$, $\breve{w}$	components of virtual displacement vector in spherical coordinate system
$\dot{\breve{\mathbf{u}}}$	virtual velocity vector (time-derivation of virtual displacement vector)
$\dot{\breve{u}}$, $\dot{\breve{v}}$, $\dot{\breve{w}}$	components of virtual velocity vector in spherical coordinate system
V	Volume of the spherical shell element
ε_{rr}	normal strain in r-(radial) direction
$\varepsilon_{\theta\theta}$	normal shear strain in θ-(polar) direction
$\varepsilon_{\varphi\varphi}$	normal shear strain in φ-(azimuthal) direction
$\varepsilon_{r\theta}$	shear strain in $r-\theta$ plane
$\varepsilon_{r\varphi}$	shear strain in $r-\varphi$ plane
$\varepsilon_{\theta\varphi}$	shear strain in $\theta-\varphi$ plane
$\varepsilon_{\varphi\theta}$	shear strain in $\varphi-\theta$ plane
$\breve{\boldsymbol{\varepsilon}}$	virtual strain rate tensor
$\breve{\varepsilon}_{rr}$	virtual normal strain rate in r-(radial) direction
$\breve{\varepsilon}_{\theta\theta}$	virtual normal strain rate in θ-(polar) direction
$\breve{\varepsilon}_{\varphi\varphi}$	virtual normal strain rate in φ-(azimuthal) direction
$\breve{\varepsilon}_{r\theta}$	virtual shear strain rate in $r-\theta$ plane
$\breve{\varepsilon}_{\theta\varphi}$	virtual shear strain rate in $\theta-\varphi$ plane
$\breve{\varepsilon}_{\varphi\theta}$	virtual shear strain rate in $\varphi-\theta$ plane
Γ, Θ, Φ	spherical coordinate system referring to the undeformed configuration
$\boldsymbol{\sigma}$	Cauchy stress tensor
σ_{rr}	normal stress in r-(radial) direction
$\sigma_{\theta\theta}$	normal stress in θ-(polar) direction
$\sigma_{\varphi\varphi}$	normal stress in φ-(azimuthal) direction
$\sigma_{r\theta}$	shear stress in $r-\theta$ plane
$\sigma_{\theta\varphi}$	shear stress in $\theta-\varphi$ plane
$\sigma_{\varphi\theta}$	shear stress in $\varphi-\theta$ plane
σ_{nr}	$= T_r$

$\sigma_{n\theta}$	$= T_\theta$
$\sigma_{n\varphi}$	$= T_\varphi$
θ_b	polar coordinate at the beginning section of the spherical shell element
θ_e	polar coordinate at the ending section of the spherical shell element
φ_b	azimuthal coordinate at the beginning section of the spherical shell element
φ_e	azimuthal coordinate at the ending section of the spherical shell element

Contents

1 Introduction

Spherical shells are widely used in civil and architecture engineering for large span roofs, concrete arch domes, liquid-retaining structures and water tanks [**1**].[1] The efficiency of load transfer by means of membrane forces and the small thickness-to-radius ratio make spherical shells very appealing structures.

In the present work, a first-order theory for thin spherical shells will be derived, based on the linearised three dimensional elasticity theory. Using the principle of virtual power as the tool for the derivation, similar to the derivations found in [**2**], the kinematics of the shell are chosen (Chapter 2). Quantification of the virtual power of the external forces (Chapter 3) and of the internal forces (Chapter 4) as well as the formulation of the principle of virtual power finally leads to the sought equilibrium equations of spherical shells (Chapter 5). Furthermore, we describe the membrane theory of spherical shells and their behaviour under rotational symmetric loads (Chapter 6).

Let us consider a thin spherical shell with a constant thickness h and a radius R of the shell midsurface, as shown in Fig. 1. By "thin" we mean that the shell thickness h is significantly smaller than the radius R

$$h \ll R \qquad \Rightarrow \qquad \frac{h}{R} \ll 1 \tag{1}$$

We use a r,θ,φ-spherical coordinate system [**5**].[2] The origin of the r-axis coincides with the center of the spherical shell. Base vectors $\mathbf{e}_r$, $\mathbf{e}_\theta$, and $\mathbf{e}_\varphi$ form a moving triad accompanying every point of the shell midsurface. $\mathbf{e}_r$ points in radial direction, $\mathbf{e}_\theta$ in polar direction, and $\mathbf{e}_\varphi$ in the azimuthal direction, respectively (Fig. 1).
The derivation of governing equations of thin spherical shells is based on the principle of virtual power [**3**, **4**, **5**, **13**], which states that the sum of virtual power performed by external forces, $\mathcal{L}^{int}$, plus the virtual power performed by internal forces, $\mathcal{L}^{ext}$, is equal to zero

$$\mathcal{L}^{int} + \mathcal{L}^{ext} = 0 \tag{2}$$

In order to describe the entire process of derivation as clearly as possible, a detailed description of assumptions for deriving a first-order theory of thin spherical shells is made. In the following chapter, we will describe the specific kinematics of spherical shells, which is a starting point for the principle of virtual power.

[1] Ventsel, E., Krauthammer, T. and Ventsel, V. Thin plates and shells: Theory, Analysis, and applications. New York: Taylor and Francis (2001) 298

[2] J. Salaçon, Handbook of Continuum Mechanics: General Concepts-Thermoelasticity, Springer Science & Business Media, (2001) 747-749

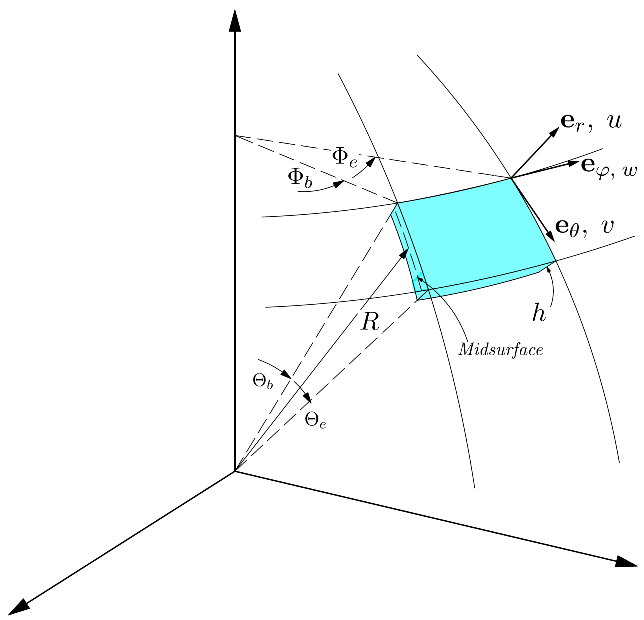

Figure 1: Spherical shell with inner surface in a radial distance $\Gamma = R - \frac{h}{2}$ from the shell center and outer surface in a radial distance $\Gamma = R + \frac{h}{2}$ from the shell center; four lateral surfaces: one at $\Theta = \Theta_b$, one at $\Theta = \Theta_e$, one at $\Phi = \Phi_b$, and one at $\Phi = \Phi_e$; accompanying orthonormal basis $\mathbf{e}_r \times \mathbf{e}_\theta = \mathbf{e}_\varphi$ and displacement components u, v, and w

2 Kinematic description and kinematic constraints

The displacement field $\mathbf{u}(\mathbf{X})$ is described through the components u, v, and w and spherical coordinates Γ, Θ, and Φ referring to the undeformed configuration

$$\mathbf{u}(\mathbf{X}) = u(\Gamma,\Theta,\Phi)\mathbf{e}_r + v(\Gamma,\Theta,\Phi)\mathbf{e}_\theta + w(\Gamma,\Theta,\Phi)\mathbf{e}_\varphi \tag{3}$$

2.1 Small shell generator rotations and constant shell thickness

We consider only small shell generator rotations and we disregard the loading-induced deformation in thickness direction. Therefore, all points $P(\Gamma,\Theta,\Phi)$ of a shell generator exhibit, in good approximation, identical displacements in radial direction, and these displacements are equal to the one of the shell midsurface $M(\Gamma\!=\!R,\Theta,\Phi)$

$$u(\Gamma,\Theta,\Phi) = u_m(\Theta,\Phi) \tag{4}$$

where index m stands for the midsurface with coordinate $\Gamma_m\!=\!R$.

2.2 Shell generator remains straight and orthogonal to the deformed midsurface

We envision that all shell generators remain, also after deformation of the shell, straight and orthogonal to the deformed midsurface. In other words, the polar displacements are linear over the shell thickness. Denoting the polar displacement component of the shell midsurface as $v_m(\Theta,\Phi)$, the polar displacement field can be expressed as

$$v(\Gamma,\Theta,\Phi) = \frac{\Gamma}{R}v_m(\Theta,\Phi) - (\Gamma - R)\frac{\partial u_m(\Theta,\Phi)}{R\partial\Theta} \tag{5}$$

The first term on the right-hand-side of (5) denotes a rotation of the shell generator around the center of the shell ($\Gamma\!=\!0$), see Fig. 2. The second term on the right-hand-side of (5) denotes a similar rotation around the local base vector $\mathbf{e}_\varphi$ in point M on the midsurface of the shell. It will turn out to be beneficial to reformulate the first term on the right-hand-side of (5) as

$$\frac{\Gamma}{R}v_m(\Theta,\Phi) = \frac{R + (\Gamma - R)}{R}v_m(\Theta,\Phi) = v_m(\Theta,\Phi) + (\Gamma - R)\frac{v_m(\Theta,\Phi)}{R} \tag{6}$$

where $v_m(\Theta,\Phi)$ is a translatory movement in local $\mathbf{e}_\theta$ direction and the last term in (6) denotes a rotation around the local $\mathbf{e}_\varphi$ vector positioned in M, as shown in Fig. 2. Specifying (5) for (6) delivers

$$v(\Gamma,\Theta,\Phi) = v_m(\Theta,\Phi) - (\Gamma - R)\left(\frac{\partial u_m(\Theta,\Phi)}{R\partial\Theta} - \frac{v_m(\Theta,\Phi)}{R}\right) \tag{7}$$

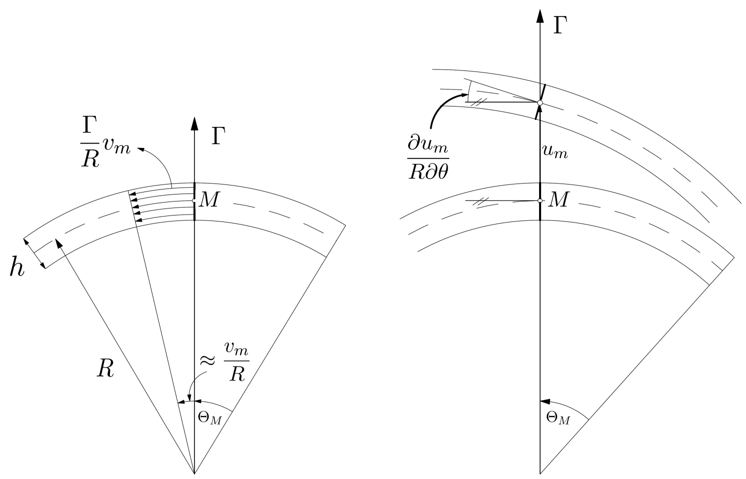

Figure 2: Kinematics of the shell generator in the Γ,Θ-plane, described in Eq. (5)

We assume that all shell generators remain straight and orthogonal, also after the deformation, to the midsurface. Therefore, also the azimuthal displacements are linear over the shell thickness. Denoting the azimuthal displacement component of the shell midsurface as $w_m(\Gamma, \Phi)$, the azimuthal displacement field can be expressed as

$$w(\Gamma, \Theta, \Phi) = w_m(\Theta, \Phi) - (\Gamma - R)\left(\frac{\partial u_m(\Theta, \Phi)}{R \sin\Theta \partial\Phi} - \frac{w_m(\Theta, \Phi)}{R}\right) \tag{8}$$

The first term on the right-hand side of (8) denotes a translatory movement of the shell generator in θ-direction, see Fig. 3. The second term on the right-hand side of (8) denotes a rotation around the local base vector $\mathbf{e}_\theta$ in point M of the midsurface of the shell.

2.3 Small displacements of the shell midsurface in comparison with the shell thickness

We assume that the displacements are very small as compared with the shell thickness. As a consequence, the deformed configuration, described by position vectors $\mathbf{x}$, will be in the immediate vicinity of the undeformed configuration, described by position vectors $\mathbf{X}$, such that both position vectors are practically the same

$$\mathbf{x} \approx \mathbf{X} \quad \Rightarrow \quad \left\{\begin{array}{c} r \\ \theta \\ \varphi \end{array}\right\} \approx \left\{\begin{array}{c} \Gamma \\ \Theta \\ \Phi \end{array}\right\} \tag{9}$$

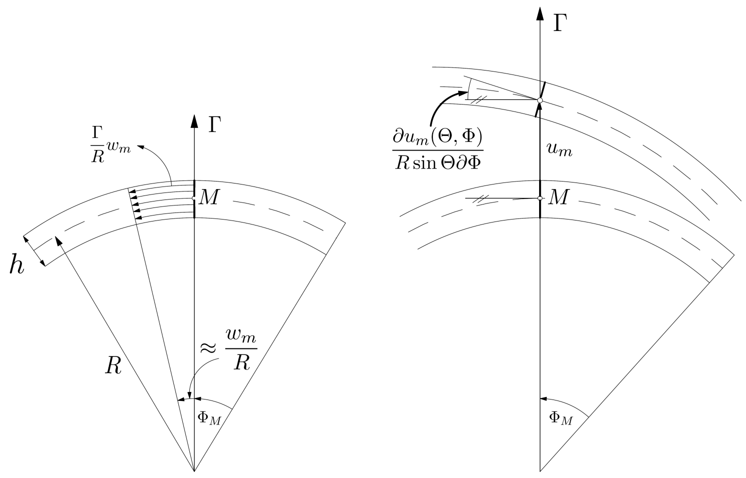

Figure 3: Kinematics of the shell generator in the Γ,Φ-plane, described in Eq. (8)

Specifying the general kinematic description (3) for kinematic constraints (4), (7), and (8) as well as for small-displacements-assumption (9) delivers

$$\mathbf{u}(\mathbf{x}) = \underbrace{u_m(\theta,\varphi)}_{u(r,\theta,\varphi)}\mathbf{e}_r + \underbrace{\left[v_m(\theta,\varphi) - (r-R)\left(\frac{\partial u_m(\theta,\varphi)}{R\partial\theta} - \frac{v_m(\theta,\varphi)}{R}\right)\right]}_{v(r,\theta,\varphi)}\mathbf{e}_\theta$$

$$+ \underbrace{\left[w_m(\theta,\varphi) - (r-R)\left(\frac{\partial u_m(\theta,\varphi)}{R\sin\theta\partial\varphi} - \frac{w_m(\theta,\varphi)}{R}\right)\right]}_{w(r,\theta,\varphi)}\mathbf{e}_\varphi \tag{10}$$

2.4 Small displacement derivatives and linear strain tensor

The displacements derivatives are considered to be very small compared to the value 1, such that a linear geometrical description is appropriate. The components of the linear strain tensor in spherical coordinates read as

$$\varepsilon_{rr} = \frac{\partial u}{\partial r} \qquad \varepsilon_{r\theta} = \frac{1}{2r}\left(\frac{\partial u}{\partial \theta} - v + \frac{r\partial v}{\partial r}\right)$$

$$\varepsilon_{\theta\theta} = \frac{1}{r}\left(\frac{\partial v}{\partial \theta} + u\right) \qquad \varepsilon_{\theta\varphi} = \frac{1}{2r}\left(\frac{1}{\sin\theta}\frac{\partial v}{\partial \varphi} + \frac{\partial w}{\partial \theta} - w\cot\theta\right)$$

$$\varepsilon_{\varphi\varphi} = \frac{1}{r}\left(\frac{1}{\sin\theta}\frac{\partial w}{\partial \varphi} + v\cot\theta + u\right) \qquad \varepsilon_{\varphi r} = \frac{1}{2r}\left(\frac{1}{\sin\theta}\frac{\partial u}{\partial \varphi} - w + \frac{r\partial w}{\partial r}\right) \tag{11}$$

Inserting the real displacements (10) into the linear strain tensor (11), yields

$$\varepsilon_{\theta\theta} = \frac{1}{r}\left[u_m + \frac{\partial v_m}{\partial \theta} - (r-R)\left(\frac{\partial^2 u_m}{R\partial\theta^2} - \frac{\partial v_m}{R\partial\theta}\right)\right]$$

$$\begin{aligned}\varepsilon_{\varphi\varphi} = {} & \frac{1}{r}\frac{1}{\sin\theta}\left[\frac{\partial w_m}{\partial\varphi} - (r-R)\left(\frac{\partial^2 u_m}{R\sin\theta\partial\varphi^2} - \frac{\partial w_m}{R\partial\varphi}\right)\right] \\ & + \frac{1}{r}\left\{\cot\theta\left[v_m - (r-R)\left(\frac{\partial u_m}{R\partial\theta} - \frac{v_m}{R}\right)\right] + u_m\right\}\end{aligned}$$

$$\begin{aligned}\varepsilon_{\theta\varphi} = {} & \frac{1}{2r}\left\{\frac{1}{\sin\theta}\left[\frac{\partial v_m}{\partial\varphi} - (r-R)\left(\frac{\partial^2 u_m}{R\partial\theta\partial\varphi} - \frac{\partial v_m}{R\partial\varphi}\right)\right]\right. \\ & + \left[\frac{\partial w_m}{\partial\theta} - (r-R)\left(\frac{\partial^2 u_m}{R\sin\theta\partial\varphi\partial\theta} - \frac{\partial u_m}{R\sin\theta\partial\varphi}\cot\theta - \frac{\partial w_m}{R\partial\theta}\right)\right] \\ & \left. - \cot\theta\left[w_m - (r-R)\left(\frac{\partial u_m}{R\sin\theta\partial\varphi} - \frac{w_m}{R}\right)\right]\right\}\end{aligned} \tag{12}$$

Notably, evaluating the derivative $\frac{\partial w}{\partial\theta}$, appearing in the expression of $\varepsilon_{\theta\varphi}$ according to (11), requires consideration of the quotient rule when it comes to the term $\frac{\partial u_m(\theta,\varphi)}{R\sin\theta\partial\varphi}$, see Eq. (10) and note that both $u(\theta,\varphi)$ and $\sin\theta$ are functions of θ. The other three independent components of the linear strain tensor, namely the transversal strain components, are equal to zero

$$\varepsilon_{rr}(r,\theta,\varphi) = \varepsilon_{r\theta}(r,\theta,\varphi) = \varepsilon_{r\varphi}(r,\theta,\varphi) = 0 \tag{13}$$

As for formulating the principle of virtual power, we now consider an element of a spherical shell, which is cut free from the structure by cutting in radial direction along parameter lines φ_b, φ_e, θ_b, and θ_e. Thus, the considered element exhibits six surfaces: an outer and an inner surface as well as four lateral surfaces obtained from fictitious cutting (Fig. 4).

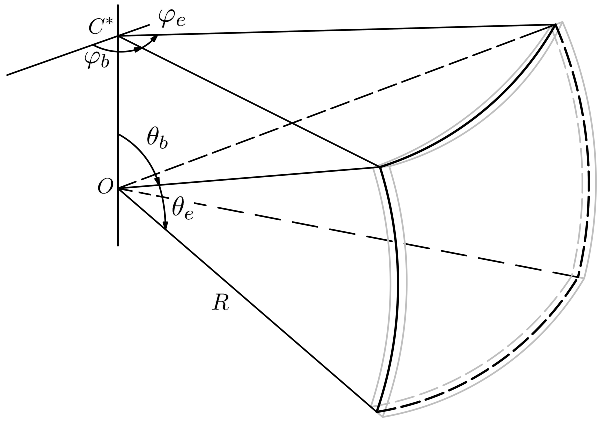

Figure 4: Shell element, with: angels of the beginning and the end of a parameter line φ_b, φ_e, θ_b, and θ_e; $O\ldots$ center of the spherical shell; $C^*\ldots$ center of the circular parameter line φ of the particular cut; and $R\ldots$ radius of the midsurface

3 Virtual power of the external forces

The virtual power of the external forces involves one volume integral and six surface integrals [**2**]

$$\mathcal{L}^{ext} = \int\limits_V \mathbf{f}(r,\theta,\varphi) \cdot \dot{\mathbf{u}}(r,\theta,\varphi;t) dV + \sum_{i=1}^{6} \int\limits_{A_i} \mathbf{T}(\mathbf{n};r,\theta,\varphi) \cdot \dot{\mathbf{u}}(r,\theta,\varphi;t) dA \tag{14}$$

where body force vectors $\mathbf{f}(r,\theta,\varphi)$ and surface traction vectors $\mathbf{T}(\mathbf{n};r,\theta,\varphi)$ perform power along the virtual velocity vectors $\dot{\mathbf{u}}(r,\theta,\varphi;t)$. The traction force vector $\mathbf{T}$ is related to the Cauchy stress tensor $\boldsymbol{\sigma}$ and to the outward unit surface normal vector, $\mathbf{n}$, via Cauchy's formula $\mathbf{T}(\mathbf{n}) = \boldsymbol{\sigma} \cdot \mathbf{n}$, see [**12**][3], reading in component-by-component representation as

$$\mathbf{T}(\mathbf{n};r,\theta,\varphi) = \sigma_{nr}(r,\theta,\varphi)\mathbf{e}_r + \sigma_{n\theta}(r,\theta,\varphi)\mathbf{e}_\theta + \sigma_{n\varphi}(r,\theta,\varphi)\mathbf{e}_\varphi \tag{15}$$

The corresponding representation of the body force vector $\mathbf{f}$ reads as

$$\mathbf{f}(r,\theta,\varphi) = f_r(r,\theta,\varphi)\mathbf{e}_r + f_\theta(r,\theta,\varphi)\mathbf{e}_\theta + f_\varphi(r,\theta,\varphi)\mathbf{e}_\varphi \tag{16}$$

The volume integral in (14) is decomposed into three integrals: one over the polar coordinate θ, one over the azimuthal coordinate φ, and one over the radial coordinate r. Similarly, the infinitesimal volume element dV is decomposed into the infinitesimal line element $rd\theta$ multiplied with the infinitesimal line elements $r\sin\theta d\varphi$ and dr (see Figs. 5 and 6)

$$\int\limits_V \bullet \, dV = \int\limits_{\theta_b}^{\theta_e} \int\limits_{\varphi_b}^{\varphi_e} \int\limits_{R-\frac{h}{2}}^{R+\frac{h}{2}} \bullet \, \overbrace{r^2 \, dr \, \sin\theta d\varphi \, d\theta}^{dV} \tag{17}$$

By analogy, the area integrals over the inner and outer surfaces in Eq. (14) are decomposed into two integrals: one over the polar coordinate θ and one over the azimuthal coordinate φ

$$\int\limits_A \bullet \, dA = \int\limits_{\theta_b}^{\theta_e} \int\limits_{\varphi_b}^{\varphi_e} \bullet \, \overbrace{\left(R \pm \frac{h}{2}\right) \sin\theta d\varphi \, \left(R \pm \frac{h}{2}\right) d\theta}^{dA} \tag{18}$$

where the positive sign applies to the outer surface and the negative sign for the inner surface. Similarly, the area integrals over the lateral surfaces of the spherical shell

[3]Mang, H. and Hofstetter, G., Festigkeitslehre, Springer Verlag Wien GmbH, Wien (2000) 46-47

element are decomposed into two integrals: one over the the polar coordinate θ

$$\int\limits_A \bullet \, dA = \int\limits_{R-\frac{h}{2}}^{R+\frac{h}{2}} \int\limits_{\theta_b}^{\theta_e} \bullet \, \overbrace{r d\theta}^{dA} \tag{19}$$

and one over the azimuthal coordinate φ

$$\int\limits_A \bullet \, dA = \int\limits_{R-\frac{h}{2}}^{R+\frac{h}{2}} \int\limits_{\varphi_b}^{\varphi_e} \bullet \, \overbrace{r \sin\theta d\varphi}^{dA} \tag{20}$$

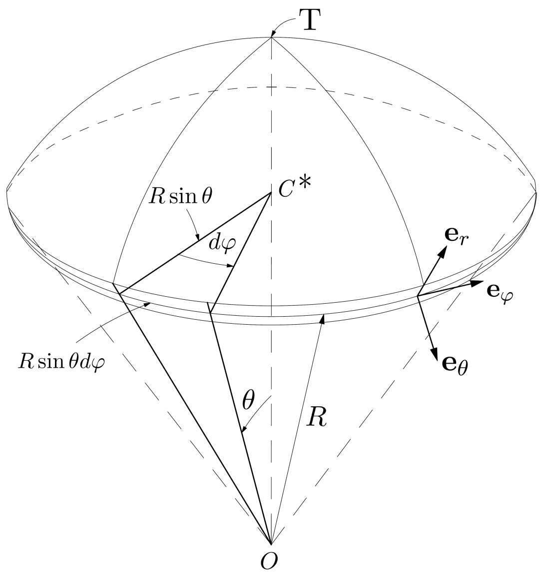

Figure 5: Cone-shaped cut through the spherical shell: O... center of the spherical shell; C^*... center of the circular parameter line φ of the particular cut; T... top of the spherical shell; R... radius of midsurface; $\mathbf{e}_r$, $\mathbf{e}_\theta$, and $\mathbf{e}_\varphi$... accompanying orthonormal basis vectors; and infinitesimal line elements $Rd\theta$ and $R\sin\theta d\varphi$

Finally, we note that time derivatives in Eq. (14) are indicated with a dot

$$\dot{\check{\mathbf{u}}}(r, \varphi, z; t) = \frac{\partial \check{\mathbf{u}}(r, \varphi, z; t)}{\partial t} \tag{21}$$

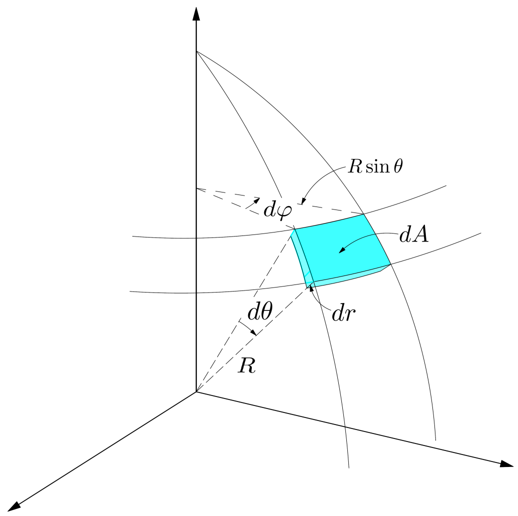

Figure 6: Infinitesimal volume element of the shell: $d\theta$... differential angle in polar direction; $d\varphi$... differential angle in azimuthal direction; dr... differential in radial direction; and dA... differential surface element

3.1 Choice of virtual velocities

When it comes to the choice of virtual displacements $\check{\mathbf{u}}(\mathbf{x};t)$, we make the same assumptions as introduced for the real displacements (10), i.e.

$$\check{\mathbf{u}}(\mathbf{x};t) = \check{u}(r,\theta,\varphi;t)\mathbf{e}_r + \check{v}(r,\theta,\varphi;t)\mathbf{e}_\theta + \check{w}(r,\theta,\varphi;t)\mathbf{e}_\varphi \tag{22}$$

with virtual displacement components in radial direction $\check{u}(r,\theta,\varphi;t)$, polar direction $\check{v}(r,\theta,\varphi;t)$, and azimuthal direction $\check{w}(r,\theta,\varphi;t)$, respectively

$$\begin{aligned}
\check{u}(r,\theta,\varphi;t) &= \check{u}_m(\theta,\varphi;t) \\
\check{v}(r,\theta,\varphi;t) &= \check{v}_m(\theta,\varphi;t) - (r-R)\left(\frac{\partial \check{u}_m(\theta,\varphi;t)}{R\partial\theta} - \frac{\check{v}_m(\theta,\varphi;t)}{R}\right) \\
\check{w}(r,\theta,\varphi;t) &= \check{w}_m(\theta,\varphi;t) - (r-R)\left(\frac{\partial \check{u}_m(\theta,\varphi;t)}{R\sin\theta\partial\varphi} - \frac{\check{w}_m(\theta,\varphi;t)}{R}\right)
\end{aligned} \tag{23}$$

The virtual velocity field follows from time-derivation of the virtual displacement field (22) as

$$\dot{\check{\mathbf{u}}}(\mathbf{x};t) = \dot{\check{u}}(r,\theta,\varphi;t)\mathbf{e}_r + \dot{\check{v}}(r,\theta,\varphi;t)\mathbf{e}_\theta + \dot{\check{w}}(r,\theta,\varphi;t)\mathbf{e}_\varphi \tag{24}$$

with virtual velocity components in respective directions

$$
\begin{aligned}
\dot{\check{u}}(r,\theta,\varphi;t) &= \dot{\check{u}}_m(\theta,\varphi;t) \\
\dot{\check{v}}(r,\theta,\varphi;t) &= \dot{\check{v}}_m(\theta,\varphi;t) - (r-R)\left(\frac{\partial \dot{\check{u}}_m(\theta,\varphi;t)}{R\partial\theta} - \frac{\dot{\check{v}}_m(\theta,\varphi;t)}{R}\right) \\
\dot{\check{w}}(r,\theta,\varphi;t) &= \dot{\check{w}}_m(\theta,\varphi;t) - (r-R)\left(\frac{\partial \dot{\check{u}}_m(\theta,\varphi;t)}{R\sin\theta\partial\varphi} - \frac{\dot{\check{w}}_m(\theta,\varphi;t)}{R}\right)
\end{aligned}
\tag{25}
$$

where time-derivations are indicated with a dot.

Now that we defined a virtual velocity field, we are able to calculate the virtual power of the external forces.

3.2 Calculating virtual power of the external forces

The considered shell element has six surfaces (see Figs. 5 and 6): an outer surface with radial distance $r = R + \frac{h}{2}$ from the shell center and normal vector $\mathbf{n} = +\mathbf{e}_r$; an inner surface with radial distance of $r = R - \frac{h}{2}$ from the shell center and normal vector $\mathbf{n} = -\mathbf{e}_r$; as well as four lateral surfaces: one at $\theta = \theta_b$ where $\mathbf{n} = -\mathbf{e}_\theta$; one at $\theta = \theta_e$ where $\mathbf{n} = +\mathbf{e}_\theta$; one at $\varphi = \varphi_b$ where $\mathbf{n} = -\mathbf{e}_\varphi$, and one at $\varphi = \varphi_e$ where $\mathbf{n} = +\mathbf{e}_\varphi$. Specifying the virtual power of external forces (14) for the volume and surface integrals Eqs. (17) to (20) delivers

$$
\begin{aligned}
\mathcal{L}^{ext} = & \int_{\varphi_b}^{\varphi_e}\int_{\theta_b}^{\theta_e}\int_{R-\frac{h}{2}}^{R+\frac{h}{2}} \mathbf{f}(r,\theta,\varphi)\cdot\check{\dot{\mathbf{u}}}(r,\theta,\varphi;t)\ \overbrace{r^2\ dr\ \sin\theta d\varphi\ d\theta}^{dV} \\
& + \int_{\varphi_b}^{\varphi_e}\int_{\theta_b}^{\theta_e} \mathbf{T}(\mathbf{n}=+\mathbf{e}_r; R+\frac{h}{2},\theta,\varphi)\cdot\check{\dot{\mathbf{u}}}(R+\frac{h}{2},\theta,\varphi;t)\ \overbrace{\left(R+\frac{h}{2}\right)^2\ \sin\theta d\varphi\ d\theta}^{dA} \\
& + \int_{\varphi_b}^{\varphi_e}\int_{\theta_b}^{\theta_e} \mathbf{T}(\mathbf{n}=-\mathbf{e}_r; R-\frac{h}{2},\theta,\varphi)\cdot\check{\dot{\mathbf{u}}}(R-\frac{h}{2},\theta,\varphi;t)\ \overbrace{\left(R-\frac{h}{2}\right)^2\ \sin\theta d\varphi\ d\theta}^{dA} \\
& + \int_{R-\frac{h}{2}}^{R+\frac{h}{2}}\int_{\theta_b}^{\theta_e} \mathbf{T}(\mathbf{n}=+\mathbf{e}_\varphi; r,\theta,\varphi_e)\cdot\check{\dot{\mathbf{u}}}(r,\theta,\varphi_e;t)\ \overbrace{rd\theta\ dr}^{dA} \\
& + \int_{R-\frac{h}{2}}^{R+\frac{h}{2}}\int_{\theta_b}^{\theta_e} \mathbf{T}(\mathbf{n}=-\mathbf{e}_\varphi; r,\theta,\varphi_b)\cdot\check{\dot{\mathbf{u}}}(r,\theta,\varphi_b;t)\ \overbrace{rd\theta\ dr}^{dA} \\
& + \int_{R-\frac{h}{2}}^{R+\frac{h}{2}}\int_{\varphi_b}^{\varphi_e} \mathbf{T}(\mathbf{n}=+\mathbf{e}_\theta; r,\theta_e,\varphi)\cdot\check{\dot{\mathbf{u}}}(r,\theta_e,\varphi;t)\ \overbrace{r\ \sin\theta d\varphi\ dr}^{dA} \\
& + \int_{R-\frac{h}{2}}^{R+\frac{h}{2}}\int_{\varphi_b}^{\varphi_e} \mathbf{T}(\mathbf{n}=-\mathbf{e}_\theta; r,\theta_b,\varphi)\cdot\check{\dot{\mathbf{u}}}(r,\theta_b,\varphi;t)\ \overbrace{r\ \sin\theta d\varphi\ dr}^{dA}
\end{aligned}
\tag{26}
$$

The term "$r^2\ dr\ \sin\theta d\varphi\ d\theta$" represents the volume of the shell infinitesimal element (dV), whilst "$\left(R\pm\frac{h}{2}\right)^2\ d\theta\ \sin\theta d\varphi$", "$rd\theta\ dr$", and "$r\ \sin\theta d\varphi\ dr$" represent surface differentials. Now, by specifying Eq. (26) for surface traction vector (15) and body force vectors (16), as well as for the virtual velocity field (24) and (25), we obtain

$$
\begin{aligned}
\mathcal{L}^{ext} = & \int\limits_{\varphi_b}^{\varphi_e} \int\limits_{R-\frac{h}{2}}^{R+\frac{h}{2}} \int\limits_{\theta_b}^{\theta_e} f_r \; \dot{\check{u}}_m \; r^2 \; dr \; \sin\theta d\varphi \; d\theta \\
& + \int\limits_{\varphi_b}^{\varphi_e} \int\limits_{R-\frac{h}{2}}^{R+\frac{h}{2}} \int\limits_{\theta_b}^{\theta_e} f_\theta \left[\dot{\check{v}}_m - (r-R) \left(\frac{\partial \dot{\check{u}}_m}{R \partial \theta} - \frac{\dot{\check{v}}_m}{R} \right) \right] \; r^2 \; dr \; \sin\theta d\varphi \; d\theta \qquad \boxed{\ldots \text{ Volume}} \\
& + \int\limits_{\varphi_b}^{\varphi_e} \int\limits_{R-\frac{h}{2}}^{R+\frac{h}{2}} \int\limits_{\theta_b}^{\theta_e} f_\varphi \left[\dot{\check{w}}_m - (r-R) \left(\frac{\partial \dot{\check{u}}_m}{R \sin\theta \partial \varphi} - \frac{\dot{\check{w}}_m}{R} \right) \right] \; r^2 \; dr \; \sin\theta d\varphi \; d\theta \\
& + \int\limits_{\varphi_b}^{\varphi_e} \int\limits_{\theta_b}^{\theta_e} \sigma_{rr} \left(R + \frac{h}{2}, \theta, \varphi \right) \; \dot{\check{u}}_m \; \left(R + \frac{h}{2} \right)^2 \; \sin\theta d\varphi \; d\theta \\
& + \int\limits_{\varphi_b}^{\varphi_e} \int\limits_{\theta_b}^{\theta_e} \sigma_{r\theta} \left(R + \frac{h}{2}, \theta, \varphi \right) \left[\dot{\check{v}}_m - \left(\frac{h}{2} \right) \left(\frac{\partial \dot{\check{u}}_m}{R \partial \theta} - \frac{\dot{\check{v}}_m}{R} \right) \right] \left(R + \frac{h}{2} \right)^2 \; \sin\theta d\varphi \; d\theta \qquad \boxed{\ldots \mathbf{n} = +\mathbf{e}_r} \\
& + \int\limits_{\varphi_b}^{\varphi_e} \int\limits_{\theta_b}^{\theta_e} \sigma_{r\varphi} \left(R + \frac{h}{2}, \theta, \varphi \right) \left[\dot{\check{w}}_m - \left(\frac{h}{2} \right) \left(\frac{\partial \dot{\check{u}}_m}{R \sin\theta \partial \varphi} - \frac{\dot{\check{w}}_m}{R} \right) \right] \left(R + \frac{h}{2} \right)^2 \; \sin\theta d\varphi \; d\theta \\
& - \int\limits_{\varphi_b}^{\varphi_e} \int\limits_{\theta_b}^{\theta_e} \sigma_{rr} \left(R - \frac{h}{2}, \theta, \varphi \right) \; \dot{\check{u}}_m \; \left(R - \frac{h}{2} \right)^2 \; \sin\theta d\varphi \; d\theta \\
& - \int\limits_{\varphi_b}^{\varphi_e} \int\limits_{\theta_b}^{\theta_e} \sigma_{r\theta} \left(R - \frac{h}{2}, \theta, \varphi \right) \left[\dot{\check{v}}_m + \left(\frac{h}{2} \right) \left(\frac{\partial \dot{\check{u}}_m}{R \partial \theta} - \frac{\dot{\check{v}}_m}{R} \right) \right] \left(R - \frac{h}{2} \right)^2 \; \sin\theta d\varphi \; d\theta \qquad \boxed{\ldots \mathbf{n} = -\mathbf{e}_r} \\
& - \int\limits_{\varphi_b}^{\varphi_e} \int\limits_{\theta_b}^{\theta_e} \sigma_{r\varphi} \left(R - \frac{h}{2}, \theta, \varphi \right) \left[\dot{\check{w}}_m + \left(\frac{h}{2} \right) \left(\frac{\partial \dot{\check{u}}_m}{R \sin\theta \partial \varphi} - \frac{\dot{\check{w}}_m}{R} \right) \right] \left(R - \frac{h}{2} \right)^2 \; \sin\theta d\varphi \; d\theta \\
& + \int\limits_{R-\frac{h}{2}}^{R+\frac{h}{2}} \int\limits_{\theta_b}^{\theta_e} \sigma_{\varphi r}(r, \theta, \varphi) \; \dot{\check{u}}_m \Big|_{\varphi_b}^{\varphi_e} r d\theta \; dr \\
& + \int\limits_{R-\frac{h}{2}}^{R+\frac{h}{2}} \int\limits_{\theta_b}^{\theta_e} \sigma_{\varphi\theta}(r, \theta, \varphi) \; \left[\dot{\check{v}}_m + (r-R) \left(\frac{\partial \dot{\check{u}}_m}{R \partial \theta} - \frac{\dot{\check{v}}_m}{R} \right) \right] \Bigg|_{\varphi_b}^{\varphi_e} r d\theta \; dr \qquad \boxed{\ldots \mathbf{n} = \pm \mathbf{e}_\varphi}
\end{aligned}
$$

$$+\int_{R-\frac{h}{2}}^{R+\frac{h}{2}}\int_{\theta_b}^{\theta_e}\sigma_{\varphi\varphi}(r,\theta,\varphi)\ \left[\dot{\check{w}}_m+(r-R)\left(\frac{\partial\dot{\check{u}}_m}{R\sin\theta\partial\varphi}-\frac{\dot{\check{w}}_m}{R}\right)\right]\Bigg|_{\varphi_b}^{\varphi_e} rd\theta\ dr$$

$$+\int_{R-\frac{h}{2}}^{R+\frac{h}{2}}\int_{\varphi_b}^{\varphi_e}\sigma_{\theta r}(r,\theta,\varphi)\ \dot{\check{u}}_m\Bigg|_{\theta_b}^{\theta_e} r\sin\theta d\varphi\ dr$$

$$+\int_{R-\frac{h}{2}}^{R+\frac{h}{2}}\int_{\varphi_b}^{\varphi_e}\sigma_{\theta\theta}(r,\theta,\varphi)\ \left[\dot{\check{v}}_m+(r-R)\left(\frac{\partial\dot{\check{u}}_m}{R\partial\theta}-\frac{\dot{\check{v}}_m}{R}\right)\right]\Bigg|_{\theta_b}^{\theta_e} r\sin\theta d\varphi\ dr \qquad \boxed{\ldots\mathbf{n}=\pm\mathbf{e}_\theta}$$

$$+\int_{R-\frac{h}{2}}^{R+\frac{h}{2}}\int_{\varphi_b}^{\varphi_e}\sigma_{\theta\varphi}(r,\varphi,\theta)\ \left[\dot{\check{w}}_m+(r-R)\left(\frac{\partial\dot{\check{u}}_m}{R\sin\theta\partial\varphi}-\frac{\dot{\check{w}}_m}{R}\right)\right]\Bigg|_{\theta_b}^{\theta_e} r\sin\theta d\varphi\ dr \tag{27}$$

Consistent with our aim to make the transition from *three*-dimensional continuum mechanics to a *two*-dimensional theory for spherical shells, we now make sure that the differential line elements referring to the *midsurface* show up in every integral in Eq. (27). This concerns differential line elements in polar direction "$Rd\theta$" and in azimuthal direction "$R\sin\theta d\varphi$", as shown in Figs. 5 and 6. To this end, we multiply $d\theta$ by 1 in the form $\frac{R}{R}$ and we represent the resulting expression as $\frac{1}{R}Rd\theta$, i.e.

$$d\theta\to\frac{1}{R}Rd\theta \quad\Rightarrow\quad rd\theta\to\frac{r}{R}Rd\theta$$

$$\left(R+\frac{h}{2}\right)d\theta\to\left(1+\frac{h}{2R}\right)Rd\theta \quad \left(R-\frac{h}{2}\right)d\theta\to\left(1-\frac{h}{2R}\right)Rd\theta \tag{28}$$

Similarly, we multiply $\sin\theta d\varphi$ by 1 in the form $\frac{R}{R}$, i.e.

$$\sin\theta d\varphi\to\frac{1}{R}R\sin\theta d\varphi \quad\Rightarrow\quad r\sin\theta d\varphi\to\frac{r}{R}R\sin\theta d\varphi$$

$$\left(R+\frac{h}{2}\right)\sin\theta d\varphi\to\left(1+\frac{h}{2R}\right)R\sin\theta d\varphi \quad \left(R-\frac{h}{2}\right)\sin\theta d\varphi\to\left(1-\frac{h}{2R}\right)R\sin\theta d\varphi \tag{29}$$

Specifying Eq. (27) for (28) and (29) delivers

$$
\begin{aligned}
\mathcal{L}^{ext} = & \int\limits_{\varphi_b}^{\varphi_e} \int\limits_{R-\frac{h}{2}}^{R+\frac{h}{2}} \int\limits_{\theta_b}^{\theta_e} f_r \; \dot{\check{u}}_m \; \frac{r^2}{R^2} \; R^2 \; dr \; \sin\theta d\varphi \; d\theta \\
& + \int\limits_{\varphi_b}^{\varphi_e} \int\limits_{R-\frac{h}{2}}^{R+\frac{h}{2}} \int\limits_{\theta_b}^{\theta_e} f_\theta \left[\dot{\check{v}}_m - (r-R) \left(\frac{\partial \dot{\check{u}}_m}{R \partial \theta} - \frac{\dot{\check{v}}_m}{R} \right) \right] \; \frac{r^2}{R^2} \; R^2 \; dr \; \sin\theta d\varphi \; d\theta \\
& + \int\limits_{\varphi_b}^{\varphi_e} \int\limits_{R-\frac{h}{2}}^{R+\frac{h}{2}} \int\limits_{\theta_b}^{\theta_e} f_\varphi \left[\dot{\check{w}}_m - (r-R) \left(\frac{\partial \dot{\check{u}}_m}{R \sin\theta \partial \varphi} - \frac{\dot{\check{w}}_m}{R} \right) \right] \; \frac{r^2}{R^2} \; R^2 \; dr \; \sin\theta d\varphi \; d\theta \\
& + \int\limits_{\varphi_b}^{\varphi_e} \int\limits_{\theta_b}^{\theta_e} \sigma_{rr} \left(R + \frac{h}{2}, \theta, \varphi \right) \; \dot{\check{u}}_m \; \left(1 + \frac{h}{2R} \right)^2 \; R^2 \; \sin\theta d\varphi \; d\theta \\
& + \int\limits_{\varphi_b}^{\varphi_e} \int\limits_{\theta_b}^{\theta_e} \sigma_{r\theta} \left(R + \frac{h}{2}, \theta, \varphi \right) \left[\dot{\check{v}}_m - \left(\frac{h}{2} \right) \left(\frac{\partial \dot{\check{u}}_m}{R \partial \theta} - \frac{\dot{\check{v}}_m}{R} \right) \right] \left(1 + \frac{h}{2R} \right)^2 \; R^2 \; \sin\theta d\varphi \; d\theta \\
& + \int\limits_{\varphi_b}^{\varphi_e} \int\limits_{\theta_b}^{\theta_e} \sigma_{r\varphi} \left(R + \frac{h}{2}, \theta, \varphi \right) \left[\dot{\check{w}}_m - \left(\frac{h}{2} \right) \left(\frac{\partial \dot{\check{u}}_m}{R \sin\theta \partial \varphi} - \frac{\dot{\check{w}}_m}{R} \right) \right] \left(1 + \frac{h}{2R} \right)^2 \; R^2 \; \sin\theta d\varphi \; d\theta \\
& - \int\limits_{\varphi_b}^{\varphi_e} \int\limits_{\theta_b}^{\theta_e} \sigma_{rr} \left(R - \frac{h}{2}, \theta, \varphi \right) \; \dot{\check{u}}_m \; \left(1 - \frac{h}{2R} \right)^2 \; R^2 \; \sin\theta d\varphi \; d\theta \\
& - \int\limits_{\varphi_b}^{\varphi_e} \int\limits_{\theta_b}^{\theta_e} \sigma_{r\theta} \left(R - \frac{h}{2}, \theta, \varphi \right) \left[\dot{\check{v}}_m + \left(\frac{h}{2} \right) \left(\frac{\partial \dot{\check{u}}_m}{R \partial \theta} - \frac{\dot{\check{v}}_m}{R} \right) \right] \left(1 - \frac{h}{2R} \right)^2 \; R^2 \; \sin\theta d\varphi \; d\theta \\
& - \int\limits_{\varphi_b}^{\varphi_e} \int\limits_{\theta_b}^{\theta_e} \sigma_{r\varphi} \left(R - \frac{h}{2}, \theta, \varphi \right) \left[\dot{\check{w}}_m + \left(\frac{h}{2} \right) \left(\frac{\partial \dot{\check{u}}_m}{R \sin\theta \partial \varphi} - \frac{\dot{\check{w}}_m}{R} \right) \right] \left(1 - \frac{h}{2R} \right)^2 \; R^2 \; \sin\theta d\varphi \; d\theta
\end{aligned}
\tag{30}
$$

$$
+ \int\limits_{R-\frac{h}{2}}^{R+\frac{h}{2}} \int\limits_{\theta_b}^{\theta_e} \sigma_{\varphi r}(r,\theta,\varphi)\ \dot{\check{u}}_m \Big|_{\varphi_b}^{\varphi_e} \frac{r}{R}\ Rd\theta\ dr
$$

$$
+ \int\limits_{R-\frac{h}{2}}^{R+\frac{h}{2}} \int\limits_{\theta_b}^{\theta_e} \sigma_{\varphi\theta}(r,\theta,\varphi)\ \left[\dot{\check{v}}_m + (r-R)\left(\frac{\partial \dot{\check{u}}_m}{R\partial\theta} - \frac{\dot{\check{v}}_m}{R}\right)\right] \Bigg|_{\varphi_b}^{\varphi_e} \frac{r}{R}\ Rd\theta\ dr
$$

$$
+ \int\limits_{R-\frac{h}{2}}^{R+\frac{h}{2}} \int\limits_{\theta_b}^{\theta_e} \sigma_{\varphi\varphi}(r,\theta,\varphi)\ \left[\dot{\check{w}}_m + (r-R)\left(\frac{\partial \dot{\check{u}}_m}{R\sin\theta\partial\varphi} - \frac{\dot{\check{w}}_m}{R}\right)\right] \Bigg|_{\varphi_b}^{\varphi_e} \frac{r}{R}\ Rd\theta\ dr
$$

$$
+ \int\limits_{R-\frac{h}{2}}^{R+\frac{h}{2}} \int\limits_{\varphi_b}^{\varphi_e} \sigma_{\theta r}(r,\theta,\varphi)\ \dot{\check{u}}_m \Big|_{\theta_b}^{\theta_e} \frac{r}{R}\ R\sin\theta d\varphi\ dr
$$

$$
+ \int\limits_{R-\frac{h}{2}}^{R+\frac{h}{2}} \int\limits_{\varphi_b}^{\varphi_e} \sigma_{\theta\theta}(r,\theta,\varphi)\ \left[\dot{\check{v}}_m + (r-R)\left(\frac{\partial \dot{\check{u}}_m}{R\partial\theta} - \frac{\dot{\check{v}}_m}{R}\right)\right] \Bigg|_{\theta_b}^{\theta_e} \frac{r}{R}\ R\sin\theta d\varphi\ dr
$$

$$
+ \int\limits_{R-\frac{h}{2}}^{R+\frac{h}{2}} \int\limits_{\varphi_b}^{\varphi_e} \sigma_{\theta\varphi}(r,\varphi,\theta)\ \left[\dot{\check{w}}_m + (r-R)\left(\frac{\partial \dot{\check{u}}_m}{R\sin\theta\partial\varphi} - \frac{\dot{\check{w}}_m}{R}\right)\right] \Bigg|_{\theta_b}^{\theta_e} \frac{r}{R}\ R\sin\theta d\varphi\ dr \qquad (31)
$$

Eq. (31) shows the existence of stress resultants, which perform power along the specific virtual velocities: external surface loads $p_r(\theta,\varphi)$, $p_\theta(\theta,\varphi)$, and $p_\varphi(\theta,\varphi)$; external surface moments $k_\theta(\theta,\varphi)$ and $k_\varphi(\theta,\varphi)$; membrane forces $n_{\theta\theta}(\theta,\varphi)$, $n_{\varphi\varphi}(\theta,\varphi)$, $n_{\theta\varphi}(\theta,\varphi)$, and $n_{\varphi\theta}(\theta,\varphi)$; transversal shear stress resultants $q_\theta(\theta,\varphi)$ and $q_\varphi(\theta,\varphi)$; as well as bending and twisting moments $m_{\theta\theta}(\theta,\varphi)$, $m_{\varphi\varphi}(\theta,\varphi)$, $m_{\theta\varphi}(\theta,\varphi)$, and $m_{\varphi\theta}(\theta,\varphi)$. Re-formulating Eq. (31) based on the described stress resultants delivers

$$
\begin{aligned}
\mathcal{L}^{ext} = &\int\limits_{\varphi_b}^{\varphi_e}\int\limits_{\theta_b}^{\theta_e} \left[p_r(\theta,\varphi)\ \dot{\check{u}}_m + p_\theta(\theta,\varphi)\ \dot{\check{v}}_m + p_\varphi(\theta,\varphi)\ \dot{\check{w}}_m\right]\ R^2\ \sin\theta d\varphi\ d\theta \\
&-\int\limits_{\varphi_b}^{\varphi_e}\int\limits_{\theta_b}^{\theta_e} \left[k_\varphi(\theta,\varphi)\left(\frac{\partial\dot{\check{u}}_m}{R\sin\theta\partial\varphi}-\frac{\dot{\check{w}}_m}{R}\right)+k_\theta(\theta,\varphi)\left(\frac{\partial\dot{\check{u}}_m}{R\partial\theta}-\frac{\dot{\check{v}}_m}{R}\right)\right]\ R^2\ \sin\theta d\varphi\ d\theta \\
&+\int\limits_{\theta_b}^{\theta_e}\left[n_{\varphi\varphi}(\theta,\varphi)\ \dot{\check{w}}_m + n_{\varphi\theta}\ \dot{\check{v}}_m + q_\varphi(\theta,\varphi)\ \dot{\check{u}}_m\right]\ Rd\theta\Big|_{\varphi_b}^{\varphi_e} \\
&-\int\limits_{\theta_b}^{\theta_e}\left[m_{\varphi\varphi}(\theta,\varphi)\left(\frac{\partial\dot{\check{u}}_m}{R\sin\theta\partial\varphi}-\frac{\dot{\check{w}}_m}{R}\right)+m_{\varphi\theta}(\theta,\varphi)\left(\frac{\partial\dot{\check{u}}_m}{R\partial\theta}-\frac{\dot{\check{v}}_m}{R}\right)\right]\ Rd\theta\Big|_{\varphi_b}^{\varphi_e} \\
&+\int\limits_{\varphi_b}^{\varphi_e}\left[n_{\theta\theta}(\theta,\varphi)\ \dot{\check{v}}_m + n_{\theta\varphi}(\theta,\varphi)\ \dot{\check{w}}_m + q_\theta(\theta,\varphi)\ \dot{\check{u}}_m\right]\ R\sin\theta d\varphi\Big|_{\theta_b}^{\theta_e} \\
&-\int\limits_{\varphi_b}^{\varphi_e}\left[m_{\theta\varphi}(\theta,\varphi)\left(\frac{\partial\dot{\check{u}}_m}{R\sin\theta\partial\varphi}-\frac{\dot{\check{w}}_m}{R}\right)+m_{\theta\theta}(\theta,\varphi)\left(\frac{\partial\dot{\check{u}}_m}{R\partial\theta}-\frac{\dot{\check{v}}_m}{R}\right)\right]\ R\sin\theta d\varphi\Big|_{\theta_b}^{\theta_e}
\end{aligned}
\tag{32}
$$

Integrating by parts, in Eq. (32), terms involving surface moments $k_\theta(\theta,\varphi)$ and $k_\varphi(\theta,\varphi)$ results in

$$
\begin{aligned}
\mathcal{L}^{ext} = & \int_{\varphi_b}^{\varphi_e}\int_{\theta_b}^{\theta_e} [p_r(\theta,\varphi)\ \dot{\check{u}}_m + p_\theta(\theta,\varphi)\ \dot{\check{v}}_m + p_\varphi(\theta,\varphi;t)\ \dot{\check{w}}_m]\ R^2\ \sin\theta d\varphi\ d\theta \\
& - \int_{\theta_b}^{\theta_e} k_\varphi(\theta,\varphi)\ \dot{\check{u}}_m \Big|_{\varphi_b}^{\varphi_e} R d\theta + \int_{\varphi_b}^{\varphi_e}\int_{\theta_b}^{\theta_e} \frac{\partial k_\varphi(\theta,\varphi)}{R\sin\theta\partial\varphi}\ \dot{\check{u}}_m\ R^2\ \sin\theta d\varphi\ d\theta \\
& + \int_{\varphi_b}^{\varphi_e}\int_{\theta_b}^{\theta_e} \frac{k_\varphi(\theta,\varphi)}{R}\ \dot{\check{w}}_m\ R^2\ \sin\theta d\varphi\ d\theta \\
& - \int_{\varphi_b}^{\varphi_e} k_\theta(\theta,\varphi)\ \dot{\check{u}}_m \Big|_{\theta_b}^{\theta_e} R\sin\theta d\varphi + \int_{\varphi_b}^{\varphi_e}\int_{\theta_b}^{\theta_e} \frac{\partial k_\theta(\theta,\varphi)}{R\partial\theta}\ \dot{\check{u}}_m\ R^2\ \sin\theta d\varphi\ d\theta \\
& + \int_{\varphi_b}^{\varphi_e}\int_{\theta_b}^{\theta_e} \frac{k_\theta(\theta,\varphi)}{R}\ \dot{\check{u}}_m\ \cot\theta\ R^2\ \sin\theta d\varphi\ d\theta + \int_{\varphi_b}^{\varphi_e}\int_{\theta_b}^{\theta_e} \frac{k_\theta(\theta,\varphi)}{R}\ \dot{\check{v}}_m\ R^2\ \sin\theta d\varphi\ d\theta \\
& + \int_{\theta_b}^{\theta_e} \left[n_{\varphi\varphi}(\theta,\varphi)\ \dot{\check{w}}_m + n_{\varphi\theta}(\theta,\varphi)\ \dot{\check{v}}_m + q_\varphi(\theta,\varphi)\ \dot{\check{u}}_m\right] \Big|_{\varphi_b}^{\varphi_e} R d\theta \\
& - \int_{\theta_b}^{\theta_e} \left[m_{\varphi\varphi}(\theta,\varphi)\left(\frac{\partial\dot{\check{u}}_m}{R\sin\theta\partial\varphi} - \frac{\dot{\check{w}}_m}{R}\right) + m_{\varphi\theta}(\theta,\varphi)\left(\frac{\partial\dot{\check{u}}_m}{R\partial\theta} - \frac{\dot{\check{v}}_m}{R}\right)\right] \Bigg|_{\varphi_b}^{\varphi_e} R d\theta \\
& + \int_{\varphi_b}^{\varphi_e} \left[n_{\theta\theta}(\theta,\varphi)\ \dot{\check{v}}_m + n_{\theta\varphi}(\theta,\varphi)\ \dot{\check{w}}_m + q_\theta(\theta,\varphi)\ \dot{\check{u}}_m\right] \Big|_{\theta_b}^{\theta_e} R\sin\theta d\varphi \\
& - \int_{\varphi_b}^{\varphi_e} \left[m_{\theta\varphi}(\theta,\varphi)\left(\frac{\partial\dot{\check{u}}_m}{R\sin\theta\partial\varphi} - \frac{\dot{\check{w}}_m}{R}\right) + m_{\theta\theta}(\theta,\varphi)\left(\frac{\partial\dot{\check{u}}_m}{R\partial\theta} - \frac{\dot{\check{v}}_m}{R}\right)\right] \Bigg|_{\theta_b}^{\theta_e} R\sin\theta d\varphi
\end{aligned}
\tag{33}
$$

3.3 Identifying power-performing stress resultants

Stress resultants p_r, p_θ, p_φ, k_θ, k_φ, $n_{\theta\theta}$, $n_{\varphi\varphi}$, $n_{\theta\varphi}$, $n_{\varphi\theta}$, q_θ, q_φ, $m_{\theta\theta}$, $m_{\varphi\varphi}$, $m_{\theta\varphi}$, and $m_{\varphi\theta}$ introduced in Eq. (32) can be determined by comparing Eq. (31) with (32). External surface loads p_r, p_θ, and p_φ (see Fig. 7), representing forces per area, perform power along the virtual velocities of the shell generator $\dot{\check{u}}_m(\theta,\varphi;t)$, $\dot{\check{v}}_m(\theta,\varphi;t)$, and $\dot{\check{w}}_m(\theta,\varphi;t)$

$$
\begin{aligned}
p_r(\theta,\varphi) &= \sigma_{rr}\left(R+\frac{h}{2},\theta,\varphi\right)\left(1+\frac{h}{2R}\right)^2 - \sigma_{rr}\left(R-\frac{h}{2},\theta,\varphi\right)\left(1-\frac{h}{2R}\right)^2 \\
&\quad + \int\limits_{R-\frac{h}{2}}^{R+\frac{h}{2}} f_r(r,\theta,\varphi)\,\frac{r^2}{R^2}\,dr \\
p_\theta(\theta,\varphi) &= \sigma_{r\theta}\left(R+\frac{h}{2},\theta,\varphi\right)\left(1+\frac{h}{2R}\right)^2 - \sigma_{r\theta}\left(R-\frac{h}{2},\theta,\varphi\right)\left(1-\frac{h}{2R}\right)^2 \\
&\quad + \int\limits_{R-\frac{h}{2}}^{R+\frac{h}{2}} f_\theta(r,\theta,\varphi)\,\frac{r^2}{R^2}\,dr \\
p_\varphi(\theta,\varphi) &= \sigma_{r\varphi}\left(R+\frac{h}{2},\theta,\varphi\right)\left(1+\frac{h}{2R}\right)^2 - \sigma_{r\varphi}\left(R-\frac{h}{2},\theta,\varphi\right)\left(1-\frac{h}{2R}\right)^2 \\
&\quad + \int\limits_{R-\frac{h}{2}}^{R+\frac{h}{2}} f_\varphi(r,\theta,\varphi)\,\frac{r^2}{R^2}\,dr \qquad (34)
\end{aligned}
$$

see also Fig. 7.

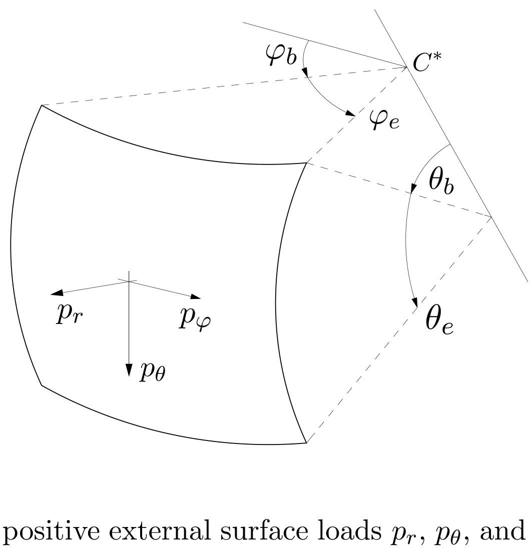

Figure 7: Directions of positive external surface loads p_r, p_θ, and p_φ, representing forces per area, described in Eq. (34); they perform positive virtual power along the virtual velocities of the shell generator $\dot{\hat{u}}_m(\theta,\varphi;t)$, $\dot{\hat{v}}_m(\theta,\varphi;t)$, and $\dot{\hat{w}}_m(\theta,\varphi;t)$

External surface moments $-k_\theta(\theta,\varphi)$ and $-k_\varphi(\theta,\varphi)$ (see Fig. 8), representing moments per area, perform power along the virtual rotations of the shell generator $\left(\frac{\partial \dot{\tilde{u}}_m}{R\partial\theta} - \frac{\dot{\tilde{v}}_m}{R}\right)$ and $\left(\frac{\partial \dot{\tilde{u}}_m}{R\sin\theta\partial\varphi} - \frac{\dot{\tilde{w}}_m}{R}\right)$

$$\begin{aligned}
k_\theta(\theta,\varphi) &= \sigma_{r\theta}\left(R+\frac{h}{2},\theta,\varphi\right)\,\frac{h}{2}\left(1+\frac{h}{2R}\right)^2 + \sigma_{r\theta}\left(R-\frac{h}{2},\theta,\varphi\right)\frac{h}{2}\left(1-\frac{h}{2R}\right)^2 \\
&\quad + \int\limits_{R-\frac{h}{2}}^{R+\frac{h}{2}} f_\theta(r,\theta,\varphi)(r-R)\,\frac{r^2}{R^2}\,dr \\
k_\varphi(\theta,\varphi) &= \sigma_{r\varphi}\left(R+\frac{h}{2},\theta,\varphi\right)\,\frac{h}{2}\left(1+\frac{h}{2R}\right)^2 + \sigma_{r\varphi}\left(R-\frac{h}{2},\theta,\varphi\right)\,\frac{h}{2}\left(1-\frac{h}{2R}\right)^2 \\
&\quad + \int\limits_{R-\frac{h}{2}}^{R+\frac{h}{2}} f_\varphi(r,\theta,\varphi)(r-R)\,\frac{r^2}{R^2}\,dr
\end{aligned} \tag{35}$$

see also Fig. 8.

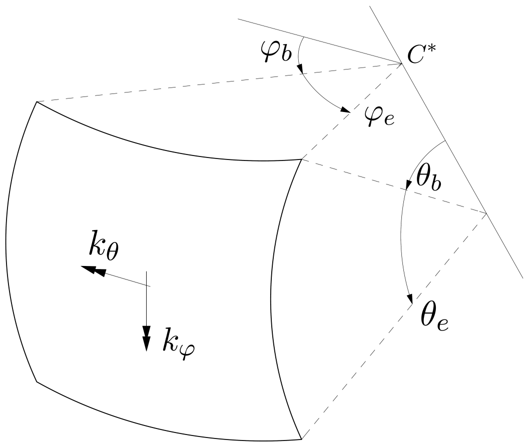

Figure 8: Directions of positive external surface moments k_θ and k_φ, representing moments per area, described in Eq. (35); they perform negative power along the virtual rotations of the shell generator $\left(\frac{\partial \dot{\tilde{u}}_m}{R\partial\theta} - \frac{\dot{\tilde{v}}_m}{R}\right)$ and $\left(\frac{\partial \dot{\tilde{u}}_m}{R\sin\theta\partial\varphi} - \frac{\dot{\tilde{w}}_m}{R}\right)$

Transversal shear stress resultants $-q_\theta(\theta_b)$ and $q_\theta(\theta_e)$, as well as membrane forces $-n_{\theta\theta}(\theta_b)$, $n_{\theta\theta}(\theta_e)$, $-n_{\theta\varphi}(\theta_b)$, and $n_{\theta\varphi}(\theta_e)$, as shown in Fig. 9, perform power along the virtual velocities, $\dot{\tilde{u}}_m(\theta_b,\varphi;t)$, $\dot{\tilde{u}}_m(\theta_e,\varphi;t)$, $\dot{\tilde{v}}_m(\theta_b,\varphi;t)$, $\dot{\tilde{v}}_m(\theta_e,\varphi;t)$, $\dot{\tilde{w}}_m(\theta_b,\varphi;t)$, and $\dot{\tilde{w}}_m(\theta_e,\varphi;t)$

$$
\begin{aligned}
q_\theta(\theta,\varphi) &= \int\limits_{R-\frac{h}{2}}^{R+\frac{h}{2}} \sigma_{\theta r}(r,\theta,\varphi)\frac{r}{R}\,dr \\
n_{\theta\theta}(\theta,\varphi) &= \int\limits_{R-\frac{h}{2}}^{R+\frac{h}{2}} \sigma_{\theta\theta}(r,\theta,\varphi)\frac{r}{R}\,dr \\
n_{\theta\varphi}(\theta,\varphi) &= \int\limits_{R-\frac{h}{2}}^{R+\frac{h}{2}} \sigma_{\theta r}(r,\theta,\varphi)\frac{r}{R}\,dr
\end{aligned} \tag{36}
$$

see also Fig. 9.

Transversal shear stress resultants $-q_\varphi(\varphi_b)$ and $q_\varphi(\varphi_e)$, as well as membrane forces $-n_{\varphi\varphi}(\varphi_b)$, $n_{\varphi\varphi}(\varphi_e)$, $-n_{\varphi\theta}(\varphi_b)$, and $n_{\varphi\theta}(\varphi_e)$, as shown in Fig. 9, perform power along the virtual velocities $\dot{\check{u}}_m(\theta,\varphi_b;t)$, $\dot{\check{u}}_m(\theta,\varphi_e;t)$, $\dot{\check{v}}_m(\theta,\varphi_b;t)$, $\dot{\check{v}}_m(\theta,\varphi_e;t)$, $\dot{\check{w}}_m(\theta,\varphi_b;t)$, and $\dot{\check{w}}_m(\theta,\varphi_e;t)$

$$
\begin{aligned}
q_\varphi(\theta,\varphi) &= \int\limits_{R-\frac{h}{2}}^{R+\frac{h}{2}} \sigma_{\varphi r}(r,\theta,\varphi)\frac{r}{R}\,dr \\
n_{\varphi\theta}(\theta,\varphi) &= \int\limits_{R-\frac{h}{2}}^{R+\frac{h}{2}} \sigma_{\varphi\theta}(r,\theta,\varphi)\frac{r}{R}\,dr \\
n_{\varphi\varphi}(\theta,\varphi) &= \int\limits_{R-\frac{h}{2}}^{R+\frac{h}{2}} \sigma_{\varphi\varphi}(r,\theta,\varphi)\frac{r}{R}\,dr
\end{aligned} \tag{37}
$$

see also Fig. 9. When comparing the definitions of stress resultants $n_{\theta\varphi}$ from (36) and $n_{\varphi\theta}$ from (37), it is noteworthy to recall the symmetry of Cauchy's stress tensor

$$
\sigma_{\theta\varphi}(r,\theta,\varphi) = \sigma_{\varphi\theta}(r,\theta,\varphi) \tag{38}
$$

and this implies that the same symmetry also applies to the stress resultants

$$
n_{\theta\varphi}(r,\theta,\varphi) = n_{\varphi\theta}(r,\theta,\varphi) \tag{39}
$$

Bending moments $m_{\theta\theta}(\theta_b)$ and $-m_{\theta\theta}(\theta_e)$, as well as twisting moments $m_{\theta\varphi}(\theta_b)$ and $-m_{\theta\varphi}(\theta_e)$, see Fig 10, perform virtual power along the shell generator ro-

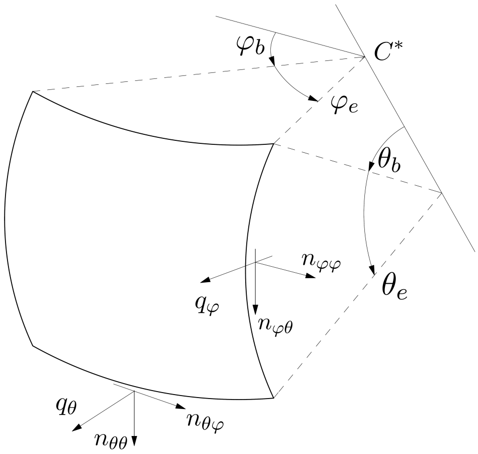

Figure 9: Directions of positive shear forces q_θ and q_φ, as well as membrane forces $n_{\theta\theta}$, $n_{\varphi\varphi}$, and $n_{\theta\varphi} = n_{\varphi\theta}$, representing forces per length, described in Eqs. (36) and (37); they perform power along the virtual velocities $\dot{\check{u}}_m(\theta, \varphi; t)$, $\dot{\check{v}}_m(\theta, \varphi; t)$, and $\dot{\check{w}}_m(\theta, \varphi; t)$

tations $\left(\frac{\partial \dot{\check{u}}_m}{R\partial\theta} - \frac{\dot{\check{v}}_m}{R}\right)\Big|_{\theta_b}$ and $\left(\frac{\partial \dot{\check{u}}_m}{R\partial\theta} - \frac{\dot{\check{v}}_m}{R}\right)\Big|_{\theta_e}$, as well as $\left(\frac{\partial \dot{\check{u}}_m}{R\sin\theta\partial\varphi} - \frac{\dot{\check{w}}_m}{R}\right)\Big|_{\theta_b}$ and $\left(\frac{\partial \dot{\check{u}}_m}{R\sin\theta\partial\varphi} - \frac{\dot{\check{w}}_m}{R}\right)\Big|_{\theta_e}$

$$m_{\theta\theta}(\theta, \varphi) = \int\limits_{R-\frac{h}{2}}^{R+\frac{h}{2}} \sigma_{\theta\theta}(r, \theta, \varphi)(r - R)\frac{r}{R}\, dr$$

$$m_{\theta\varphi}(\theta, \varphi) = \int\limits_{R-\frac{h}{2}}^{R+\frac{h}{2}} \sigma_{\theta\varphi}(r, \theta, \varphi)(r - R)\frac{r}{R}\, dr \tag{40}$$

see also Fig. 10.

Bending moments $m_{\varphi\varphi}(\varphi)$ and $-m_{\varphi\varphi}(\varphi)$, as well as twisting moments $m_{\varphi\theta}(\varphi)$ and $-m_{\varphi\theta}(\varphi)$, see Fig. 10, perform virtual power along the shell generator rotations $\left(\frac{\partial \dot{\check{u}}_m}{R\sin\theta\partial\varphi} - \frac{\dot{\check{w}}_m}{R}\right)\Big|_{\varphi_b}$ and $\left(\frac{\partial \dot{\check{u}}_m}{R\sin\theta\partial\varphi} - \frac{\dot{\check{w}}_m}{R}\right)\Big|_{\varphi_e}$, as well as $\left(\frac{\partial \dot{\check{u}}_m}{R\partial\theta} - \frac{\dot{\check{v}}_m}{R}\right)\Big|_{\varphi_b}$ and $\left(\frac{\partial \dot{\check{u}}_m}{R\partial\theta} - \frac{\dot{\check{v}}_m}{R}\right)\Big|_{\varphi_e}$

$$m_{\varphi\varphi}(\theta,\varphi) = \int\limits_{R-\frac{h}{2}}^{R+\frac{h}{2}} \sigma_{\varphi\varphi}(r,\theta,\varphi)(r-R)\frac{r}{R}\,dr$$

$$m_{\varphi\theta}(\theta,\varphi) = \int\limits_{R-\frac{h}{2}}^{R+\frac{h}{2}} \sigma_{\varphi\theta}(r,\theta,\varphi)(r-R)\frac{r}{R}\,dr \tag{41}$$

see also Fig. 10. By analogy to the membrane shear forces, we can recognise the symmetry of twisting moments, compare (40) and (41) under consideration of (38), i.e.

$$m_{\theta\varphi}(r,\theta,\varphi) = m_{\varphi\theta}(r,\theta,\varphi) \tag{42}$$

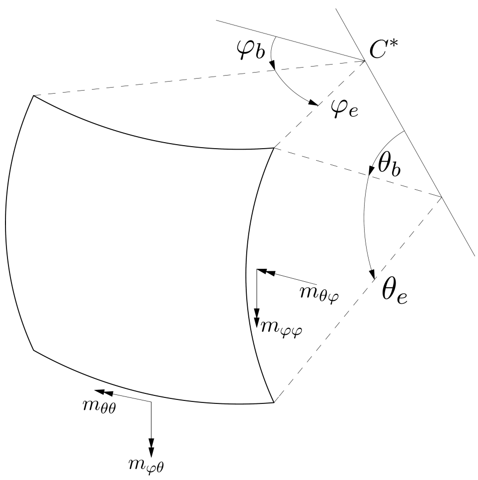

Figure 10: Directions of positive bending moments $m_{\theta\theta}$ and $m_{\varphi\varphi}$, as well as twisting moments $m_{\theta\varphi} = m_{\varphi\theta}$, representing moments per length, described in Eq. (40) and (41); they perform virtual power along the shell generator rotations $\left(\frac{\partial \dot{u}_m}{R\sin\theta\partial\varphi} - \frac{\dot{w}_m}{R}\right)$ and $\left(\frac{\partial \dot{u}_m}{R\partial\theta} - \frac{\dot{v}_m}{R}\right)$

3.4 Constitutive relations and relations between stresses and stress resultants

Normal stresses $\sigma_{\theta\theta}$, $\sigma_{\varphi\varphi}$ and shear stresses $\sigma_{\theta\varphi} = \sigma_{\varphi\theta}$ appearing in the membrane forces $n_{\theta\theta}$, $n_{\varphi\varphi}$, and $n_{\theta\varphi} = n_{\varphi\theta}$, as well as in the bending moments $m_{\theta\theta}$, $m_{\varphi\varphi}$ and twisting moments $m_{\theta\varphi} = m_{\varphi\theta}$, can be determined by applying Hooke's law. Considering that the transversal stresses σ_{rr}, $\sigma_{r\theta}$, and $\sigma_{r\varphi}$ are significantly smaller than the membrane stresses $\sigma_{\theta\theta}$, $\sigma_{\varphi\varphi}$, and $\sigma_{\theta\varphi}$ is the motivation to apply Hooke's law for a *plane* stress state in θ, φ planes:

$$\begin{aligned}
\sigma_{\theta\theta}(r,\theta,\varphi) &= \frac{E}{1-\nu^2}\left[\varepsilon_{\theta\theta}(r,\theta,\varphi)+\nu\varepsilon_{\varphi\varphi}(r,\theta,\varphi)\right] \\
\sigma_{\varphi\varphi}(r,\theta,\varphi) &= \frac{E}{1-\nu^2}\left[\varepsilon_{\varphi\varphi}(r,\theta,\varphi)+\nu\varepsilon_{\theta\theta}(r,\theta,\varphi)\right] \\
\sigma_{\theta\varphi}(r,\theta,\varphi) &= \sigma_{\varphi\theta}(r,\theta,\varphi) = \frac{E}{1+\nu}\varepsilon_{\theta\varphi}(r,\theta,\varphi)
\end{aligned} \tag{43}$$

Specifying stresses (43) for the relation between strains and displacements according to (12) delivers

$$\begin{aligned}
\sigma_{\theta\theta}(r,\theta,\varphi) &= \frac{E}{r(1-\nu^2)}\Bigg\{\left[u_m+\frac{\partial v_m}{\partial\theta}-(r-R)\left(\frac{\partial^2 u_m}{R\partial\theta^2}-\frac{\partial v_m}{R\partial\theta}\right)\right] \\
&+\nu\frac{1}{\sin\theta}\left[\frac{\partial w_m}{\partial\varphi}-(r-R)\left(\frac{\partial^2 u_m}{R\sin\theta\partial\varphi^2}-\frac{\partial w_m}{R\partial\varphi}\right)\right] \\
&+\nu\cot\theta\left[v_m-(r-R)\left(\frac{\partial u_m}{R\partial\theta}-\frac{v_m}{R}\right)\right]+\nu u_m\Bigg\} \\
\sigma_{\varphi\varphi}(r,\theta,\varphi) &= \frac{E}{r(1-\nu^2)}\Bigg\{\frac{1}{\sin\theta}\left[\frac{\partial w_m}{\partial\varphi}-(r-R)\left(\frac{\partial^2 u_m}{R\sin\theta\partial\varphi^2}-\frac{\partial w_m}{R\partial\varphi}\right)\right] \\
&+\cot\theta\left[v_m-(r-R)\left(\frac{\partial u_m}{R\partial\theta}-\frac{v_m}{R}\right)\right]+u_m \\
&+\nu\left[u_m+\frac{\partial v_m}{\partial\theta}-(r-R)\left(\frac{\partial^2 u_m}{R\partial\theta^2}-\frac{\partial v_m}{R\partial\theta}\right)\right] \\
\sigma_{\theta\varphi}(r,\theta,\varphi) &= \sigma_{\varphi\theta}(r,\theta,\varphi) = \frac{E}{2r(1+\nu)}\Bigg\{\frac{1}{\sin\theta}\left[\frac{\partial v_m}{\partial\varphi}-(r-R)\left(\frac{\partial^2 u_m}{R\partial\theta\partial\varphi}-\frac{\partial v_m}{R\partial\varphi}\right)\right] \\
&+\left[\frac{\partial w_m}{\partial\theta}-(r-R)\left(\frac{\partial^2 u_m}{R\sin\theta\partial\varphi\partial\theta}-\frac{\partial^2 u_m}{R\sin\theta\partial\varphi}\cot\theta-\frac{\partial w_m}{R\partial\theta}\right)\right] \\
&-\cot\theta\left[w_m-(r-R)\left(\frac{\partial u_m}{R\sin\theta\partial\varphi}-\frac{w_m}{R}\right)\right]\Bigg\}
\end{aligned} \tag{44}$$

Since the shear strains $\varepsilon_{r\theta}$ and $\varepsilon_{r\varphi}$ are zero in the context of the chosen kinematic description, it is impossible to determine the shear stresses $\sigma_{r\theta}$ and $\sigma_{r\varphi}$ from Hooke's law, although they intervene in the descriptions of the shear forces q_θ and q_φ, see Eqs. (36) and (37). As a remedy, the relation between shear forces and shear stresses can be determined through equilibrium equations in radial direction, by analogy to shear-rigid beam theory [**12**].

3.4.1 Constitutive equations for membrane forces

• Specifying normal forces $n_{\theta\theta}$ according to (36) for normal stresses $\sigma_{\theta\theta}$ given in (44) delivers

$$
\begin{aligned}
n_{\theta\theta}(\theta,\varphi) &= \int\limits_{R-\frac{h}{2}}^{R+\frac{h}{2}} \sigma_{\theta\theta}(\theta,\varphi)\frac{r}{R}dr \\
&= \int\limits_{R-\frac{h}{2}}^{R+\frac{h}{2}} \frac{E}{1-\nu^2}\Bigg\{\frac{1}{r}\left[u_m + \frac{\partial v_m}{\partial\theta} - (r-R)\left(\frac{\partial^2 u_m}{R\partial\theta^2} - \frac{\partial v_m}{R\partial\theta}\right)\right] \\
&+ \nu\frac{1}{r\sin\theta}\left[\frac{\partial w_m}{\partial\varphi} - (r-R)\left(\frac{\partial^2 u_m}{R\sin\theta\partial\varphi^2} - \frac{\partial w_m}{R\partial\varphi}\right)\right] \\
&+ \frac{\nu}{r}\cot\theta\left[v_m - (r-R)\left(\frac{\partial u_m}{R\partial\theta} - \frac{v_m}{R}\right)\right] + \nu\,\frac{u_m}{r}\Bigg\}\frac{r}{R}dr \\
&= \int\limits_{R-\frac{h}{2}}^{R+\frac{h}{2}} \frac{E}{1-\nu^2}\Bigg\{\left[u_m + \frac{\partial v_m}{\partial\theta} - (r-R)\left(\frac{\partial^2 u_m}{R\partial\theta^2} - \frac{\partial v_m}{R\partial\theta}\right)\right] \\
&+ \frac{\nu}{\sin\theta}\left[\frac{\partial w_m}{\partial\varphi} - (r-R)\left(\frac{\partial^2 u_m}{R\sin\theta\partial\varphi^2} - \frac{\partial w_m}{R\partial\varphi}\right)\right] \\
&+ \nu\,\cot\theta\left[v_m - (r-R)\left(\frac{\partial u_m}{R\partial\theta} - \frac{v_m}{R}\right)\right] + \nu\,u_m\Bigg\}\frac{1}{R}dr
\end{aligned} \tag{45}
$$

Eq. (45) contains the following two integrals over the shell thickness

$$
\int\limits_{R-\frac{h}{2}}^{R+\frac{h}{2}} 1\,dr = h \qquad \int\limits_{R-\frac{h}{2}}^{R+\frac{h}{2}} (r-R)\,dr = 0 \tag{46}
$$

Evaluating normal forces $n_{\theta\theta}$ according to (45) based on (46) delivers

$$
n_{\theta\theta}(\theta,\varphi) = \frac{E}{1-\nu^2}\left[\frac{h}{R}u_m + \frac{h}{R}\frac{\partial v_m}{\partial\theta} + \frac{h}{R}\nu\left(u_m + \frac{1}{\sin\theta}\frac{\partial w_m}{\partial\varphi} + v_m\cot\theta\right)\right] \tag{47}
$$

Factorising the shell thickness h out of the squared brackets in Eq. (47), and defining the extensional stiffness of the shell as

$$
C = \frac{Eh}{1-\nu^2} \tag{48}
$$

allows for re-writing (47) as

$$n_{\theta\theta}(\theta,\varphi) = C\left[\frac{u_m}{R} + \frac{\partial v_m}{R\partial\theta} + \nu\left(\frac{u_m}{R} + \frac{\partial w_m}{R\sin\theta\partial\varphi} + \cot\theta\frac{v_m}{R}\right)\right] \tag{49}$$

• Specifying normal forces $n_{\varphi\varphi}$ according to (37) for normal stresses $\sigma_{\varphi\varphi}$ given in (44) delivers

$$\begin{aligned}
n_{\varphi\varphi}(\theta,\varphi) &= \int\limits_{R-\frac{h}{2}}^{R+\frac{h}{2}} \sigma_{\varphi\varphi}(r,\theta,\varphi)\frac{r}{R}dr \\
&= \int\limits_{R-\frac{h}{2}}^{R+\frac{h}{2}} \frac{E}{1-\nu^2}\Bigg\{\frac{1}{r}\frac{1}{\sin\theta}\left[\frac{\partial w_m}{\partial\varphi} - (r-R)\left(\frac{\partial^2 u_m}{R\sin\theta\partial\varphi^2} - \frac{\partial w_m}{R\partial\varphi}\right)\right] \\
&+ \frac{1}{r}\cot\theta\left[v_m - (r-R)\left(\frac{\partial u_m}{R\partial\theta} - \frac{v_m}{R}\right)\right] + \frac{1}{r}u_m \\
&+ \nu\,\frac{1}{r}\left[u_m + \frac{\partial v_m}{\partial\theta} - (r-R)\left(\frac{\partial^2 u_m}{R\partial\theta^2} - \frac{\partial v_m}{R\partial\theta}\right)\right]\Bigg\}\frac{r}{R}dr \\
&= \int\limits_{R-\frac{h}{2}}^{R+\frac{h}{2}} \frac{E}{1-\nu^2}\Bigg\{\frac{1}{R\sin\theta}\left[\frac{\partial w_m}{\partial\varphi} - (r-R)\left(\frac{\partial^2 u_m}{R\sin\theta\partial\varphi^2} - \frac{\partial w_m}{R\partial\varphi}\right)\right] \\
&+ \frac{\cot\theta}{R}\left[v_m - (r-R)\left(\frac{\partial u_m}{R\partial\theta} - \frac{v_m}{R}\right)\right] + \frac{u_m}{R} \\
&+ \nu\,\frac{1}{R}\left[u_m + \frac{\partial v_m}{\partial\theta} - (r-R)\left(\frac{\partial^2 u_m}{R\partial\theta^2} - \frac{\partial v_m}{R\partial\theta}\right)\right]\Bigg\}\,dr
\end{aligned} \tag{50}$$

Evaluating the integrals in (50) based on (46) delivers

$$n_{\varphi\varphi}(\theta,\varphi) = \frac{E}{1-\nu^2}\left[\frac{h}{R\sin\theta}\frac{\partial w_m}{\partial\varphi} + \frac{h\cot\theta}{R}v_m + \frac{h}{R}u_m + \frac{h}{R}\nu\left(u_m + \frac{\partial v_m}{\partial\theta}\right)\right] \tag{51}$$

Factorising the shell thickness h out of the squared brackets in Eq. (51) and considering the definition of extensional stiffness of the shell according to (48), we get

$$n_{\varphi\varphi}(\theta,\varphi) = C\left[\frac{u_m}{R} + \frac{\partial w_m}{R\sin\theta\partial\varphi} + \frac{\cot\theta}{R}v_m + \nu\left(\frac{u_m}{R} + \frac{\partial v_m}{R\partial\theta}\right)\right] \tag{52}$$

• Specifying the expression for $n_{\theta\varphi}=n_{\varphi\theta}$ according to (35) for normal stresses $\sigma_{\theta\varphi}=\sigma_{\varphi\theta}$ given in (44) delivers

$$
\begin{aligned}
n_{\theta\varphi}(\theta,\varphi) = n_{\varphi\theta}(\theta,\varphi) &= \int\limits_{R-\frac{h}{2}}^{R+\frac{h}{2}} \sigma_{\theta\varphi}\frac{r}{R}dr \\
&= \frac{E}{1+\nu}\frac{1}{2r}\left\{\frac{1}{\sin\theta}\left[\frac{\partial v_m}{\partial\varphi} - (r-R)\left(\frac{\partial^2 u_m}{R\partial\theta\partial\varphi} - \frac{\partial v_m}{R\partial\varphi}\right)\right]\right. \\
&+ \left[\frac{\partial w_m}{\partial\theta} - (r-R)\left(\frac{\partial^2 u_m}{R\sin\theta\partial\varphi\partial\theta} - \frac{\partial u_m}{R\sin\theta\partial\varphi}\cot\theta - \frac{\partial w_m}{R\partial\theta}\right)\right] \\
&- \left.\cot\theta\left[w_m - (r-R)\left(\frac{\partial u_m}{R\sin\theta\partial\varphi} - \frac{w_m}{R}\right)\right]\right\}\frac{r}{R}dr \\
&= \int\limits_{R-\frac{h}{2}}^{R+\frac{h}{2}} \frac{E}{2(1+\nu)}\left\{\frac{1}{\sin\theta}\left[\frac{\partial v_m}{\partial\varphi} - (r-R)\left(\frac{\partial^2 u_m}{R\partial\theta\partial\varphi} - \frac{\partial v_m}{R\partial\varphi}\right)\right]\right. \\
&+ \left[\frac{\partial w_m}{\partial\theta} - (r-R)\left(\frac{\partial^2 u_m}{R\sin\theta\partial\varphi\partial\theta} - \frac{\partial u_m}{R\sin\theta\partial\varphi}\cot\theta - \frac{\partial w_m}{R\partial\theta}\right)\right] \\
&- \left.\cot\theta\left[w_m - (r-R)\left(\frac{\partial u_m}{R\sin\theta\partial\varphi} - \frac{w_m}{R}\right)\right]\right\}\frac{1}{R}dr
\end{aligned} \tag{53}
$$

Evaluating the integrals in Eq. (53) based on (46)

$$
n_{\theta\varphi}(\theta,\varphi) = n_{\varphi\theta}(\theta,\varphi) = \frac{E}{2(1+\nu)}\left(\frac{h}{R\sin\theta}\frac{\partial v_m}{\partial\varphi} + \frac{h}{R}\frac{\partial w_m}{\partial\theta} - \frac{h}{R}\,w_m\cot\theta\right) \tag{54}
$$

Factorising the shell thickness h out of the brackets in Eq. (54) and considering the definition of the extensional stiffness of the shell according to (48) as

$$
\frac{Eh}{2(1+\nu)} = \frac{Eh}{2(1+\nu)}\frac{1-\nu}{1-\nu} = C\,\frac{1-\nu}{2} \tag{55}
$$

allows for re-writing (54) as follows

$$
n_{\theta\varphi}(\theta,\varphi) = n_{\varphi\theta}(\theta,\varphi) = C\,\frac{1-\nu}{2}\left(\frac{\partial v_m}{R\sin\theta\partial\varphi} + \frac{\partial w_m}{R\partial\theta} - \frac{w_m}{R}\cot\theta\right) \tag{56}
$$

3.4.2 Constitutive equations for bending and twisting moments

• Specifying $m_{\theta\theta}$ according to (39) for normal stresses $\sigma_{\theta\theta}$ given in (44) delivers

$$
\begin{aligned}
m_{\theta\theta}(\theta,\varphi) = & \int\limits_{R-\frac{h}{2}}^{R+\frac{h}{2}} \sigma_{\theta\theta}(r-R)\frac{r}{R}dr \\
= & \int\limits_{R-\frac{h}{2}}^{R+\frac{h}{2}} \frac{E}{1-\nu^2}\Bigg\{\frac{1}{r}\left[u_m + \frac{\partial v_m}{\partial\theta} - (r-R)\left(\frac{\partial^2 u_m}{R\partial\theta^2} - \frac{\partial v_m}{R\partial\theta}\right)\right] \\
& + \nu\frac{1}{r\sin\theta}\left[\frac{\partial w_m}{\partial\varphi} - (r-R)\left(\frac{\partial^2 u_m}{R\sin\theta\partial\varphi^2} - \frac{\partial w_m}{R\partial\varphi}\right)\right] \\
& + \frac{\nu}{r}\cot\theta\left[v_m - (r-R)\left(\frac{\partial u_m}{R\partial\theta} - \frac{v_m}{R}\right)\right] + \frac{\nu}{r}u_m\Bigg\}(r-R)\frac{r}{R}dr \\
= & \int\limits_{R-\frac{h}{2}}^{R+\frac{h}{2}} \frac{E}{1-\nu^2}\Bigg\{\frac{1}{R}\left[u_m + \frac{\partial v_m}{\partial\theta} - (r-R)\left(\frac{\partial^2 u_m}{R\partial\theta^2} - \frac{\partial v_m}{R\partial\theta}\right)\right] \\
& + \nu\frac{1}{R\sin\theta}\left[\frac{\partial w_m}{\partial\varphi} - (r-R)\left(\frac{\partial^2 u_m}{R\sin\theta\partial\varphi^2} - \frac{\partial w_m}{R\partial\varphi}\right)\right] \\
& + \nu\frac{\cot\theta}{R}\left[v_m - (r-R)\left(\frac{\partial u_m}{R\partial\theta} - \frac{v_m}{R}\right)\right] + \frac{\nu}{R}u_m\Bigg\}(r-R)\; dr
\end{aligned} \tag{57}
$$

The following integrals show up in Eq. (57)

$$
\int\limits_{R-\frac{h}{2}}^{R+\frac{h}{2}} (r-R)\; dr = 0 \qquad \int\limits_{R-\frac{h}{2}}^{R+\frac{h}{2}} (r-R)^2\; dr = \frac{h^3}{12} \tag{58}
$$

Evaluating the integrals in (57) based on (58) delivers

$$
\begin{aligned}
m_{\theta\theta}(\theta,\theta) = & -\frac{E}{1-\nu^2}\frac{h^3}{12}\Bigg\{\frac{1}{R}\left(\frac{\partial^2 u_m}{R\partial\theta^2} - \frac{\partial v_m}{R\partial\theta}\right) + \frac{\nu}{R\sin\theta}\left(\frac{\partial^2 u_m}{R\sin\theta\partial\varphi^2} - \frac{\partial w_m}{R\partial\varphi}\right) \\
& + \nu\frac{\cot\theta}{R}\left(\frac{\partial u_m}{R\partial\theta} - \frac{v_m}{R}\right)\Bigg\}
\end{aligned} \tag{59}
$$

The term multiplied in (59) with the expression in the curled brackets can be defined as the negative bending stiffness of the shell. The latter reads as

$$K = \frac{Eh^3}{12(1-\nu^2)} \tag{60}$$

Consideration of (60) in (59) results in

$$\begin{aligned} m_{\theta\theta}(\theta,\varphi) =& -K\left\{\frac{1}{R}\left(\frac{\partial^2 u_m}{R\partial\theta^2} - \frac{\partial v_m}{R\partial\theta}\right) + \nu\frac{1}{R\sin\theta}\left(\frac{\partial^2 u_m}{R\sin\theta\partial\varphi^2} - \frac{\partial w_m}{R\partial\varphi}\right)\right. \\ &\left. + \nu\frac{\cot\theta}{R}\left(\frac{\partial u_m}{R\partial\theta} - \frac{v_m}{R}\right)\right\} \end{aligned} \tag{61}$$

- Specifying $m_{\varphi\varphi}$ according to (41) for normal stresses $\sigma_{\varphi\varphi}$ given in (44) delivers

$$\begin{aligned} m_{\varphi\varphi}(\theta,\varphi) =& \int\limits_{R-\frac{h}{2}}^{R+\frac{h}{2}} \sigma_{\varphi\varphi}(r-R)\frac{r}{R}dr \\ =& \int\limits_{R-\frac{h}{2}}^{R+\frac{h}{2}} \frac{E}{1-\nu^2}\left\{\frac{1}{r}\frac{1}{\sin\theta}\left[\frac{\partial w_m}{\partial\varphi} - (r-R)\left(\frac{\partial^2 u_m}{R\sin\theta\partial\varphi^2} - \frac{\partial w_m}{R\partial\varphi}\right)\right]\right. \\ &+ \frac{1}{r}\cot\theta\left[v_m - (r-R)\left(\frac{\partial u_m}{R\partial\theta} - \frac{v_m}{R}\right)\right] + \frac{1}{r}u_m \\ &\left. + \nu\,\frac{1}{r}\left[u_m + \frac{\partial v_m}{\partial\theta} - (r-R)\left(\frac{\partial^2 u_m}{R\partial\theta^2} - \frac{\partial v_m}{R\partial\theta}\right)\right]\right\}(r-R)\frac{r}{R}dr \\ =& \int\limits_{R-\frac{h}{2}}^{R+\frac{h}{2}} \frac{E}{1-\nu^2}\left\{\frac{1}{R\sin\theta}\left[\frac{\partial w_m}{\partial\varphi} - (r-R)\left(\frac{\partial^2 u_m}{R\sin\theta\partial\varphi^2} - \frac{\partial w_m}{R\partial\varphi}\right)\right]\right. \\ &+ \frac{\cot\theta}{R}\left[v_m - (r-R)\left(\frac{\partial u_m}{R\partial\theta} - \frac{v_m}{R}\right)\right] + \frac{u_m}{R} \\ &\left. + \frac{\nu}{R}\left[u_m + \frac{\partial v_m}{\partial\theta} - (r-R)\left(\frac{\partial^2 u_m}{R\partial\theta^2} - \frac{\partial v_m}{R\partial\theta}\right)\right]\right\}(r-R)dr \end{aligned} \tag{62}$$

Evaluating the integrals in (62) based on (58) delivers

$$\begin{aligned} m_{\varphi\varphi}(\theta,\varphi) =& -\frac{E}{1-\nu^2}\frac{h^3}{12}\left\{\frac{1}{R\sin\theta}\left(\frac{\partial^2 u_m}{R\sin\theta\partial\varphi^2} - \frac{\partial w_m}{R\partial\varphi}\right) + \frac{\cot\theta}{R}\left(\frac{\partial u_m}{R\partial\theta} - \frac{v_m}{R}\right)\right. \\ &\left. + \frac{\nu}{R}\left(\frac{\partial^2 u_m}{R\partial\theta^2} - \frac{\partial v_m}{R\partial\theta}\right)\right\} \end{aligned} \tag{63}$$

Introduction of the bending stiffness (60) in (63) delivers

$$
\begin{aligned}
m_{\varphi\varphi}(\theta,\varphi) = & -K\left[\frac{1}{R\sin\theta}\left(\frac{\partial^2 u_m}{R\sin\theta\partial\varphi^2}-\frac{\partial w_m}{R\partial\varphi}\right)+\frac{\cot\theta}{R}\left(\frac{\partial u_m}{R\partial\theta}-\frac{v_m}{R}\right)\right.\\
& \left.+\frac{\nu}{R}\left(\frac{\partial^2 u_m}{R\partial\theta^2}-\frac{\partial v_m}{R\partial\theta}\right)\right]
\end{aligned}
\tag{64}
$$

• Specifying $m_{\theta\varphi} = m_{\varphi\theta}$ according to (41) for normal stresses $\sigma_{\theta\varphi} = \sigma_{\varphi\theta}$ given in (44) delivers

$$
\begin{aligned}
m_{\theta\varphi}(\theta,\varphi) = & m_{\varphi\theta}(\theta,\varphi) = \int\limits_{R-\frac{h}{2}}^{R+\frac{h}{2}} \sigma_{\theta\varphi}(r-R)\frac{r}{R}dr \\
& = \int\limits_{R-\frac{h}{2}}^{R+\frac{h}{2}} \frac{E}{1+\nu}\frac{1}{2r}\left\{\frac{1}{\sin\theta}\left[\frac{\partial v_m}{\partial\varphi}-(r-R)\left(\frac{\partial^2 u_m}{R\partial\theta\partial\varphi}-\frac{\partial v_m}{R\partial\varphi}\right)\right]\right.\\
& +\left[\frac{\partial w_m}{\partial\theta}-(r-R)\left(\frac{\partial^2 u_m}{R\sin\theta\partial\varphi\partial\theta}-\frac{\partial u_m}{R\sin\theta\partial\varphi}\cot\theta-\frac{\partial w_m}{R\partial\theta}\right)\right]\\
& \left.-\cot\theta\left[w_m-(r-R)\left(\frac{\partial u_m}{\sin\theta R\partial\varphi}-\frac{w_m}{R}\right)\right]\right\}(r-R)\frac{r}{R}dr\\
& = \int\limits_{R-\frac{h}{2}}^{R+\frac{h}{2}} \frac{E}{2(1+\nu)}\left\{\frac{1}{\sin\theta}\left[\frac{\partial v_m}{\partial\varphi}-(r-R)\left(\frac{\partial^2 u_m}{R\partial\theta\partial\varphi}-\frac{\partial v_m}{R\partial\varphi}\right)\right]\right.\\
& +\left[\frac{\partial w_m}{\partial\theta}-(r-R)\left(\frac{\partial^2 u_m}{R\sin\theta\partial\varphi\partial\theta}-\frac{\partial u_m}{R\sin\theta\partial\varphi}\cot\theta-\frac{\partial w_m}{R\partial\theta}\right)\right]\\
& \left.-\cot\theta\left[w_m-(r-R)\left(\frac{\partial u_m}{R\sin\theta\partial\varphi}-\frac{w_m}{R}\right)\right]\right\}(r-R)\frac{1}{R}dr
\end{aligned}
\tag{65}
$$

Evaluating the integrals in (65) based on (58) and consideration of the bending stiffness (60) delivers

$$
\begin{aligned}
m_{\theta\varphi}(\theta,\varphi) = & m_{\varphi\theta}(\theta,\varphi) = -K\frac{(1-\nu)}{2R}\left\{\frac{1}{\sin\theta}\left(\frac{\partial^2 u_m}{R\partial\theta\partial\varphi}-\frac{\partial v_m}{R\partial\varphi}\right)\right.\\
& \left.+\left(\frac{\partial^2 u_m}{R\sin\theta\partial\varphi\partial\theta}-\frac{\partial u_m}{R\sin\theta\partial\varphi}\cot\theta-\frac{\partial w_m}{R\partial\theta}\right)-\cot\theta\left(\frac{\partial u_m}{R\sin\theta\partial\varphi}-\frac{w_m}{R}\right)\right\}
\end{aligned}
\tag{66}
$$

3.4.3 Relations between membrane stresses and membrane stress resultants

Introducing the expressions for stress resultants, i.e. the expressions for $n_{\theta\theta}$ according to (49), for $n_{\varphi\varphi}$ from (52), for $n_{\theta\varphi}$ from (56), for $m_{\theta\theta}$ from (61), for $m_{\varphi\varphi}$ from (64), and for $m_{\theta\varphi}$ from (66), into the expressions for stresses (44) results in

$$\begin{aligned}
\sigma_{\theta\theta}(r,\theta,\varphi) &= \frac{n_{\theta\theta}(\theta,\varphi)}{h} + \frac{m_{\theta\theta}(\theta,\varphi)}{h^3/12}(r-R) \\
\sigma_{\varphi\varphi}(r,\theta,\varphi) &= \frac{n_{\varphi\varphi}(\theta,\varphi)}{h} + \frac{m_{\varphi\varphi}(\theta,\varphi)}{h^3/12}(r-R) \\
\sigma_{\theta\varphi}(r,\theta,\varphi) &= \frac{n_{\theta\varphi}(\theta,\varphi)}{h} + \frac{m_{\theta\varphi}(\theta,\varphi)}{h^3/12}(r-R)
\end{aligned} \tag{67}$$

This completes the identification of constitutive equations.

After identifying the virtual power of external forces, our next goal is identifying the virtual power of internal forces, which leads us to identification of equilibrium conditions.

4 Virtual power of the internal forces

The general expression for the virtual power of the internal forces [**2**] reads as

$$\mathcal{L}^{int} = -\int_V \boldsymbol{\sigma} : \dot{\check{\boldsymbol{\varepsilon}}} dV \tag{68}$$

where real stresses $\boldsymbol{\sigma}$ perform power along the virtual strain rates $\dot{\check{\boldsymbol{\varepsilon}}}$. Therefore, we need to define a field of virtual strain rates.

4.1 Choice of virtual strain rates

The virtual strain rates are chosen by analogy to the real strains given in (12)

$$\begin{aligned}
\dot{\check{\varepsilon}}_{\theta\theta} =& \frac{1}{r}\left[\dot{\check{u}}_m + \frac{\partial \dot{\check{v}}_m}{\partial \theta} - (r-R)\left(\frac{\partial^2 \dot{\check{u}}_m}{R\partial\theta^2} - \frac{\partial \dot{\check{v}}_m}{R\partial\theta}\right)\right] \\
\dot{\check{\varepsilon}}_{\varphi\varphi} =& \frac{1}{r}\left\{\dot{\check{u}}_m + \frac{1}{\sin\theta}\left[\frac{\partial \dot{\check{w}}_m}{\partial\varphi} - (r-R)\left(\frac{\partial^2 \dot{\check{u}}_m}{R\sin\theta\partial\varphi^2} - \frac{\partial \dot{\check{w}}_m}{R\partial\varphi}\right)\right]\right. \\
& \left. + \cot\theta\left[\dot{\check{v}}_m - (r-R)\left(\frac{\partial \dot{\check{u}}_m}{R\partial\theta} - \frac{\dot{\check{v}}_m}{R}\right)\right]\right\} \\
\dot{\check{\varepsilon}}_{\theta\varphi} =& \frac{1}{2r}\left\{\frac{1}{\sin\theta}\left[\frac{\partial \dot{\check{v}}_m}{\partial\varphi} - (r-R)\left(\frac{\partial^2 \dot{\check{u}}_m}{R\partial\theta\partial\varphi} - \frac{\partial \dot{\check{v}}_m}{R\partial\varphi}\right)\right]\right. \\
& + \left[\frac{\partial \dot{\check{w}}_m}{\partial\theta} - (r-R)\left(\frac{\partial^2 \dot{\check{u}}_m}{R\sin\theta\partial\varphi\partial\theta} - \frac{\partial \dot{\check{u}}_m}{R\sin\theta\partial\varphi}\cot\theta - \frac{\partial \dot{\check{w}}_m}{R\partial\theta}\right)\right] \\
& \left. - \cot\theta\left[\dot{\check{w}}_m - (r-R)\left(\frac{\partial \dot{\check{u}}_m}{R\sin\theta\partial\varphi} - \frac{\dot{\check{w}}_m}{R}\right)\right]\right\}
\end{aligned} \tag{69}$$

The other virtual strain rates vanish

$$\dot{\check{\varepsilon}}_{rr} = \dot{\check{\varepsilon}}_{r\theta} = \dot{\check{\varepsilon}}_{r\varphi} = 0 \tag{70}$$

4.2 Calculating virtual power of internal forces

The power of internal forces is performed from membrane stresses $\sigma_{\theta\theta}$, $\sigma_{\varphi\varphi}$, and $\sigma_{\theta\varphi}=\sigma_{\varphi\theta}$ along the corresponding *non-vanishing* virtual membrane strain rates $\dot{\check{\varepsilon}}_{\theta\theta}$, $\dot{\check{\varepsilon}}_{\varphi\varphi}$, and $\dot{\check{\varepsilon}}_{\theta\varphi}=\dot{\check{\varepsilon}}_{\varphi\theta}$

$$\mathcal{L}^{int} = -\int\limits_{V} \sigma_{\theta\theta}\, \dot{\check{\varepsilon}}_{\theta\theta}\, dV - \int\limits_{V} \sigma_{\varphi\varphi}\, \dot{\check{\varepsilon}}_{\varphi\varphi}\, dV - 2\int\limits_{V} \sigma_{\theta\varphi}\, \dot{\check{\varepsilon}}_{\theta\varphi}\, dV \tag{71}$$

4.2.1 Power of stresses $\sigma_{\theta\theta}$ along the virtual strain rates $\dot{\check{\varepsilon}}_{\theta\theta}$

Specifying the first term on the right-hand of Eq. (71) for the virtual strain rates $\dot{\check{\varepsilon}}_{\theta\theta}$ given in (69) and making use of stress resultants $n_{\theta\theta}$ and $m_{\theta\theta}$ according to (36) and (40) delivers

$$\begin{aligned}
-\int\limits_{V} \sigma_{\theta\theta}\, \dot{\check{\varepsilon}}_{\theta\theta}\, dV &= -\int\limits_{\varphi_b}^{\varphi_e}\int\limits_{\theta_b}^{\theta_e}\int\limits_{R-\frac{h}{2}}^{R+\frac{h}{2}} \sigma_{\theta\theta}\, \dot{\check{\varepsilon}}_{\theta\theta}\, r^2 dr\, \sin\theta d\varphi\, d\theta \\
&= -\int\limits_{\varphi_b}^{\varphi_e}\int\limits_{\theta_b}^{\theta_e}\int\limits_{R-\frac{h}{2}}^{R+\frac{h}{2}} \sigma_{\theta\theta}\, \frac{1}{r}\left[\dot{\check{u}}_m + \frac{\partial \dot{\check{v}}_m}{\partial\theta} - (r-R)\left(\frac{\partial^2 \dot{\check{u}}_m}{R\partial\theta^2} - \frac{\partial \dot{\check{v}}_m}{R\partial\theta}\right)\right]\frac{r^2}{R^2}\, R^2 dr\, \sin\theta d\varphi\, d\theta \\
&= -\int\limits_{\varphi_b}^{\varphi_e}\int\limits_{\theta_b}^{\theta_e} \left[\frac{n_{\theta\theta}}{R}\left(\dot{\check{u}}_m + \frac{\partial \dot{\check{v}}_m}{\partial\theta}\right) - \frac{m_{\theta\theta}}{R}\left(\frac{\partial^2 \dot{\check{u}}_m}{R\partial\theta^2} - \frac{\partial \dot{\check{v}}_m}{R\partial\theta}\right)\right] R^2\, \sin\theta d\varphi\, d\theta
\end{aligned} \tag{72}$$

In order to identify the equilibrium conditions, it turns out to be beneficial to collect terms multiplying the same virtual velocity quantities. To this end, we decompose terms inside brackets of Eq. (72) and we integrate them by parts, which leads to

$$
\begin{aligned}
-\int\limits_V \sigma_{\theta\theta}\,\dot{\tilde{\varepsilon}}_{\theta\theta}\,dV = &-\int\limits_{\varphi_b}^{\varphi_e}\int\limits_{\theta_b}^{\theta_e}\frac{n_{\theta\theta}}{R}\,\dot{\tilde{u}}_m\,R^2\,\sin\theta d\varphi\,d\theta-\int\limits_{\varphi_b}^{\varphi_e} n_{\theta\theta}\,\dot{\tilde{v}}_m\Big|_{\theta_b}^{\theta_e} R\sin\theta d\varphi\\
&+\int\limits_{\varphi_b}^{\varphi_e}\int\limits_{\theta_b}^{\theta_e}\frac{\partial n_{\theta\theta}}{R\partial\theta}\,\dot{\tilde{v}}_m\,R^2\,\sin\theta d\varphi\,d\theta+\int\limits_{\varphi_b}^{\varphi_e}\int\limits_{\theta_b}^{\theta_e}\frac{n_{\theta\theta}}{R}\,\dot{\tilde{v}}_m\cot\theta\,R^2\,\sin\theta d\varphi\,d\theta\\
&-\int\limits_{\varphi_b}^{\varphi_e}\frac{m_{\theta\theta}}{R}\,\dot{\tilde{v}}_m\Big|_{\theta_b}^{\theta_e} R\sin\theta d\varphi+\int\limits_{\varphi_b}^{\varphi_e}\int\limits_{\theta_b}^{\theta_e}\frac{\partial m_{\theta\theta}}{R^2\partial\theta}\,\dot{\tilde{v}}_m\,R^2\,\sin\theta d\varphi\,d\theta\\
&+\int\limits_{\varphi_b}^{\varphi_e}\int\limits_{\theta_b}^{\theta_e}\frac{m_{\theta\theta}}{R^2}\,\dot{\tilde{v}}_m\cot\theta\,R^2\,\sin\theta d\varphi\,d\theta+\int\limits_{\varphi_b}^{\varphi_e}\frac{m_{\theta\theta}}{R}\,\frac{\partial\dot{\tilde{u}}_m}{\partial\theta}\Big|_{\theta_b}^{\theta_e} R\sin\theta d\varphi\\
&-\int\limits_{\varphi_b}^{\varphi_e}\frac{\partial m_{\theta\theta}}{R\partial\theta}\,\dot{\tilde{u}}_m\Big|_{\theta_b}^{\theta_e} R\sin\theta d\varphi-\int\limits_{\varphi_b}^{\varphi_e}\frac{m_{\theta\theta}}{R}\,\dot{\tilde{u}}_m\Big|_{\theta_b}^{\theta_e}\cot\theta\,R\sin\theta d\varphi\\
&+\int\limits_{\varphi_b}^{\varphi_e}\int\limits_{\theta_b}^{\theta_e}\frac{\partial^2 m_{\theta\theta}}{R^2\partial\theta^2}\,\dot{\tilde{u}}_m\,R^2\,\sin\theta d\varphi\,d\theta+\int\limits_{\varphi_b}^{\varphi_e}\int\limits_{\theta_b}^{\theta_e}\frac{\partial m_{\theta\theta}}{R^2\partial\theta}\,\dot{\tilde{u}}_m\cot\theta\,R^2\,\sin\theta d\varphi\,d\theta\\
&+\int\limits_{\varphi_b}^{\varphi_e}\int\limits_{\theta_b}^{\theta_e}\frac{\partial m_{\theta\theta}}{R^2\partial\theta}\,\dot{\tilde{u}}_m\cot\theta\,R^2\,\sin\theta d\varphi\,d\theta-\int\limits_{\varphi_b}^{\varphi_e}\int\limits_{\theta_b}^{\theta_e}\frac{m_{\theta\theta}}{R^2}\,\dot{\tilde{u}}_m\,R^2\,\sin\theta d\varphi\,d\theta
\end{aligned}
\tag{73}
$$

4.2.2 Power of stresses $\sigma_{\varphi\varphi}$ along the virtual strain rates $\dot{\tilde{\varepsilon}}_{\varphi\varphi}$

Specifying the second term on the right-hand of Eq. (71) for the virtual strain rates $\dot{\tilde{\varepsilon}}_{\varphi\varphi}$ given in (69) delivers

$$
-\int\limits_V \sigma_{\varphi\varphi}\,\dot{\tilde{\varepsilon}}_{\varphi\varphi}\,dV = -\int\limits_{\varphi_b}^{\varphi_e}\int\limits_{\theta_b}^{\theta_e}\int\limits_{R-\frac{h}{2}}^{R+\frac{h}{2}}\sigma_{\varphi\varphi}\,\dot{\tilde{\varepsilon}}_{\varphi\varphi}\,r^2dr\,\sin\theta d\varphi\,d\theta
$$

$$
\begin{aligned}
&=-\int\limits_{\varphi_b}^{\varphi_e}\int\limits_{\theta_b}^{\theta_e}\int\limits_{R-\frac{h}{2}}^{R+\frac{h}{2}}\sigma_{\varphi\varphi}\frac{1}{r}\Bigg\{\dot{\tilde{u}}_m+\frac{1}{\sin\theta}\left[\frac{\partial\dot{\tilde{w}}_m}{\partial\varphi}-(r-R)\left(\frac{\partial^2\dot{\tilde{u}}_m}{R\sin\theta\partial\varphi^2}-\frac{\partial\dot{\tilde{w}}_m}{R\partial\varphi}\right)\right]\\
&+\cot\theta\left[\dot{\tilde{v}}_m-(r-R)\left(\frac{\partial\dot{\tilde{u}}_m}{R\partial\theta}-\frac{\dot{\tilde{v}}_m}{R}\right)\right]\Bigg\}\,\frac{r^2}{R^2}dr\,R^2\,\sin\theta d\varphi\,d\theta
\end{aligned}
$$

Sorting by terms proportional to $\frac{r}{R}$ and to $(r-R)\,\frac{r}{R}$, respectively, and making use of stress resultants $n_{\varphi\varphi}$ and $m_{\varphi\varphi}$ according to (37) and (41) delivers

$$
\begin{aligned}
&-\int\limits_V \sigma_{\varphi\varphi}\,\dot{\varepsilon}_{\varphi\varphi}\,dV = -\int\limits_{\varphi_b}^{\varphi_e}\int\limits_{\theta_b}^{\theta_e}\int\limits_{R-\frac{h}{2}}^{R+\frac{h}{2}} \sigma_{\varphi\varphi}\Bigg\{\left(\frac{1}{\sin\theta}\frac{\partial\dot{w}_m}{\partial\varphi}+\cot\theta\dot{v}_m+\dot{u}_m\right)\\
&-(r-R)\left[\frac{1}{\sin\theta}\left(\frac{\partial^2\dot{u}_m}{R\sin\theta\partial\varphi^2}-\frac{\partial\dot{w}_m}{R\partial\varphi}\right)+\cot\theta\left(\frac{\partial\dot{u}_m}{R\partial\theta}-\frac{\dot{v}_m}{R}\right)\right]\Bigg\}\,\frac{r}{R^2}dr\,R^2\,\sin\theta d\varphi\,d\theta\\
&=-\int\limits_{\varphi_b}^{\varphi_e}\int\limits_{\theta_b}^{\theta_e}\frac{n_{\varphi\varphi}}{R}\left(\frac{1}{\sin\theta}\frac{\partial\dot{w}_m}{\partial\varphi}+\cot\theta\,\dot{v}_m+\dot{u}_m\right)R^2\,\sin\theta d\varphi\,d\theta\\
&+\int\limits_{\varphi_b}^{\varphi_e}\int\limits_{\theta_b}^{\theta_e}\frac{m_{\varphi\varphi}}{R}\left[\frac{1}{\sin\theta}\left(\frac{\partial^2\dot{u}_m}{R\sin\theta\partial\varphi^2}-\frac{\partial\dot{w}_m}{R\partial\varphi}\right)+\cot\theta\left(\frac{\partial\dot{u}_m}{R\partial\theta}-\frac{\dot{v}_m}{R}\right)\right]R^2\,\sin\theta d\varphi\,d\theta
\end{aligned}
\tag{74}
$$

By analogy to the normal stresses $\sigma_{\theta\theta}$, we decompose terms inside the brackets of Eq. (74) and we integrate them by parts, which leads to

$$
\begin{aligned}
-\int\limits_V \sigma_{\varphi\varphi}\,\dot{\varepsilon}_{\varphi\varphi}\,dV = &-\int\limits_{\theta_b}^{\theta_e} n_{\varphi\varphi}\,\dot{w}_m\Big|_{\varphi_b}^{\varphi_e} Rd\theta+\int\limits_{\varphi_b}^{\varphi_e}\int\limits_{\theta_b}^{\theta_e}\frac{\partial n_{\varphi\varphi}}{R\sin\theta\partial\varphi}\,\dot{w}_m\,R^2\,\sin\theta d\varphi\,d\theta\\
&-\int\limits_{\varphi_b}^{\varphi_e}\int\limits_{\theta_b}^{\theta_e}\frac{n_{\varphi\varphi}}{R}\,\dot{v}_m\cot\theta\,R^2\,\sin\theta d\varphi\,d\theta-\int\limits_{\varphi_b}^{\varphi_e}\int\limits_{\theta_b}^{\theta_e}\frac{n_{\varphi\varphi}}{R}\,\dot{u}_m\,R^2\,\sin\theta d\varphi\,d\theta\\
&+\int\limits_{\theta_b}^{\theta_e} m_{\varphi\varphi}\,\frac{\partial\dot{u}_m}{R\sin\theta\partial\varphi}\Big|_{\varphi_b}^{\varphi_e} Rd\theta-\int\limits_{\theta_b}^{\theta_e}\frac{\partial m_{\varphi\varphi}}{R\sin\theta\partial\varphi}\,\dot{u}_m\Big|_{\varphi_b}^{\varphi_e} Rd\theta\\
&+\int\limits_{\varphi_b}^{\varphi_e}\int\limits_{\theta_b}^{\theta_e}\frac{\partial^2 m_{\varphi\varphi}}{R^2\sin^2\theta\partial\varphi^2}\,\dot{u}_m\,R^2\,\sin\theta d\varphi\,d\theta-\int\limits_{\theta_b}^{\theta_e}\frac{m_{\varphi\varphi}}{R}\,\dot{w}_m\Big|_{\varphi_b}^{\varphi_e} Rd\theta\\
&+\int\limits_{\varphi_b}^{\varphi_e}\int\limits_{\theta_b}^{\theta_e}\frac{\partial m_{\varphi\varphi}}{R^2\sin\theta\partial\varphi}\,\dot{w}_m\,R^2\,\sin\theta d\varphi\,d\theta-\int\limits_{\varphi_b}^{\varphi_e}\int\limits_{\theta_b}^{\theta_e}\frac{m_{\varphi\varphi}}{R^2}\,\dot{v}_m\cot\theta\,R^2\,\sin\theta d\varphi\,d\theta\\
&+\int\limits_{\varphi_b}^{\varphi_e}\frac{m_{\varphi\varphi}}{R}\,\dot{u}_m\Big|_{\theta_b}^{\theta_e}\cot\theta\,R\sin\theta d\varphi-\int\limits_{\varphi_b}^{\varphi_e}\int\limits_{\theta_b}^{\theta_e}\frac{\partial m_{\varphi\varphi}}{R^2\partial\theta}\,\dot{u}_m\cot\theta\,R^2\,\sin\theta d\varphi\,d\theta\\
&+\int\limits_{\varphi_b}^{\varphi_e}\int\limits_{\theta_b}^{\theta_e}\frac{m_{\varphi\varphi}}{R^2}\,\dot{u}_m\,R^2\,\sin\theta d\varphi\,d\theta
\end{aligned}
\tag{75}
$$

4.2.3 Power of stresses $\sigma_{\theta\varphi}$ along the virtual strain rates $\dot{\tilde{\varepsilon}}_{\theta\varphi}$

Specifying the third term on the right-hand of (71) for the virtual strain rates $\dot{\tilde{\varepsilon}}_{\theta\varphi}$ given in (69) and making use of stress resultants $n_{\theta\varphi} = n_{\varphi\theta}$ and $m_{\theta\varphi} = m_{\varphi\theta}$ according to (36) and (40) delivers

$$
\begin{aligned}
-2\int\limits_V \sigma_{\theta\varphi}\,\dot{\tilde{\varepsilon}}_{\theta\varphi}\,dV = &-2\int\limits_{\varphi_b}^{\varphi_e}\int\limits_{\theta_b}^{\theta_e}\int\limits_{R-\frac{h}{2}}^{R+\frac{h}{2}} \sigma_{\theta\varphi}\,\dot{\tilde{\varepsilon}}_{\theta\varphi}\,r^2 dr\ \sin\theta d\varphi\, d\theta \\
= &-2\int\limits_{\varphi_b}^{\varphi_e}\int\limits_{\theta_b}^{\theta_e}\int\limits_{R-\frac{h}{2}}^{R+\frac{h}{2}} \sigma_{\theta\varphi}\,\frac{1}{2r}\left\{\frac{1}{\sin\theta}\left[\frac{\partial\dot{\tilde{v}}_m}{\partial\varphi} - (r-R)\left(\frac{\partial^2\dot{\tilde{u}}_m}{R\partial\theta\partial\varphi} - \frac{\partial\dot{\tilde{v}}_m}{R\partial\varphi}\right)\right]\right. \\
&+\left[\frac{\partial\dot{\tilde{w}}_m}{\partial\theta} - (r-R)\left(\frac{\partial^2\dot{\tilde{u}}_m}{R\sin\theta\partial\varphi\partial\theta} - \frac{\partial\dot{\tilde{u}}_m}{R\sin\theta\partial\varphi}\cot\theta - \frac{\partial\dot{\tilde{w}}_m}{R\partial\theta}\right)\right] \\
&\left.-\cot\theta\left[\dot{\tilde{w}}_m - (r-R)\left(\frac{\partial\dot{\tilde{u}}_m}{R\sin\theta\partial\varphi} - \frac{\dot{\tilde{w}}_m}{R}\right)\right]\right\} r^2 dr\ \sin\theta d\varphi\, d\theta \\
= &-\int\limits_{\varphi_b}^{\varphi_e}\int\limits_{\theta_b}^{\theta_e}\int\limits_{R-\frac{h}{2}}^{R+\frac{h}{2}} \sigma_{\theta\varphi}\left(\frac{1}{\sin\theta}\frac{\partial\dot{\tilde{v}}_m}{\partial\varphi} + \frac{\partial\dot{\tilde{w}}_m}{\partial\theta} - \cot\theta\,\dot{\tilde{w}}_m\right)\frac{r}{R^2}R^2\,dr\ \sin\theta d\varphi\, d\theta \\
&+\int\limits_{\varphi_b}^{\varphi_e}\int\limits_{\theta_b}^{\theta_e}\int\limits_{R-\frac{h}{2}}^{R+\frac{h}{2}} \sigma_{\theta\varphi}\left\{\frac{1}{\sin\theta}\left(\frac{\partial^2\dot{\tilde{u}}_m}{R\partial\theta\partial\varphi} - \frac{\partial\dot{\tilde{v}}_m}{R\partial\varphi}\right)\right. \\
&+\left(\frac{\partial^2\dot{\tilde{u}}_m}{R\sin\theta\partial\varphi\partial\theta} - \frac{\partial\dot{\tilde{u}}_m}{R\sin\theta\partial\varphi}\cot\theta - \frac{\partial\dot{\tilde{w}}_m}{R\partial\theta}\right) \\
&\left.-\cot\theta\left(\frac{\partial\dot{\tilde{u}}_m}{R\sin\theta\partial\varphi} - \frac{\dot{\tilde{w}}_m}{R}\right)\right\}(r-R)\,\frac{r}{R^2}R^2\,dr\ \sin\theta d\varphi\, d\theta \\
= &-\int\limits_{\varphi_b}^{\varphi_e}\int\limits_{\theta_b}^{\theta_e} \frac{n_{\theta\varphi}}{R}\left(\frac{1}{\sin\theta}\frac{\partial\dot{\tilde{v}}_m}{\partial\varphi} + \frac{\partial\dot{\tilde{w}}_m}{\partial\theta} - \cot\theta\,\dot{\tilde{w}}_m\right) R^2\ \sin\theta d\varphi\, d\theta \\
&+\int\limits_{\varphi_b}^{\varphi_e}\int\limits_{\theta_b}^{\theta_e} \frac{m_{\theta\varphi}}{R}\left\{\frac{1}{\sin\theta}\left(\frac{\partial^2\dot{\tilde{u}}_m}{R\partial\theta\partial\varphi} - \frac{\partial\dot{\tilde{v}}_m}{R\partial\varphi}\right)\right. \\
&+\left(\frac{\partial^2\dot{\tilde{u}}_m}{R\sin\theta\partial\varphi\partial\theta} - \frac{\partial\dot{\tilde{u}}_m}{R\sin\theta\partial\varphi}\cot\theta - \frac{\partial\dot{\tilde{w}}_m}{R\partial\theta}\right) \\
&\left.-\cot\theta\left(\frac{\partial\dot{\tilde{u}}_m}{R\sin\theta\partial\varphi} - \frac{\dot{\tilde{w}}_m}{R}\right)\right\} R^2\ \sin\theta d\varphi\, d\theta
\end{aligned}
\tag{76}
$$

Partial integration of Eq. (76) results in

$$
\begin{aligned}
-2\int\limits_V \sigma_{\theta\varphi}\,\dot{\tilde{\varepsilon}}_{\theta\varphi}\,dV = &-\int\limits_{\theta_b}^{\theta_e} n_{\theta\varphi}\,\dot{v}_m\Big|_{\varphi_b}^{\varphi_e} Rd\theta + \int\limits_{\varphi_b}^{\varphi_e}\int\limits_{\theta_b}^{\theta_e} \frac{\partial n_{\theta\varphi}}{R\sin\theta\partial\varphi}\,\dot{v}_m\,R^2\sin\theta d\varphi\,d\theta \\
&-\int\limits_{\varphi_b}^{\varphi_e} n_{\theta\varphi}\,\dot{w}_m\Big|_{\theta_b}^{\theta_e} R\sin\theta d\varphi + \int\limits_{\varphi_b}^{\varphi_e}\int\limits_{\theta_b}^{\theta_e} \frac{\partial n_{\theta\varphi}}{R\partial\theta}\,\dot{w}_m\,R^2\,\sin\theta d\varphi\,d\theta \\
&+\int\limits_{\varphi_b}^{\varphi_e}\int\limits_{\theta_b}^{\theta_e} \frac{n_{\theta\varphi}}{R}\,\dot{w}_m\cot\theta\,R^2\,\sin\theta d\varphi\,d\theta \\
&+\int\limits_{\varphi_b}^{\varphi_e}\int\limits_{\theta_b}^{\theta_e} \frac{n_{\theta\varphi}}{R}\,\dot{w}_m\cot\theta\,R^2\,\sin\theta d\varphi\,d\theta + \int\limits_{\varphi_b}^{\varphi_e} m_{\theta\varphi}\,\frac{\partial\dot{u}_m}{R\sin\theta\partial\varphi}\Big|_{\theta_b}^{\theta_e} R\sin\theta d\varphi \\
&-\int\limits_{\theta_b}^{\theta_e} \frac{\partial m_{\theta\varphi}}{R\partial\theta}\,\dot{u}_m\Big|_{\varphi_b}^{\varphi_e} Rd\theta + \int\limits_{\varphi_b}^{\varphi_e}\int\limits_{\theta_b}^{\theta_e} \frac{\partial^2 m_{\theta\varphi}}{R^2\sin\theta\partial\theta\partial\varphi}\,\dot{u}_m\,R^2\,\sin\theta d\varphi\,d\theta \\
&-\int\limits_{\theta_b}^{\theta_e} \frac{m_{\theta\varphi}}{R}\,\dot{v}_m\Big|_{\varphi_b}^{\varphi_e} Rd\theta + \int\limits_{\varphi_b}^{\varphi_e}\int\limits_{\theta_b}^{\theta_e} \frac{\partial m_{\theta\varphi}}{R^2\sin\theta\partial\varphi}\,\dot{v}_m\,R^2\,\sin\theta d\varphi\,d\theta \\
&+\int\limits_{\theta_b}^{\theta_e} \frac{m_{\theta\varphi}}{R}\frac{\partial\dot{u}_m}{\partial\theta}\Big|_{\varphi_b}^{\varphi_e} Rd\theta - \int\limits_{\varphi_b}^{\varphi_e} \frac{\partial m_{\theta\varphi}}{R\sin\theta\partial\varphi}\,\dot{u}_m\Big|_{\theta_b}^{\theta_e} R\sin\theta d\varphi \\
&+\int\limits_{\varphi_b}^{\varphi_e}\int\limits_{\theta_b}^{\theta_e} \frac{\partial^2 m_{\theta\varphi}}{R^2\sin\theta\partial\varphi\partial\theta}\,\dot{u}_m\,R^2\,\sin\theta d\varphi\,d\theta - \int\limits_{\theta_b}^{\theta_e} \frac{m_{\theta\varphi}}{R}\,\dot{u}_m\Big|_{\varphi_b}^{\varphi_e} \cot\theta Rd\theta \\
&+\int\limits_{\varphi_b}^{\varphi_e}\int\limits_{\theta_b}^{\theta_e} \frac{\partial m_{\theta\varphi}}{R^2\sin\theta\partial\varphi}\,\dot{u}_m\,\cot\theta R^2\,\sin\theta d\varphi\,d\theta - \int\limits_{\varphi_b}^{\varphi_e} \frac{m_{\theta\varphi}}{R}\,\dot{w}_m\Big|_{\theta_b}^{\theta_e} R\sin\theta d\varphi \\
&+\int\limits_{\varphi_b}^{\varphi_e}\int\limits_{\theta_b}^{\theta_e} \frac{\partial m_{\theta\varphi}}{R^2\partial\theta}\,\dot{w}_m\,R^2\,\sin\theta d\varphi\,d\theta + \int\limits_{\varphi_b}^{\varphi_e}\int\limits_{\theta_b}^{\theta_e} \frac{m_{\theta\varphi}}{R^2}\,\dot{w}_m\,\cot\theta\,R^2\,\sin\theta d\varphi\,d\theta \\
&-\int\limits_{\theta_b}^{\theta_e} \frac{m_{\theta\varphi}}{R}\,\dot{u}_m\Big|_{\varphi_b}^{\varphi_e} \cot\theta\,Rd\theta + \int\limits_{\varphi_b}^{\varphi_e}\int\limits_{\theta_b}^{\theta_e} \frac{\partial m_{\theta\varphi}}{R^2\sin\theta\partial\varphi}\,\dot{u}_m\,\cot\theta\,R^2\,\sin\theta d\varphi\,d\theta \\
&+\int\limits_{\varphi_b}^{\varphi_e}\int\limits_{\theta_b}^{\theta_e} \frac{m_{\theta\varphi}}{R^2}\,\dot{w}_m\,\cot\theta\,R^2\,\sin\theta d\varphi\,d\theta \qquad (77)
\end{aligned}
$$

5 Applying the principle of virtual power: identification of the equilibrium equations in stress resultants

The description of shell kinematics led to identification of virtual power of internal forces and external forces. Furthermore, we aim to apply the principle of virtual power, which means equating the sum of virtual power of internal forces and external forces to zero (Eq. (2)). Specifying the principle of virtual power (2) for the virtual power of external forces (33) as well as for the virtual power of internal forces (73), (75) and (77), yields

$$
\begin{aligned}
\mathcal{L}^{int} + \mathcal{L}^{ext} = & - \int\limits_{\varphi_b}^{\varphi_e} \int\limits_{\theta_b}^{\theta_e} \frac{n_{\theta\theta}}{R} \, \dot{\hat{u}}_m \, R^2 \, \sin\theta d\varphi \, d\theta - \int\limits_{\varphi_b}^{\varphi_e} n_{\theta\theta} \, \dot{\hat{v}}_m \Big|_{\theta_b}^{\theta_e} R \sin\theta d\varphi \\
& + \int\limits_{\varphi_b}^{\varphi_e} \int\limits_{\theta_b}^{\theta_e} \frac{\partial n_{\theta\theta}}{R\partial\theta} \, \dot{\hat{v}}_m \, R^2 \, \sin\theta d\varphi \, d\theta + \int\limits_{\varphi_b}^{\varphi_e} \int\limits_{\theta_b}^{\theta_e} \frac{n_{\theta\theta}}{R} \, \dot{\hat{v}}_m \cot\theta \, R^2 \, \sin\theta d\varphi \, d\theta \\
& - \int\limits_{\varphi_b}^{\varphi_e} \frac{m_{\theta\theta}}{R} \, \dot{\hat{v}}_m \Big|_{\theta_b}^{\theta_e} R \sin\theta d\varphi + \int\limits_{\varphi_b}^{\varphi_e} \int\limits_{\theta_b}^{\theta_e} \frac{\partial m_{\theta\theta}}{R^2 \partial\theta} \, \dot{\hat{v}}_m \, R^2 \, \sin\theta d\varphi \, d\theta \\
& + \int\limits_{\varphi_b}^{\varphi_e} \int\limits_{\theta_b}^{\theta_e} \frac{m_{\theta\theta}}{R^2} \, \dot{\hat{v}}_m \cot\theta \, R^2 \, \sin\theta d\varphi \, d\theta + \int\limits_{\varphi_b}^{\varphi_e} \frac{m_{\theta\theta}}{R} \, \frac{\partial \dot{\hat{u}}_m}{\partial\theta} \Big|_{\theta_b}^{\theta_e} R \sin\theta d\varphi \\
& - \int\limits_{\varphi_b}^{\varphi_e} \frac{\partial m_{\theta\theta}}{R\partial\theta} \, \dot{\hat{u}}_m \Big|_{\theta_b}^{\theta_e} R \sin\theta d\varphi - \int\limits_{\varphi_b}^{\varphi_e} \frac{m_{\theta\theta}}{R} \, \dot{\hat{u}}_m \Big|_{\theta_b}^{\theta_e} \cot\theta \, R \sin\theta d\varphi \\
& + \int\limits_{\varphi_b}^{\varphi_e} \int\limits_{\theta_b}^{\theta_e} \frac{\partial^2 m_{\theta\theta}}{R^2 \partial\theta^2} \, \dot{\hat{u}}_m \, R^2 \, \sin\theta d\varphi \, d\theta + \int\limits_{\varphi_b}^{\varphi_e} \int\limits_{\theta_b}^{\theta_e} \frac{\partial m_{\theta\theta}}{R^2 \partial\theta} \, \dot{\hat{u}}_m \cot\theta \, R^2 \, \sin\theta d\varphi \, d\theta \\
& + \int\limits_{\varphi_b}^{\varphi_e} \int\limits_{\theta_b}^{\theta_e} \frac{\partial m_{\theta\theta}}{R^2 \partial\theta} \, \dot{\hat{u}}_m \cot\theta \, R^2 \, \sin\theta d\varphi \, d\theta - \int\limits_{\varphi_b}^{\varphi_e} \int\limits_{\theta_b}^{\theta_e} \frac{m_{\theta\theta}}{R^2} \, \dot{\hat{u}}_m \, R^2 \, \sin\theta d\varphi \, d\theta \\
& - \int\limits_{\theta_b}^{\theta_e} n_{\varphi\varphi} \, \dot{\hat{w}}_m \Big|_{\varphi_b}^{\varphi_e} R d\theta + \int\limits_{\varphi_b}^{\varphi_e} \int\limits_{\theta_b}^{\theta_e} \frac{\partial n_{\varphi\varphi}}{R \sin\theta \partial\varphi} \, \dot{\hat{w}}_m \, R^2 \, \sin\theta d\varphi \, d\theta \\
& - \int\limits_{\varphi_b}^{\varphi_e} \int\limits_{\theta_b}^{\theta_e} \frac{n_{\varphi\varphi}}{R} \, \dot{\hat{v}}_m \cot\theta \, R^2 \, \sin\theta d\varphi \, d\theta - \int\limits_{\varphi_b}^{\varphi_e} \int\limits_{\theta_b}^{\theta_e} \frac{n_{\varphi\varphi}}{R} \, \dot{\hat{u}}_m \, R^2 \, \sin\theta d\varphi \, d\theta
\end{aligned}
$$

$$+\int\limits_{\theta_b}^{\theta_e} m_{\varphi\varphi}\ \frac{\partial \dot{\breve{u}}_m}{R\sin\theta\partial\varphi}\bigg|_{\varphi_b}^{\varphi_e} Rd\theta - \int\limits_{\theta_b}^{\theta_e} \frac{\partial m_{\varphi\varphi}}{R\sin\theta\partial\varphi}\ \dot{\breve{u}}_m\bigg|_{\varphi_b}^{\varphi_e} Rd\theta$$

$$+\int\limits_{\varphi_b}^{\varphi_e}\int\limits_{\theta_b}^{\theta_e} \frac{\partial^2 m_{\varphi\varphi}}{R^2\sin^2\theta\partial\varphi^2}\ \dot{\breve{u}}_m\ R^2\ \sin\theta d\varphi\ d\theta - \int\limits_{\theta_b}^{\theta_e} \frac{m_{\varphi\varphi}}{R}\ \dot{\breve{w}}_m\bigg|_{\varphi_b}^{\varphi_e} Rd\theta$$

$$+\int\limits_{\varphi_b}^{\varphi_e}\int\limits_{\theta_b}^{\theta_e} \frac{\partial m_{\varphi\varphi}}{R^2\sin\theta\partial\varphi}\ \dot{\breve{w}}_m\ R^2\ \sin\theta d\varphi\ d\theta - \int\limits_{\varphi_b}^{\varphi_e}\int\limits_{\theta_b}^{\theta_e} \frac{m_{\varphi\varphi}}{R^2}\ \dot{\breve{v}}_m \cot\theta\ R^2\ \sin\theta d\varphi\ d\theta$$

$$+\int\limits_{\varphi_b}^{\varphi_e} \frac{m_{\varphi\varphi}}{R}\ \dot{\breve{u}}_m\bigg|_{\theta_b}^{\theta_e} \cot\theta\ R\sin\theta d\varphi - \int\limits_{\varphi_b}^{\varphi_e}\int\limits_{\theta_b}^{\theta_e} \frac{\partial m_{\varphi\varphi}}{R^2\partial\theta}\ \dot{\breve{u}}_m \cot\theta\ R^2\ \sin\theta d\varphi\ d\theta$$

$$+\int\limits_{\varphi_b}^{\varphi_e}\int\limits_{\theta_b}^{\theta_e} \frac{m_{\varphi\varphi}}{R^2}\ \dot{\breve{u}}_m\ R^2\ \sin\theta d\varphi\ d\theta - \int\limits_{\theta_b}^{\theta_e} n_{\theta\varphi}\ \dot{\breve{v}}_m\bigg|_{\varphi_b}^{\varphi_e} Rd\theta$$

$$+\int\limits_{\varphi_b}^{\varphi_e}\int\limits_{\theta_b}^{\theta_e} \frac{\partial n_{\theta\varphi}}{R\sin\theta\partial\varphi}\ \dot{\breve{v}}_m\ R^2\ \sin\theta d\varphi\ d\theta - \int\limits_{\varphi_b}^{\varphi_e} n_{\theta\varphi}\ \dot{\breve{w}}_m\bigg|_{\theta_b}^{\theta_e} R\sin\theta d\varphi$$

$$+\int\limits_{\varphi_b}^{\varphi_e}\int\limits_{\theta_b}^{\theta_e} \frac{\partial n_{\theta\varphi}}{R\partial\theta}\ \dot{\breve{w}}_m\ R^2\ \sin\theta d\varphi\ d\theta + \int\limits_{\varphi_b}^{\varphi_e}\int\limits_{\theta_b}^{\theta_e} \frac{n_{\theta\varphi}}{R}\ \dot{\breve{w}}_m \cot\theta\ R^2\ \sin\theta d\varphi\ d\theta$$

$$+\int\limits_{\varphi_b}^{\varphi_e}\int\limits_{\theta_b}^{\theta_e} \frac{n_{\theta\varphi}}{R}\ \dot{\breve{w}}_m \cot\theta\ R^2\ \sin\theta d\varphi\ d\theta + \int\limits_{\varphi_b}^{\varphi_e} m_{\theta\varphi}\ \frac{\partial \dot{\breve{u}}_m}{R\sin\theta\partial\varphi}\bigg|_{\theta_b}^{\theta_e} R\sin\theta d\varphi$$

$$-\int\limits_{\theta_b}^{\theta_e} \frac{\partial m_{\theta\varphi}}{R\partial\theta}\ \dot{\breve{u}}_m\bigg|_{\varphi_b}^{\varphi_e} Rd\theta + \int\limits_{\varphi_b}^{\varphi_e}\int\limits_{\theta_b}^{\theta_e} \frac{\partial^2 m_{\theta\varphi}}{R^2\sin\theta\partial\theta\partial\varphi}\ \dot{\breve{u}}_m\ R^2\ \sin\theta d\varphi\ d\theta$$

$$-\int\limits_{\theta_b}^{\theta_e} \frac{m_{\theta\varphi}}{R}\ \dot{\breve{v}}_m\bigg|_{\varphi_b}^{\varphi_e} Rd\theta + \int\limits_{\varphi_b}^{\varphi_e}\int\limits_{\theta_b}^{\theta_e} \frac{\partial m_{\theta\varphi}}{R^2\sin\theta\partial\varphi}\ \dot{\breve{v}}_m\ R^2\ \sin\theta d\varphi\ d\theta$$

$$+\int\limits_{\theta_b}^{\theta_e} \frac{m_{\theta\varphi}}{R}\frac{\partial \dot{\breve{u}}_m}{\partial\theta}\bigg|_{\varphi_b}^{\varphi_e} Rd\theta - \int\limits_{\varphi_b}^{\varphi_e} \frac{\partial m_{\theta\varphi}}{R\sin\theta\partial\varphi}\ \dot{\breve{u}}_m\bigg|_{\theta_b}^{\theta_e} R\sin\theta d\varphi$$

$$+\int\limits_{\varphi_b}^{\varphi_e}\int\limits_{\theta_b}^{\theta_e} \frac{\partial^2 m_{\theta\varphi}}{R^2\sin\theta\partial\varphi\partial\theta}\ \dot{\breve{u}}_m\ R^2\ \sin\theta d\varphi\ d\theta - \int\limits_{\theta_b}^{\theta_e} \frac{m_{\theta\varphi}}{R}\ \dot{\breve{u}}_m\bigg|_{\varphi_b}^{\varphi_e} \cot\theta\ Rd\theta$$

$$+\int\limits_{\varphi_b}^{\varphi_e}\int\limits_{\theta_b}^{\theta_e} \frac{\partial m_{\theta\varphi}}{R^2\sin\theta\partial\varphi}\ \dot{\breve{u}}_m \cot\theta\ R^2\ \sin\theta d\varphi\ d\theta - \int\limits_{\varphi_b}^{\varphi_e} \frac{m_{\theta\varphi}}{R}\ \dot{\breve{w}}_m\bigg|_{\theta_b}^{\theta_e} R\sin\theta d\varphi$$

$$
+\int_{\varphi_b}^{\varphi_e}\int_{\theta_b}^{\theta_e} \frac{\partial m_{\theta\varphi}}{R^2\partial\theta}\ \dot{\check{w}}_m\ R^2\ \sin\theta d\varphi\ d\theta + \int_{\varphi_b}^{\varphi_e}\int_{\theta_b}^{\theta_e} \frac{m_{\theta\varphi}}{R^2}\ \dot{\check{w}}_m \cot\theta\ R^2\ \sin\theta d\varphi\ d\theta
$$

$$
-\int_{\theta_b}^{\theta_e} \frac{m_{\theta\varphi}}{R}\ \dot{\check{u}}_m\Big|_{\varphi_b}^{\varphi_e}\ \cot\theta R d\theta + \int_{\varphi_b}^{\varphi_e}\int_{\theta_b}^{\theta_e} \frac{\partial m_{\theta\varphi}}{R^2\sin\theta\partial\varphi}\ \dot{\check{u}}_m\ \cot\theta\ R^2\ \sin\theta d\varphi\ d\theta
$$

$$
+\int_{\varphi_b}^{\varphi_e}\int_{\theta_b}^{\theta_e} \frac{m_{\theta\varphi}}{R^2}\ \dot{\check{w}}_m \cot\theta\ R^2\ \sin\theta d\varphi\ d\theta
$$

$$
+\int_{\varphi_b}^{\varphi_e}\int_{\theta_b}^{\theta_e} [p_r\ \dot{\check{u}}_m + p_\theta\ \dot{\check{v}}_m + p_\varphi\ \dot{\check{w}}_m]\ R^2\ \sin\theta d\varphi\ d\theta
$$

$$
-\int_{\theta_b}^{\theta_e} k_\varphi\ \dot{\check{u}}_m\Big|_{\varphi_b}^{\varphi_e} R d\theta + \int_{\varphi_b}^{\varphi_e}\int_{\theta_b}^{\theta_e} \frac{\partial k_\varphi}{R\sin\theta\partial\varphi}\ \dot{\check{u}}_m\ R^2\ \sin\theta d\varphi\ d\theta
$$

$$
+\int_{\varphi_b}^{\varphi_e}\int_{\theta_b}^{\theta_e} \frac{k_\varphi}{R}\ \dot{\check{w}}_m\ R^2\ \sin\theta d\varphi\ d\theta
$$

$$
-\int_{\varphi_b}^{\varphi_e} k_\theta\ \dot{\check{u}}_m\Big|_{\theta_b}^{\theta_e} R\sin\theta d\varphi + \int_{\varphi_b}^{\varphi_e}\int_{\theta_b}^{\theta_e} \frac{\partial k_\theta}{R\partial\theta}\ \dot{\check{u}}_m\ R^2\ \sin\theta d\varphi\ d\theta
$$

$$
+\int_{\varphi_b}^{\varphi_e}\int_{\theta_b}^{\theta_e} \frac{k_\theta}{R}\ \dot{\check{u}}_m \cot\theta\ R^2\ \sin\theta d\varphi\ d\theta + \int_{\varphi_b}^{\varphi_e}\int_{\theta_b}^{\theta_e} \frac{k_\theta}{R}\ \dot{\check{v}}_m\ R^2\ \sin\theta d\varphi\ d\theta
$$

$$
+\int_{\theta_b}^{\theta_e} \left[n_{\varphi\varphi}\ \dot{\check{w}}_m + n_{\varphi\theta}\ \dot{\check{v}}_m + q_\varphi\ \dot{\check{u}}_m\right]\Big|_{\varphi_b}^{\varphi_e} R d\theta
$$

$$
-\int_{\theta_b}^{\theta_e} \left[m_{\varphi\varphi}\left(\frac{\partial\dot{\check{u}}_m}{R\sin\theta\partial\varphi} - \frac{\dot{\check{w}}_m}{R}\right) + m_{\varphi\theta}\left(\frac{\partial\dot{\check{u}}_m}{R\partial\theta} - \frac{\dot{\check{v}}_m}{R}\right)\right]\Bigg|_{\varphi_b}^{\varphi_e} R d\theta
$$

$$
+\int_{\varphi_b}^{\varphi_e} \left[n_{\theta\theta}\ \dot{\check{v}}_m + n_{\theta\varphi}\ \dot{\check{w}}_m + q_\theta\ \dot{\check{u}}_m\right]\Big|_{\theta_b}^{\theta_e} R\sin\theta d\varphi
$$

$$
-\int_{\varphi_b}^{\varphi_e} \left[m_{\theta\varphi}\left(\frac{\partial\dot{\check{u}}_m}{R\sin\theta\partial\varphi} - \frac{\dot{\check{w}}_m}{R}\right) + m_{\theta\theta}\left(\frac{\partial\dot{\check{u}}_m}{R\partial\theta} - \frac{\dot{\check{v}}_m}{R}\right)\right]\Bigg|_{\theta_b}^{\theta_e} R\sin\theta d\varphi = 0 \tag{78}
$$

Furthermore, eliminating identical terms with different signs and collecting terms multiplied with the same virtual velocity quantities, while considering the symmetry of membrane forces $n_{\theta\varphi}=n_{\varphi\theta}$ and twisting moments $m_{\theta\varphi}=m_{\varphi\theta}$, Eq. (78) reduces to

$$
\begin{aligned}
&\mathcal{L}^{int}+\mathcal{L}^{ext}= \\
&\int\limits_{\varphi_b}^{\varphi_e}\int\limits_{\theta_b}^{\theta_e}\left[-\frac{n_{\theta\theta}}{R}+\frac{\partial^2 m_{\theta\theta}}{R^2\partial\theta^2}+2\frac{\partial m_{\theta\theta}}{R^2\partial\theta}\cot\theta-\frac{m_{\theta\theta}}{R^2}-\frac{n_{\varphi\varphi}}{R}+\frac{\partial^2 m_{\varphi\varphi}}{R^2\sin^2\theta\partial\varphi^2}\right. \\
&-\frac{\partial m_{\varphi\varphi}}{R^2\partial\theta}\cot\theta+\frac{m_{\varphi\varphi}}{R^2}+\frac{\partial^2 m_{\theta\varphi}}{R^2\sin\theta\partial\theta\partial\varphi}+\frac{\partial^2 m_{\theta\varphi}}{R^2\sin\theta\partial\varphi\partial\theta}+2\frac{\partial m_{\theta\varphi}}{R^2\sin\theta\partial\varphi}\cot\theta \\
&\left.+p_r+\frac{\partial k_{\varphi}}{R\sin\theta\partial\varphi}+\frac{\partial k_{\theta}}{R\partial\theta}+\frac{k_{\theta}}{R}\cot\theta\right]\dot{\check{u}}_m\ R^2\ \sin\theta d\varphi\ d\theta \\
&+\int\limits_{\varphi_b}^{\varphi_e}\int\limits_{\theta_b}^{\theta_e}\left[\frac{\partial n_{\theta\theta}}{R\partial\theta}+\frac{n_{\theta\theta}}{R}\cot\theta+\frac{\partial m_{\theta\theta}}{R^2\partial\theta}+\frac{m_{\theta\theta}}{R^2}\cot\theta-\frac{n_{\varphi\varphi}}{R}\cot\theta-\frac{m_{\varphi\varphi}}{R^2}\cot\theta\right. \\
&\left.+\frac{\partial n_{\theta\varphi}}{R\sin\theta\partial\varphi}+\frac{\partial m_{\theta\varphi}}{R^2\sin\theta\partial\varphi}+p_{\theta}+\frac{k_{\theta}}{R}\right]\dot{\check{v}}_m\ R^2\ \sin\theta d\varphi\ d\theta \\
&+\int\limits_{\varphi_b}^{\varphi_e}\int\limits_{\theta_b}^{\theta_e}\left[\frac{\partial n_{\varphi\varphi}}{R\sin\theta\partial\varphi}+\frac{\partial m_{\varphi\varphi}}{R^2\sin\theta\partial\varphi}+\frac{\partial n_{\theta\varphi}}{R\partial\theta}+2\frac{n_{\theta\varphi}}{R}\cot\theta+\frac{\partial m_{\theta\varphi}}{R^2\partial\theta}\right. \\
&\left.+2\frac{m_{\theta\varphi}}{R^2}\cot\theta+p_{\varphi}+\frac{k_{\varphi}}{R}\right]\dot{\check{w}}_m\ R^2\ \sin\theta d\varphi\ d\theta \\
&+\int\limits_{\theta_b}^{\theta_e}\left[-\frac{\partial m_{\varphi\varphi}}{R\sin\theta\partial\varphi}-\frac{\partial m_{\theta\varphi}}{R\partial\theta}-2\frac{m_{\theta\varphi}}{R}\cot\theta+q_{\varphi}-k_{\varphi}\right]\dot{\check{u}}_m\Bigg|_{\varphi_b}^{\varphi_e}R d\theta \\
&+\int\limits_{\varphi_b}^{\varphi_e}\left[-\frac{m_{\theta\theta}}{R}\cot\theta-\frac{\partial m_{\theta\theta}}{R\partial\theta}+\frac{m_{\varphi\varphi}}{R}\cot\theta-\frac{\partial m_{\theta\varphi}}{R\sin\theta\partial\varphi}+q_{\theta}-k_{\theta}\right]\dot{\check{u}}_m\Bigg|_{\theta_b}^{\theta_e}R\sin\theta d\varphi=0
\end{aligned}
\tag{79}
$$

Finally, from Eq. (79) we can identify the equilibrium equations for thin spherical shells

$$\begin{aligned}
&-\frac{n_{\theta\theta}}{R}+\frac{\partial^2 m_{\theta\theta}}{R^2\partial\theta^2}+2\frac{\partial m_{\theta\theta}}{R^2\partial\theta}\cot\theta-\frac{m_{\theta\theta}}{R^2}-\frac{n_{\varphi\varphi}}{R}+\frac{\partial^2 m_{\varphi\varphi}}{R^2\sin^2\theta\partial\varphi^2}-\frac{\partial m_{\varphi\varphi}}{R^2\partial\theta}\cot\theta\\
&+\frac{m_{\varphi\varphi}}{R^2}+\frac{\partial^2 m_{\theta\varphi}}{R^2\sin\theta\partial\theta\partial\varphi}+\frac{\partial^2 m_{\theta\varphi}}{R^2\sin\theta\partial\varphi\partial\theta}+2\frac{\partial m_{\theta\varphi}}{R^2\sin\theta\partial\varphi}\cot\theta\\
&+p_r+\frac{\partial k_\varphi}{R\sin\theta\partial\varphi}+\frac{\partial k_\theta}{R\partial\theta}+\frac{k_\theta}{R}\cot\theta=0
\end{aligned}\tag{80}$$

$$\begin{aligned}
&\frac{\partial n_{\theta\theta}}{R\partial\theta}+\frac{n_{\theta\theta}}{R}\cot\theta+\frac{\partial m_{\theta\theta}}{R^2\partial\theta}+\frac{m_{\theta\theta}}{R^2}\cot\theta-\frac{n_{\varphi\varphi}}{R}\cot\theta-\frac{m_{\varphi\varphi}}{R^2}\cot\theta\\
&+\frac{\partial n_{\theta\varphi}}{R\sin\theta\partial\varphi}+\frac{\partial m_{\theta\varphi}}{R^2\sin\theta\partial\varphi}+p_\theta+\frac{k_\theta}{R}=0
\end{aligned}\tag{81}$$

$$\begin{aligned}
&\frac{\partial n_{\varphi\varphi}}{R\sin\theta\partial\varphi}+\frac{\partial m_{\varphi\varphi}}{R^2\sin\theta\partial\varphi}+\frac{\partial n_{\theta\varphi}}{R\partial\theta}+2\frac{n_{\theta\varphi}}{R}\cot\theta+\frac{\partial m_{\theta\varphi}}{R^2\partial\theta}\\
&+2\frac{m_{\theta\varphi}}{R^2}\cot\theta+p_\varphi+\frac{k_\varphi}{R}=0
\end{aligned}\tag{82}$$

$$-\frac{\partial m_{\varphi\varphi}}{R\sin\theta\partial\varphi}-\frac{\partial m_{\theta\varphi}}{R\partial\theta}-2\frac{m_{\theta\varphi}}{R}\cot\theta+q_\varphi-k_\varphi=0\tag{83}$$

$$-\frac{m_{\theta\theta}}{R}\cot\theta-\frac{\partial m_{\theta\theta}}{R\partial\theta}+\frac{m_{\varphi\varphi}}{R}\cot\theta-\frac{\partial m_{\theta\varphi}}{R\sin\theta\partial\varphi}+q_\theta-k_\theta=0\tag{84}$$

By further simplification, equilibrium equations take the following form

$$-\frac{n_{\theta\theta}}{R}-\frac{n_{\varphi\varphi}}{R}+\frac{1}{R\sin\theta}\frac{\partial}{\partial\theta}\left(q_{\theta}\sin\theta\right)+\frac{\partial q_{\varphi}}{R\sin\theta\partial\varphi}+p_r=0 \tag{85}$$

$$\frac{1}{R\sin\theta}\frac{\partial}{\partial\theta}\left(n_{\theta\theta}\sin\theta\right)+\frac{\partial n_{\theta\varphi}}{R\sin\theta\partial\varphi}+\frac{q_{\theta}}{R}+p_{\theta}=0 \tag{86}$$

$$\frac{\partial n_{\varphi\varphi}}{R\sin\theta\partial\varphi}+\frac{1}{R\sin^2\theta}\frac{\partial}{\partial\theta}\left(n_{\theta\varphi}\sin^2\theta\right)+\frac{q_{\varphi}}{R}+p_{\varphi}=0 \tag{87}$$

$$q_{\varphi}=\frac{\partial m_{\varphi\varphi}}{R\sin\theta\partial\varphi}+\frac{1}{R\sin^2}\frac{\partial}{\partial\theta}\left(m_{\theta\varphi}\sin^2\theta\right)+k_{\varphi} \tag{88}$$

$$q_{\theta}=\frac{1}{R\sin\theta}\frac{\partial}{\partial\theta}\left(m_{\theta\theta}\sin\theta\right)-\frac{m_{\varphi\varphi}}{R}\cot\theta+\frac{\partial m_{\theta\varphi}}{R\sin\theta\partial\varphi}+k_{\theta} \tag{89}$$

where $n_{\theta\theta}$, $n_{\varphi\varphi}$, and $n_{\theta\varphi}$ represent the membrane forces, $m_{\theta\theta}$ and $m_{\varphi\varphi}$ bending moments, $m_{\theta\varphi}$ twisting moments, as well as $q_{\theta\theta}$ and $q_{\varphi\varphi}$ represent shear forces, k_{θ} and k_{φ} area moments.

The general load-carrying behaviour of a spherical shell can be categorised as follows: load transfer to the supports by means of (i) membrane forces alone (no bending), (ii) moments and transfersal shear forces alone (no membrane forces), and (iii) a mixed state, see [**1**].[4] In the following chapter we will consider in more detail only the membrane theory of spherical shells.

[4]Ventsel, E., Krauthammer, T. and Ventsel, V. Thin plates and shells: Theory, Analysis, and applications. New York: Taylor and Francis (2001) 353-355

6 Membrane theory of spherical shells under rotational symmetric loading

The effectiveness of spherical shells as building structures is related to their ability of carrying loads mainly through membrane forces. Membrane behaviour may occur only after considering particular loading and boundary conditions, which was described by many authors, see among others [**1**, **6**, **7**, **8**].[5]

Membrane behaviour implies that loads are carried exclusively through membrane forces $n_{\theta\theta}$, $n_{\varphi\varphi}$, and $n_{\theta\varphi}$, i.e. bending moments $m_{\theta\theta}$ and $m_{\varphi\varphi}$, twisting moments $m_{\theta\varphi}$, as well as shear forces $q_{\theta\theta}$ and $q_{\varphi\varphi}$ are zero. Specifying (88) and (89) for the vanishing stress resultants delivers the necessary condition that surface moments k_θ and k_φ must be equal to zero: $k_\theta = k_\varphi = 0$. Specifying (85) to (87) for the vanishing stress resultants delivers

$$-\frac{n_{\theta\theta}}{R} - \frac{n_{\varphi\varphi}}{R} + p_r = 0 \tag{90}$$

$$\frac{\partial n_{\theta\theta}}{R\partial\theta} + \frac{n_{\theta\theta}}{R}\cot\theta - \frac{n_{\varphi\varphi}}{R}\cot\theta + \frac{\partial n_{\theta\varphi}}{R\sin\theta\partial\varphi} + p_\theta = 0 \tag{91}$$

$$\frac{\partial n_{\varphi\varphi}}{R\sin\theta\partial\varphi} + \frac{\partial n_{\theta\varphi}}{R\partial\theta} + 2\frac{n_{\theta\varphi}}{R}\cot\theta + p_\varphi = 0 \tag{92}$$

Additional consideration of rotational symmetric loading $p_r = p_r(\theta)$, $p_\theta = p_\theta(\theta)$, and $p_\varphi = 0$, results in a rotational symmetric answer of the shell. This implies that terms depending on φ in Eq. (90) and (91) become zero. Specifying Eq. (92) for these properties implies $n_{\theta\varphi} = 0$, and Eq. (90) and (91) reduce to

$$-\frac{n_{\theta\theta}}{R} - \frac{n_{\varphi\varphi}}{R} + p_r = 0 \tag{93}$$

$$\frac{dn_{\theta\theta}}{Rd\theta} + \frac{n_{\theta\theta}}{R}\cot\theta - \frac{n_{\varphi\varphi}}{R}\cot\theta + p_\theta = 0 \tag{94}$$

Rewriting Eq. (93) as follows

$$\frac{n_{\varphi\varphi}}{R} = p_r - \frac{n_{\theta\theta}}{R} \tag{95}$$

[5] Ventsel, E., Krauthammer, T. and Ventsel, V. Thin plates and shells: Theory, Analysis, and applications. New York: Taylor and Francis (2001) 379-384; VCH. Der Ingenieurbau - Grundwissen. Edition. Wiley-VCH Verlag GmbH (1995), (Kapitel 4, Mang, H.) 113-118; Girkmann, K., Flächentragwerke, 6. Auflage, Springer, Wien (1963) 359-361; Timoshenko, S., Woinowsky-Krieger, S., Timoshenko, S.P. and Woinowsky-Kreiger, S. Theory of plates and shells (McGraw-Hill classic textbook reissue series). 2nd edn. Auckland: McGraw Hill Higher Education (1964) 436-439

and substituting it into Eq. (94), we obtain

$$\frac{dn_{\theta\theta}}{Rd\theta} + 2\frac{n_{\theta\theta}}{R}\cot\theta - p_r\cot\theta + p_\theta = 0 \tag{96}$$

Rewriting the above equation as follows

$$\frac{1}{R\sin^2\theta}\frac{d}{d\theta}\left(n_{\theta\theta}\sin^2\theta\right) = p_r\ \cot\theta - p_\theta \tag{97}$$

and solving the differential equation leads to the sought condition for the membrane behaviour

$$n_{\theta\theta} = \frac{1}{\sin^2\theta}\left[\int_{\theta_0}^{\theta}(p_r\cos\theta - p_\theta\sin\theta)\sin\theta\ Rd\theta + C_1\right] \tag{98}$$

The integration constant C_1 in Eq. (98) is to be identified from the boundary conditions. For $\theta = \theta_0$ the integral vanishes, which leads to the identification of the integration constant C_1 as $C_1 = n_{\theta\theta}\sin^2(\theta_0)$. Subsequently, substituting $n_{\theta\theta}$ in Eq. (95) delivers $n_{\varphi\varphi}$

$$n_{\varphi\varphi} = p_r\ R - \frac{1}{\sin^2\theta}\left[\int_{\theta_0}^{\theta}(p_r\cos\theta - p_\theta\sin\theta)\sin\theta\ Rd\theta + C_1\right] \tag{99}$$

In the following we will consider some of the typical loading conditions, in which loads are carried exclusively through membrane forces. Because of the assumption for "thin" spherical shells, loads are applied on the midsurface of the spherical shell:

a) ***Interior pressure***

Consider a spherical shell subjected to a uniformly distributed radial load (Fig. 11)

$$p_r = const. \quad p_\theta = 0 \tag{100}$$

Substitution of the load definitions p_r and p_θ (Eq. (100)) into Eq. (98), yields

$$n_{\theta\theta} = \frac{p_r}{\sin^2(\theta)}\int_{\theta_0}^{\theta}\cos\theta\sin\theta\ Rd\theta \tag{101}$$

The solution for the above integral reads as

$$n_{\theta\theta} = p_r\frac{R}{2} \tag{102}$$

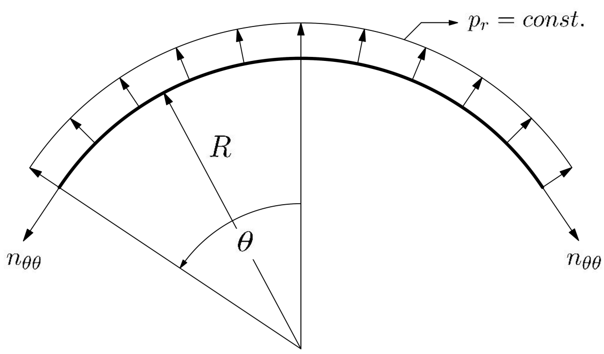

Figure 11: Spherical shell loaded with a constant radial load $p_r = const$

and $n_{\varphi\varphi}$ results from Eq. (99)

$$n_{\varphi\varphi} = p_r \frac{R}{2} \tag{103}$$

As it can be recognised from Eq. (102) and (103), membrane forces $n_{\theta\theta}$ and $n_{\varphi\varphi}$ are not dependent from θ and φ, which means that they are also constant $n_{\theta\theta} = n_{\varphi\varphi} = const.$

b) ***Self-weight***

Consider a spherical shell with a constant thickness h and a constant radius R, as shown in Fig. 12. Self-weight load g can be decomposed into two components, one in radial direction r and another one in polar direction θ

$$p_r = -g\cos\theta, \qquad p_\theta = g\sin\theta \tag{104}$$

Substituting Eq. (104) into Eq. (98) and (99), and considering the integral constant $C_1 = 0$ for $\theta = 0$, delivers the membrane forces $n_{\theta\theta}$

$$n_{\theta\theta} = -\frac{g}{\sin^2\theta}\left[\int_{\theta_0}^{\theta}\left(\cos^2\theta + \sin^2\theta\right)\ R\sin\theta d\theta\right] = -\frac{gR(1-\cos\theta)}{\sin^2\theta} = -\frac{gR}{1+\cos\theta} \tag{105}$$

as well as $n_{\varphi\varphi}$

$$n_{\varphi\varphi} = p_r\, R - n_{\theta\theta} = -gR\left(\cos\theta - \frac{1}{1+\cos\theta}\right) \tag{106}$$

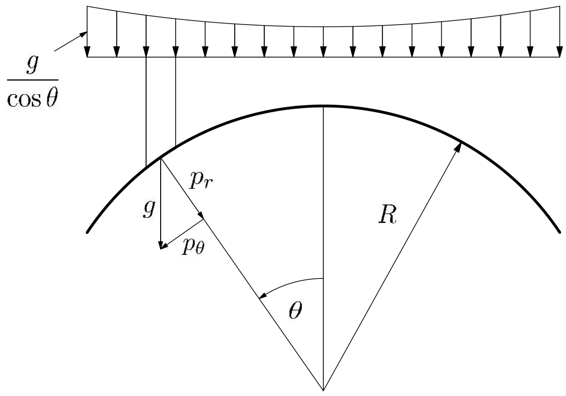

Figure 12: Self-weight g decomposed into a radial component p_r and a polar component p_θ

For $\theta = 0$ Eq. (105) and (106) deliver

$$n_{\theta\theta}(\theta = 0) = n_{\varphi\varphi}(\theta = 0) = -\frac{1}{2}\, gR \tag{107}$$

and for $\theta = \frac{\pi}{2}$

$$-n_{\theta\theta}\left(\theta = \frac{\pi}{2}\right) = n_{\varphi\varphi}\left(\theta = \frac{\pi}{2}\right) = gR \tag{108}$$

As is seen from Eq. (107) and (108), $n_{\theta\theta}$ progresses from its maximum value at the top of the spherical shell $-\frac{1}{2}gR$ to its minimum value $-gR$ for $\theta = \frac{\pi}{2}$. On the other hand, $n_{\varphi\varphi}$ varies from $-\frac{1}{2}gR$ at the top of the spherical shell to gR for $\theta = \frac{\pi}{2}$, which leads to $n_{\varphi\varphi} = 0$ for $\theta = 51,49°$.

c) ***Constant projected load***

Constant projected load q is distributed uniformly over the surface of the spherical shell and can be dissolved into a radial component p_r and a polar component p_θ (see Fig. 13)

$$p_r = -q\cos^2\theta, \qquad p_\theta = q\sin\theta\cos\theta \tag{109}$$

Substituting Eq. (109) into Eqs. (98) and (99) delivers

$$n_{\theta\theta} = -\frac{q}{\sin^2\theta}\int_{\theta_0}^{\theta}(\cos^3\theta + \sin^2\theta\cos\theta)R\sin\theta d\theta = -\frac{1}{2}q\ R \tag{110}$$

and

$$n_{\varphi\varphi} = -q\, R \cos^2\theta + \frac{q\, R}{2} = q\, R \left(\frac{1 - 2\cos^2\theta}{2} \right) = -\frac{1}{2}\, q\, R \cos 2\theta \tag{111}$$

From the Eq. (110) and (111) we recognise that $n_{\theta\theta}$ is a constant and $n_{\varphi\varphi}$ is a function of θ. For $\theta = 0$ Eqs. (110) and (111) deliver

$$n_{\theta\theta}(\theta = 0) = n_{\varphi\varphi}(\theta = 0) = -\frac{1}{2}\, q\, R \tag{112}$$

and for $\theta = \frac{\pi}{2}$

$$-n_{\theta\theta}\left(\theta = \frac{\pi}{2}\right) = n_{\varphi\varphi}\left(\theta = \frac{\pi}{2}\right) = \frac{1}{2}\, q\, R \tag{113}$$

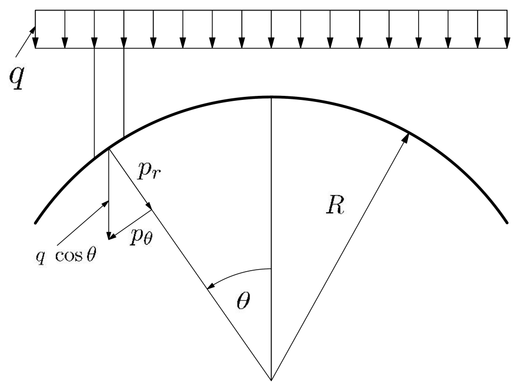

Figure 13: Constant projected load q decomposed into a radial component p_r and a polar component p_θ

According to Eq. (112) and (113), membrane forces $n_{\theta\theta}$ run constantly over the height of the spherical shell $n_{\theta\theta} = -\frac{1}{2}qR$, while $n_{\varphi\varphi}$ progresses from $n_{\varphi\varphi} = -\frac{1}{2}qR$ on top of the spherical shell ($\theta = 0$) to $n_{\varphi\varphi} = \frac{1}{2}qR$ for $\theta = \frac{\pi}{2}$.

In Chapter 6 we described the membrane theory of spherical shells and ended by identifying typical loading conditions, which led to carrying loads exclusively over membrane forces. The latter shows an extraordinary feature of spherical shells, underlining that the geometric shape of a structure plays an important role when it comes to transferring loads to the supports. In comparison to plates, where bending moments are the dominant internal forces, spherical shells carry their loads predominantly by membrane forces. In order to avoid bending at the supports, boundary conditions need to be chosen carefully. Using an edge ring at the supports, as shown in the work of Timoshenko,[6] may reduce bending of the shell.

[6] Timoshenko, S., Woinowsky-Krieger, S., Timoshenko, S.P. and Woinowsky-Kreiger, S. Theory of

7 Summary and conclusions

In classical structural analysis, the equilibrium conditions of a spherical shell are identified by considering the equilibrium of an infinitesimal shell element (see Appendix A). However, these approaches lead very often to a lack of clarity of the underlying assumptions. With the aim of clarification of the underlying assumptions, a first-order theory for thin spherical shells was derived using the principle of virtual power as a tool for derivation. The theory is applicable to thin spherical shell, meaning a small thickness-to-radius ratio and a constant thickness. The aim of this thesis was to derive, from a kinematical description of the shell, the definitions of work-conjugated stress resultants, the corresponding constitutive relations, and the equilibrium conditions.

Instead of analysing the very *general* displacement and deformation possibilities of three-dimensional continua, we focused on the *typical* displacement and deformation possibilities of a spherical shell, which allowed for deriving a two-dimensional theory referring to the midsurface of the structure. In this context, we considered that the shell generator rotations remain small and we disregarded the loading-induced deformation of the shell in thickness direction. In addition, we assumed that the shell generator remains straight and orthogonal to the deformed midsurface and that the displacements of the midsurface are very small as compared with the shell thickness. Constraining the kinematics of the spherical shell like that, resulted in introducing five degrees of freedom for the shell generator: one displacement in radial direction, one in polar direction, and another one in azimuthal direction, as well as two rotations, one around the local base vector in polar direction and another one around the local base vector in azimuthal direction. Finally, the validity of the linearised strain tensor was assumed.

In the course of the mathematical formulation of the virtual power of the external forces, we were able to identify the power conjugated stress resultants, which performed power along the characteristic displacement and rotation possibilities of the shell generator. In order to derive constitutive equations, Hooke's law was used to express membrane stresses as functions of isotropic elasticity constants and of the components of the linearised strain tensor; the latter expressed through the displacement and rotation possibilities of the shell generator. Those expressions for the membrane stresses were inserted into the identified definitions of the bending and twisting moments as well as of the membrane forces, delivering the sought constitutive conditions. They include external stress resultants and internal stress resultants.

As part of identifying the virtual power of internal forces, membrane stresses performed power along the virtual strain rates. The latter were chosen by analogy to the real strains. Finally, summing up the virtual power performed by external forces and by internal forces, and equating the sum to zero, led to the identification of five

plates and shells (McGraw-Hill classic textbook reissue series). 2nd edn. Auckland: McGraw Hill Higher Education (1964) 555-558 equilibrium equations involving the identified stress resultants.

Because of the effectiveness of spherical shells carrying loads mainly through membrane forces, we elaborated the membrane theory in more detail and described some specific loading conditions. Notably, transferring loads through compressive membrane forces includes the risks of buckling and snap through [**9**, **10**, **11**]. However, loss of stability is beyond the scope of this thesis.

A Classical structural analysis interpretation of equilibrium conditions

In classical structural analysis, the equilibrium conditions are identified by considering the equilibrium of an infinitesimal shell element (see Fig. 14), as found in [**14**]

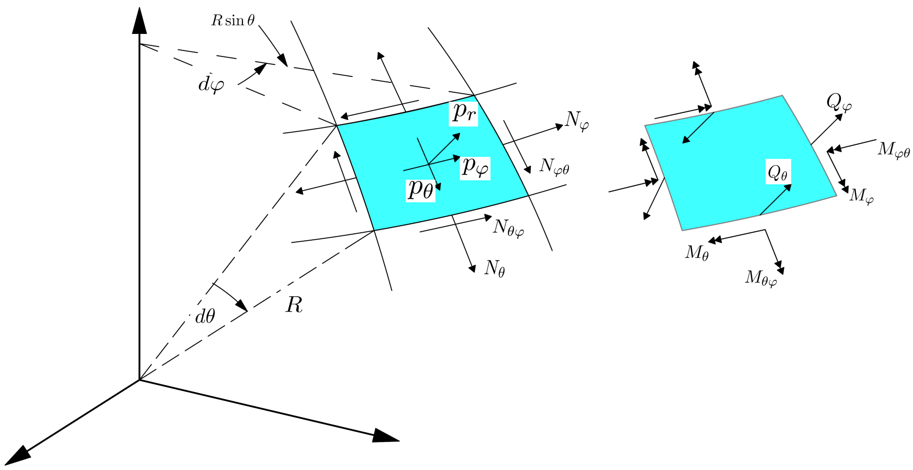

Figure 14: An infinitesimal shell element with: loads in radial p_r, polar p_θ, and azimuthal direction p_φ; membrane forces N_θ, N_φ, and $N_{\theta\varphi} = N_{\varphi\theta}$; bending moments M_θ, M_φ, and twisting moments $M_{\theta\varphi} = M_{\varphi\theta}$; as well as shear forces Q_θ and Q_φ

$$-N_\varphi R\sin\theta - N_\theta R\sin\theta + \frac{\partial}{\partial\theta}\left(Q_\theta R\sin\theta\right) + \frac{\partial Q_\varphi}{\partial\varphi}R = -p_r R^2\sin\theta \tag{114}$$

$$\frac{\partial}{\partial\theta}\left(N_\theta R\sin\theta\right) - N_\varphi R\cos\theta + \frac{\partial N_{\theta\varphi}}{\partial\varphi}R + Q_\theta R\sin\theta = -p_\theta R^2\sin\theta \tag{115}$$

$$\frac{\partial N_{\theta\varphi}}{\partial\theta}R\sin\theta + \frac{\partial N_\varphi}{\partial\varphi}R + N_{\varphi\theta}R\cos\theta + Q_\varphi R\sin\theta = -p_\varphi R^2\sin\theta \tag{116}$$

$$-Q_\varphi R^2\sin\theta + \frac{\partial M_{\theta\varphi}}{\partial\theta}R\sin\theta + \frac{\partial M_\varphi}{\partial\varphi}R + M_{\varphi\theta}R\cos\theta = 0 \tag{117}$$

$$-Q_\theta R^2\sin\theta + \frac{\partial}{\partial\theta}\left(M_\theta R\sin\theta\right) - M_\varphi R\cos\theta + \frac{\partial M_{\varphi\theta}}{\partial\varphi}R = 0 \tag{118}$$

Re-formulating Eq. (117) and (118) as follows

$$Q_\varphi = \frac{\partial M_{\theta\varphi}}{R\partial\theta} + \frac{M_{\theta\varphi}}{R}\cot\theta + \frac{\partial M_\varphi}{R\sin\theta\partial\varphi} + \frac{M_{\theta\varphi}}{R}\cot\theta \tag{119}$$

$$Q_\theta = \frac{\partial M_\theta}{R\partial\theta} + \frac{M_\theta}{R}\cot\theta - \frac{M_\varphi}{R}\cot\theta + \frac{\partial M_{\theta\varphi}}{R\sin\theta\partial\varphi} \tag{120}$$

and decomposing terms inside brackets in Eqs. (114) to (116) under consideration of (119) and (120) results in

$$-\frac{N_\varphi}{R} - \frac{N_\theta}{R} + \frac{\partial^2 M_\theta}{R^2\partial\theta^2} + 2\frac{\partial M_\theta}{R^2\partial\theta}\cot\theta - \frac{M_\theta}{R^2} - \frac{\partial M_\varphi}{R^2\partial\theta}\cot\theta + \frac{M_\varphi}{R^2} + 2\frac{\partial^2 M_{\theta\varphi}}{R^2\sin\theta\partial\varphi\partial\theta}$$

$$+2\frac{\partial M_{\theta\varphi}}{R^2\sin\theta\partial\varphi}\cot\theta + \frac{\partial^2 M_\varphi}{R^2\sin^2\theta\partial\varphi^2} + p_r = 0 \tag{121}$$

$$\frac{\partial N_\theta}{R\partial\theta} + \frac{N_\theta}{R}\cot\theta - \frac{N_\varphi}{R}\cot\theta + \frac{\partial N_{\theta\varphi}}{R\sin\theta\partial\varphi} + \frac{\partial M_\theta}{R^2\partial\theta} + \frac{M_\theta}{R^2}\cot\theta - \frac{M_\varphi}{R^2}\cot\theta$$
$$+\frac{\partial M_{\theta\varphi}}{R^2\sin\theta\partial\varphi} + p_\theta = 0 \tag{122}$$

$$\frac{\partial N_{\theta\varphi}}{R\partial\theta} + 2\frac{N_{\theta\varphi}}{R}\cot\theta + \frac{\partial N_\varphi}{R\sin\theta\partial\varphi} + \frac{\partial M_{\theta\varphi}}{R^2\partial\theta} + 2\frac{M_{\theta\varphi}}{R^2}\cot\theta + \frac{\partial M_\varphi}{R^2\sin\theta\partial\varphi} + p_\varphi = 0 \tag{123}$$

$$-\frac{\partial M_{\theta\varphi}}{R\partial\theta} - \frac{M_{\theta\varphi}}{R}\cot\theta - \frac{\partial M_\varphi}{R\sin\theta\partial\varphi} - \frac{M_{\theta\varphi}}{R}\cot\theta + Q_\varphi = 0 \tag{124}$$

$$-\frac{\partial M_\theta}{R\partial\theta} - \frac{M_\theta}{R}\cot\theta + \frac{M_\varphi}{R}\cot\theta - \frac{\partial M_{\theta\varphi}}{R\sin\theta\partial\varphi} + Q_\theta = 0 \tag{125}$$

Considering only membrane forces N_θ, N_φ, and $N_{\theta\varphi}$, Eq. (124) and (125) vanish, while Eqs. (121) to (123) reduce to

$$-\frac{N_\varphi}{R} - \frac{N_\theta}{R} + p_r = 0 \tag{126}$$

$$\frac{\partial N_\theta}{R\partial\theta} + \frac{N_\theta}{R}\cot\theta - \frac{N_\varphi}{R}\cot\theta + \frac{\partial N_{\theta\varphi}}{R\sin\theta\partial\varphi} + p_\theta = 0 \tag{127}$$

$$\frac{\partial N_{\theta\varphi}}{R\partial\theta} + 2\frac{N_{\theta\varphi}}{R}\cot\theta + \frac{\partial N_\varphi}{R\sin\theta\partial\varphi} + p_\varphi = 0 \tag{128}$$

B Derivation of the first-order theory for slender circular arches, based on the principle of virtual power

Consider a slender circular arch, with constant cross section and an axial radius amounting to R, as shown Fig. 15. By "slender" we mean that the arch length is significantly larger than the cross-sectional dimensions. We use a r,φ,z-cylinder coordinate system. The origin of the r-axis coincides with the center of the arch. Base vectors $\mathbf{e}_r$, $\mathbf{e}_\varphi$ and $\mathbf{e}_z$ form a moving triad accompanying the arch axis. $\mathbf{e}_r$ points in radial direction, $\mathbf{e}_\varphi$ in circumferential direction and $\mathbf{e}_z$ is orthogonal to the plane containing the arch axis (Fig. 15).

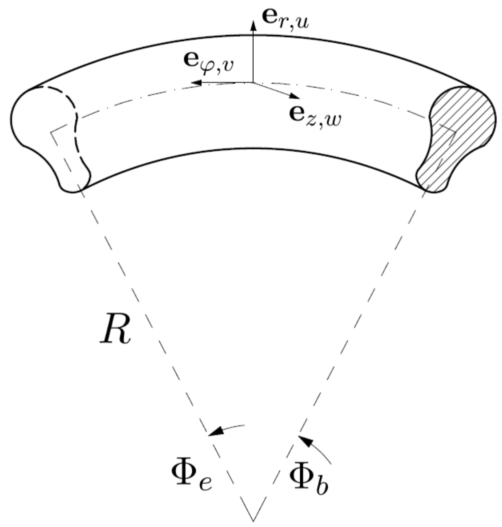

Figure 15: Circular arch with radius R; base vectors $\mathbf{e}_r$, $\mathbf{e}_\varphi$ and $\mathbf{e}_z$; Lagrangian coordinates Φ_b and Φ_e denote cross sections at the arch beginning and the arch end, respectively

Our goal is to use the principle of virtual power, in order to derive a first-order theory for slender circular arches, similar to the derivations found in [**2**]. This principle states that the virtual power performed by the internal forces plus the virtual power performed by the external forces is equal to zero

$$\mathcal{L}^{int} + \mathcal{L}^{ext} = 0 \tag{129}$$

B.1 Kinematic description and kinematic constraints

The displacement field $\mathbf{u}(\mathbf{X})$ is described through the components u, v and w and through cylinder coordinates Γ, Φ and Z referring to the undeformed configuration

$$\mathbf{u}(\mathbf{X}) = u(\Gamma, \Phi, Z)\mathbf{e}_r + v(\Gamma, \Phi, Z)\mathbf{e}_\varphi + w(\Gamma, \Phi, Z)\mathbf{e}_z \tag{130}$$

B.1.1 Plane problem in r,φ-plane

We consider a plane problem in the r,φ-plane. Consequently, all variables $\bullet$ are constant along the Z-direction, i.e.

$$\frac{\partial \bullet}{\partial Z} = 0 \tag{131}$$

In addition, the displacements component in Z-direction is equal to zero

$$w(\Gamma, \Phi, Z) = 0 \tag{132}$$

such that the displacement field (129) takes the following simpler form

$$\mathbf{u}(\mathbf{X}) = u(\Gamma, \Phi)\mathbf{e}_r + v(\Gamma, \Phi)\mathbf{e}_\varphi \tag{133}$$

B.1.2 Small cross sectional rotation and constant cross sectional dimensions

We consider only small cross-sectional rotations and we disregard the loading-induced deformation of the cross-sectional dimensions. Therefore, all points $P(\Gamma, \Phi, Z)$ of a cross section exhibit, in good approximation, identical displacement in radial direction, and this displacement is equal to the one of the arch's axis $S(R, \Phi, 0)$

$$u(\Gamma, \Phi) = u_a(\Phi) \tag{134}$$

where index a stands for the arch axis $\Gamma_a = R$.

B.1.3 Bernoulli hypothesis

We envision that all cross-sections remain, also after deformation of the arch, plane and orthogonal to the deformed arch axis. In other words, the displacement in circumferential direction is linear over the height of the arch. Denoting the circumferential displacement of the arch axis as $v_a(\Phi)$, the circumferential displacement field can be expressed as

$$v(\Gamma, \Phi) = \frac{\Gamma}{R} v_a(\Phi) - (\Gamma - R)\frac{\partial u_a(\Phi)}{R\partial \Phi} \tag{135}$$

The first term on the right-hand side of (135) denotes a rotation around the arch's center O, while the second term denotes a rotation around the midsurface point M, see Fig. 16. In this context, it will turn out to be beneficial to reformulate the first term as

$$\frac{\Gamma}{R}\, v_a(\Phi) = \frac{R + (\Gamma - R)}{R}\, v_a(\Phi) = v_a(\Phi) + (\Gamma - R)\frac{v_a(\Phi)}{R} \tag{136}$$

where $v_a(\Phi)$ denotes a translation in local $\mathbf{e}_\varphi$ direction and the last term in (136) denotes a rotation around the local $\mathbf{e}_z$ vector positioned in M, see Fig. 16. Specifying (135) for (136) delivers

$$v(\Gamma, \Phi, Z) = v_a(\Phi) - (\Gamma - R)\left(\frac{\partial u_a(\Phi)}{R\partial \Phi} - \frac{v_a(\Phi)}{R}\right) \tag{137}$$

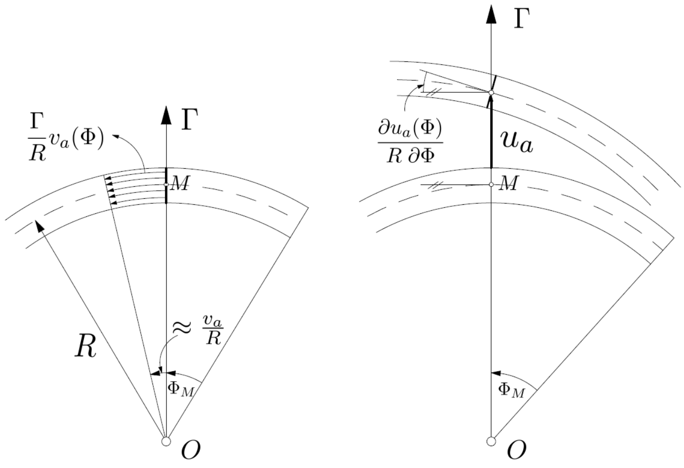

Figure 16: Kinematic constraints in the Γ,Φ-plane

B.1.4 Small displacements compared to cross-section dimensions

We assume that the displacements are very small compared with the cross-sectional dimensions. As a consequence, the deformed configuration, described by position vectors $\mathbf{x}$, will be in the immediate vicinity of the undeformed configuration, described by position vectors $\mathbf{X}$, such that both position vectors are practically the same

$$\mathbf{x} \approx \mathbf{X} \quad \Rightarrow \quad \left\{ \begin{array}{c} r \\ \varphi \\ z \end{array} \right\} \approx \left\{ \begin{array}{c} \Gamma \\ \Phi \\ Z \end{array} \right\} \tag{138}$$

Specifying the general kinematic description (133) for kinematic constraints (134) and (137), as well as for the small-displacements-assumption (138) delivers

$$\mathbf{u}(\mathbf{x}) = \underbrace{u_a(\varphi)}_{u(\varphi)} \mathbf{e}_r + \underbrace{\left[v_a(\varphi) - (r - R) \left(\frac{\partial u_a(\varphi)}{R \partial \varphi} - \frac{v_a(\varphi)}{R} \right) \right]}_{v(\varphi)} \mathbf{e}_\varphi \tag{139}$$

B.1.5 Small displacement derivatives and linear strain tensor

The displacement derivatives are considered to be very small compared to the value 1, such that a linear geometrical description is appropriate. The components of the linear strain tensor in cylinder coordinates read as

$$\varepsilon_{rr} = \frac{\partial u}{\partial r}, \qquad \varepsilon_{\varphi\varphi} = \frac{u}{r} + \frac{1}{r} \frac{\partial v}{\partial \varphi}, \qquad \varepsilon_{zz} = \frac{\partial w}{\partial z}, \tag{140}$$

$$\varepsilon_{r\varphi} = \frac{1}{2}\left(\frac{1}{r}\frac{\partial u}{\partial \varphi} + \frac{\partial v}{\partial \varphi} - \frac{v}{r}\right), \quad \varepsilon_{\varphi z} = \frac{1}{2}\left(\frac{\partial v}{\partial z} + \frac{1}{r}\frac{\partial w}{\partial \varphi}\right), \quad \varepsilon_{zr} = \frac{1}{2}\left(\frac{\partial w}{\partial r} + \frac{\partial u}{\partial z}\right)$$

Specifying (140) for the constrained displacements (139), yields

$$\varepsilon_{\varphi\varphi}(r,\varphi,z) = \frac{u_a(\varphi)}{r} + \frac{1}{r}\frac{\partial v_a(\varphi)}{\partial \varphi} - \frac{r-R}{r}\left(\frac{\partial^2 u_a(\varphi)}{R\partial\varphi^2} - \frac{\partial v_a(\varphi)}{R\partial\varphi}\right) \tag{141}$$

while all other five independent components of the linear strain tensor (140) are equal to zero

$$\varepsilon_{rr} = \varepsilon_{zz} = \varepsilon_{r\varphi} = \varepsilon_{\varphi z} = \varepsilon_{zr} = 0 \tag{142}$$

The terms on the right side of (141) are approximately of the same order of magnitude

$$\left|\frac{u_a}{R}\right| \approx \left|\frac{\partial v_a}{R\partial\varphi}\right| \approx \left|\left(\frac{h}{2R}\right)\frac{\partial^2 u_a}{R\partial\varphi^2}\right| \approx \left|\left(\frac{h}{2R}\right)\frac{\partial v_a}{R\partial\varphi}\right| \tag{143}$$

B.2 Virtual power of external forces

The virtual power of the external forces involves a volume integral and a surface integral

$$\mathcal{L}^{ext} = \int\limits_V \mathbf{f}(r,\varphi,z)\cdot\dot{\hat{\mathbf{u}}}(r,\varphi,z;t)\,dV + \int\limits_{\partial V} \mathbf{T}(\mathbf{n};r,\varphi,z)\cdot\dot{\hat{\mathbf{u}}}(r,\varphi,z;t)\,dA \tag{144}$$

where body forces $\mathbf{f}(r,\varphi,z)$ and surface tractions $\mathbf{T}(\mathbf{n};r,\varphi,z)$ perform power along the virtual velocity field $\dot{\hat{\mathbf{u}}}(r,\varphi,z;t)$. The traction vectors $\mathbf{T}$ are related to the Cauchy stress tensor $\boldsymbol{\sigma}$ and to the outward unit surface normal vector, $\mathbf{n}$, via Cauchy's formula $\mathbf{T}(\mathbf{n}) = \boldsymbol{\sigma}\cdot\mathbf{n}$, reading in component-by-component representation as

$$\mathbf{T}(\mathbf{n};r,\varphi,z) = \sigma_{nr}(r,\varphi,z)\mathbf{e}_r(\varphi) + \sigma_{n\varphi}(r,\varphi,z)\mathbf{e}_\varphi(\varphi) + \sigma_{nz}(r,\varphi,z)\mathbf{e}_z \tag{145}$$

The component representation of the body forces $\mathbf{f}$ reads as

$$\mathbf{f}(r,\varphi,z) = f_r(r,\varphi,z)\mathbf{e}_r(\varphi) + f_\varphi(r,\varphi,z)\mathbf{e}_\varphi(\varphi) + f_z(r,\varphi,z)\mathbf{e}_z \tag{146}$$

The volume integral in (144) will be decomposed into two integrals: one over the cross-sectional area A and another one over the circumferential coordinate φ. Thereby, the infinitesimal volume element dV is decomposed into the infinitesimal line element $rd\varphi$ multiplied with the infinitesimal cross section element dA

$$\int\limits_V \bullet\, dV = \int\limits_{\varphi_b}^{\varphi_e}\int\limits_A \bullet\, r\,dA\,d\varphi \tag{147}$$

The surface integral in (144) will be decomposed into three sub-integrals, one over the cross section at $\varphi = \varphi_b$, one over the cross section at $\varphi = \varphi_e$ and one over the remaining local surface of the arch

$$\int\limits_{\partial V} \bullet \, dA = \int\limits_{A(\varphi_b)} \bullet \, dA + \int\limits_{A(\varphi_e)} \bullet \, dA + \int\limits_{\partial V_l} \bullet \, dA \tag{148}$$

The last integral in (148), will be decomposed into a line integral along the cross-sectional contour C and a line integral in circumferential direction

$$\int\limits_{\partial V} \bullet \, dA = \int\limits_{\varphi_b}^{\varphi_e} \int\limits_{C} \bullet \, r \, ds \, d\varphi \tag{149}$$

Finally, we note that time derivatives in (144) are indicated with a dot

$$\dot{\check{\mathbf{u}}}(r, \varphi, z; t) = \frac{\partial \check{\mathbf{u}}(r, \varphi, z; t)}{\partial t} \tag{150}$$

B.2.1 Constraining virtual velocities

When it comes to the virtual displacement vectors $\check{\mathbf{u}}(\mathbf{x}; t)$, we make the same assumption as introduced for the real displacements, i.e. $\check{w} = 0$ such that

$$\check{\mathbf{u}}(\mathbf{x}; t) = \check{u}(r, \varphi, z; t)\mathbf{e}_r + \check{v}(r, \varphi, z; t)\mathbf{e}_\varphi \tag{151}$$

and

$$\begin{aligned} \check{u}(r, \varphi, z; t) &= \check{u}_a(\varphi; t) \\ \check{v}(r, \varphi, z; t) &= \check{v}_a(\varphi; t) - (r - R)\left(\frac{\partial \check{u}_a(\varphi; t)}{R \partial \varphi} - \frac{\check{v}_a(\varphi; t)}{R}\right) \end{aligned} \tag{152}$$

The virtual velocity field follows from time-derivation of the virtual displacement field as

$$\dot{\check{\mathbf{u}}}(\mathbf{x}; t) = \dot{\check{u}}(r, \varphi, z; t)\mathbf{e}_r + \dot{\check{v}}(r, \varphi, z; t)\mathbf{e}_\varphi \tag{153}$$

with

$$\begin{aligned} \dot{\check{u}}(r, \varphi, z; t) &= \dot{\check{u}}_a(\varphi; t) \\ \dot{\check{v}}(r, \varphi, z; t) &= \dot{\check{v}}_a(\varphi; t) - (r - R)\left(\frac{\partial \dot{\check{u}}_a(\varphi; t)}{R \partial \varphi} - \frac{\dot{\check{v}}_a(\varphi; t)}{R}\right) \end{aligned} \tag{154}$$

B.2.2 Calculating virtual power of the external forces

Specifying the virtual power of the external forces (144) for traction vectors (145), for body force vectors (146), as well as for virtual velocities (153) and (154); also taking into account the volume integral decomposition (147) as well as the surface integral decomposition (148) and (149) delivers

$$
\begin{aligned}
\mathcal{L}^{ext} = & \int_{\varphi_b}^{\varphi_e} \int_A f_r(r,\varphi,z)\, \dot{\check{u}}_a(\varphi;t)\; r\; dA\; d\varphi \\
& + \int_{\varphi_b}^{\varphi_e} \int_A f_\varphi(r,\varphi,z) \left[\dot{\check{v}}_a(\varphi;t) - (r-R) \left(\frac{\partial \dot{\check{u}}_a(\varphi;t)}{R\partial\varphi} - \frac{\dot{\check{v}}_a(\varphi;t)}{R} \right) \right]\; r\; dA\; d\varphi \\
& + \int_{\varphi_b}^{\varphi_e} \int_C T_r(\mathbf{n}_s; r,\varphi,z)\, \dot{\check{u}}_a(\varphi;t)\; r\; ds\; d\varphi \\
& + \int_{\varphi_b}^{\varphi_e} \int_C T_\varphi(\mathbf{n}_s; r,\varphi,z) \left[\dot{\check{v}}_a(\varphi;t) - (r-R) \left(\frac{\partial \dot{\check{u}}_a(\varphi;t)}{R\partial\varphi} - \frac{\dot{\check{v}}_a(\varphi;t)}{R} \right) \right]\; r\; ds\; d\varphi \\
& + \int_{A(\varphi_b)} T_r(\mathbf{n} = -\mathbf{e}_\varphi; r,\varphi_b,z)\, \dot{\check{u}}_a(\varphi_b;t)\; dA \\
& + \int_{A(\varphi_b)} T_\varphi(\mathbf{n} = -\mathbf{e}_\varphi; r,\varphi_b,z) \left[\dot{\check{v}}_a(\varphi_b;t) - (r-R) \left(\frac{\partial \dot{\check{u}}_a(\varphi_b;t)}{R\partial\varphi} - \frac{\dot{\check{v}}_a(\varphi_b;t)}{R} \right) \right]\; dA \\
& + \int_{A(\varphi_e)} T_r(\mathbf{n} = +\mathbf{e}_\varphi; r,\varphi_e,z)\, \dot{\check{u}}_a(\varphi_e;t)\; dA \\
& + \int_{A(\varphi_e)} T_\varphi(\mathbf{n} = +\mathbf{e}_\varphi; r,\varphi_e,z) \left[\dot{\check{v}}_a(\varphi_e;t) - (r-R) \left(\frac{\partial \dot{\check{u}}_a(\varphi_e;t)}{R\partial\varphi} - \frac{\dot{\check{v}}_a(\varphi_e;t)}{R} \right) \right] dA
\end{aligned}
\tag{155}
$$

where $\mathbf{n}_s$ denotes the unit surface normal vector at any point along the contour (Fig. 17).

In the next step, we want to make sure that the differential line element along the arch axis "$Rd\varphi$" shows up in every integral along the circumferential direction. To this end,

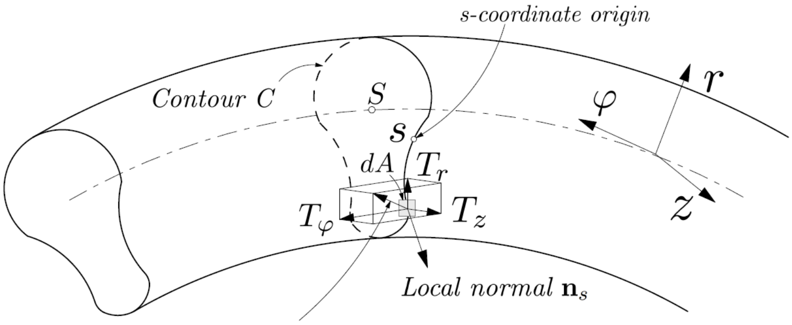

$$\begin{aligned}\mathbf{T}(\mathbf{n}_s) &= T_r\mathbf{e}_r + T_\varphi\mathbf{e}_\varphi + T_z\mathbf{e}_z \\ &= \sigma_{nr}\mathbf{e}_r + \sigma_{n\varphi}\mathbf{e}_\varphi + \sigma_{nz}\mathbf{e}_z\end{aligned}$$

Figure 17: Cross-section contour C, s-coordinate which runs along the contour, traction vectors $\mathbf{T}(\mathbf{n}_s)$, and the unit surface normal vector $\mathbf{n}_s$

we multiply $d\varphi$ by 1 in the form $\frac{R}{R}$, and we represent the resulting expression as $\frac{1}{R}Rd\varphi$

$$\begin{aligned}
\mathcal{L}^{ext} = & \int\limits_{\varphi_b}^{\varphi_e}\int\limits_{A} f_r(r,\varphi,z)\;\dot{\check{u}}_a(\varphi;t)\;\frac{r}{R}\;dA\;Rd\varphi \\
& + \int\limits_{\varphi_b}^{\varphi_e}\int\limits_{A} f_\varphi(r,\varphi,z)\left[\dot{\check{v}}_a(\varphi;t) - (r-R)\left(\frac{\partial\dot{\check{u}}_a(\varphi;t)}{R\partial\varphi} - \frac{\dot{\check{v}}_a(\varphi;t)}{R}\right)\right]\;\frac{r}{R}\;dA\;Rd\varphi \\
& + \int\limits_{\varphi_b}^{\varphi_e}\int\limits_{C} T_r(\mathbf{n}_s;r,\varphi,z)\;\dot{\check{u}}_a(\varphi;t)\;\frac{r}{R}\;ds\;Rd\varphi \\
& + \int\limits_{\varphi_b}^{\varphi_e}\int\limits_{C} T_\varphi(\mathbf{n}_s;r,\varphi,z)\left[\dot{\check{v}}_a(\varphi;t) - (r-R)\left(\frac{\partial\dot{\check{u}}_a(\varphi;t)}{R\partial\varphi} - \frac{\dot{\check{v}}_a(\varphi;t)}{R}\right)\right]\;\frac{r}{R}\;ds\;Rd\varphi \\
& + \int\limits_{A(\varphi_b)} T_r(\mathbf{n}=-\mathbf{e}_\varphi;r,\varphi_b,z)\;\dot{\check{u}}_a(\varphi_b;t)\;dA \\
& + \int\limits_{A(\varphi_b)} T_\varphi(\mathbf{n}=-\mathbf{e}_\varphi;r,\varphi_b,z)\left[\dot{\check{v}}_a(\varphi_b;t) - (r-R)\left(\frac{\partial\dot{\check{u}}_a(\varphi_b;t)}{R\partial\varphi} - \frac{\dot{\check{v}}_a(\varphi_b;t)}{R}\right)\right]\;dA \\
& + \int\limits_{A(\varphi_e)} T_r(\mathbf{n}=+\mathbf{e}_\varphi;r,\varphi_e,z)\;\dot{\check{u}}_a(\varphi_e;t)\;dA \\
& + \int\limits_{A(\varphi_e)} T_\varphi(\mathbf{n}=+\mathbf{e}_\varphi;r,\varphi_e,z)\left[\dot{\check{v}}_a(\varphi_e;t) - (r-R)\left(\frac{\partial\dot{\check{u}}_a(\varphi_e;t)}{R\partial\varphi} - \frac{\dot{\check{v}}_a(\varphi_e;t)}{R}\right)\right]\;dA
\end{aligned} \tag{156}$$

Equation (156) indicates the existence of the stress resultants: line loads $q_r(\varphi)$ and $q_\varphi(\varphi)$; distributed moments $m(\varphi)$; normal forces $N(\varphi)$; shear forces $V(\varphi)$; and bending moments $M(\varphi)$, which perform power along the virtual velocities $\dot{\check{u}}_a$, $\dot{\check{v}}_a$ and virtual rotations $\frac{\partial \dot{\check{u}}_a}{R\partial\varphi} - \frac{\dot{\check{v}}_a}{R}$, respectively, such that (156) can be re-formulated equivalently as

$$\begin{aligned}\mathcal{L}^{ext} = &\int\limits_{\varphi_b}^{\varphi_e} q_r(\varphi)\, \dot{\check{u}}_a(\varphi;t)\, Rd\varphi + \int\limits_{\varphi_b}^{\varphi_e} q_\varphi(\varphi)\, \dot{\check{v}}_a(\varphi;t)\, Rd\varphi \\ &- \int\limits_{\varphi_b}^{\varphi_e} m(\varphi) \left(\frac{\partial \dot{\check{u}}_a(\varphi;t)}{R\partial\varphi} - \frac{\dot{\check{v}}_a(\varphi;t)}{R} \right) Rd\varphi + N(\varphi)\, \dot{\check{v}}_a(\varphi;t) \Big|_{\varphi_b}^{\varphi_e} \\ &- M(\varphi) \left(\frac{\partial \dot{\check{u}}_a(\varphi;t)}{R\partial\varphi} - \frac{\dot{\check{v}}_a(\varphi;t)}{R} \right) \Big|_{\varphi_b}^{\varphi_e} + V(\varphi)\, \dot{\check{u}}_a(\varphi;t) \Big|_{\varphi_b}^{\varphi_e}\end{aligned} \tag{157}$$

Notably, a positive value of $\frac{\partial \dot{\check{u}}_a}{R\partial\varphi} - \frac{\dot{\check{v}}_a}{R}$ indicates a negative rotation around the Z-axis, see Fig. 16, and this explains the minus sign in (157), where positive moments $m(\varphi)$ and $M(\varphi)$ rotate positively around the Z-axis. Integrating (157) by parts, yields

$$\begin{aligned}\mathcal{L}^{ext} = &\int\limits_{\varphi_b}^{\varphi_e} q_r(\varphi)\, \dot{\check{u}}_a(\varphi;t)\, Rd\varphi + \int\limits_{\varphi_b}^{\varphi_e} q_\varphi(\varphi)\, \dot{\check{v}}_a(\varphi;t)\, Rd\varphi \\ &- m(\varphi)\, \dot{\check{u}}_a(\varphi;t) \Big|_{\varphi_b}^{\varphi_e} + \int\limits_{\varphi_b}^{\varphi_e} \frac{\partial m(\varphi)}{R\partial\varphi}\, \dot{\check{u}}_a(\varphi;t)\, Rd\varphi \\ &+ \int\limits_{\varphi_b}^{\varphi_e} \frac{m(\varphi)}{R}\, \dot{\check{v}}_a(\varphi;t)\, Rd\varphi + N(\varphi)\, \dot{\check{v}}_a(\varphi;t) \Big|_{\varphi_b}^{\varphi_e} \\ &- M(\varphi) \left(\frac{\partial \dot{\check{u}}_a(\varphi;t)}{R\partial\varphi} - \frac{\dot{\check{v}}_a(\varphi;t)}{R} \right) \Big|_{\varphi_b}^{\varphi_e} + V(\varphi)\, \dot{\check{u}}_a(\varphi;t) \Big|_{\varphi_b}^{\varphi_e}\end{aligned} \tag{158}$$

We can further simplify (158) by collecting terms multiplied with the same virtual velocity quantities. This yields

$$
\begin{aligned}
\mathcal{L}^{ext} = & \int\limits_{\varphi_b}^{\varphi_e} \left[q_r(\varphi) + \frac{\partial m(\varphi)}{R \partial \varphi} \right] \, \dot{\check{u}}_a(\varphi;t) \, R d\varphi \\
& + \int\limits_{\varphi_b}^{\varphi_e} \left[q_\varphi(\varphi) + \frac{m(\varphi)}{R} \right] \, \dot{\check{v}}_a(\varphi;t) \, R d\varphi \\
& + \left[V(\varphi) - m(\varphi) \right] \, \dot{\check{u}}_a(\varphi;t) \Big|_{\varphi_b}^{\varphi_e} + N(\varphi) \, \dot{\check{v}}_a(\varphi;t) \Big|_{\varphi_b}^{\varphi_e} \\
& - M(\varphi) \left(\frac{\partial \dot{\check{u}}_a(\varphi;t)}{R \partial \varphi} - \frac{\dot{\check{v}}_a(\varphi;t)}{R} \right) \Bigg|_{\varphi_b}^{\varphi_e}
\end{aligned}
\tag{159}
$$

B.2.3 Identifying power-performing stress resultants

The stress resultants $q_\varphi(\varphi)$, $q_r(\varphi)$, $m(\varphi)$, $N(\varphi)$, $V(\varphi)$ and $M(\varphi)$ introduced in (157) are determined by comparing (156) with (157) (see Fig. 18 and Fig. 19). Line loads $q_r(\varphi)$

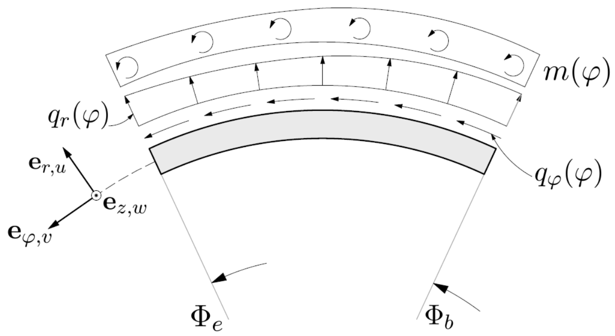

Figure 18: Positive line loads $q_\varphi(\varphi)$ and $q_r(\varphi)$ as well as positive distributed moments $m(\varphi)$ are acting in the direction of the local base vectors $\mathbf{e}_r$, $\mathbf{e}_\varphi$, $\mathbf{e}_z$

and $q_\varphi(\varphi)$ perform virtual power along the virtual velocities $\dot{\check{u}}_a(\varphi;t)$ and $\dot{\check{v}}_a(\varphi;t)$

$$
q_r(\varphi) = \int\limits_A f_r(r,\varphi,z) \, \frac{r}{R} \, dA + \int\limits_C T_r(\mathbf{n}_s; r,\varphi,z) \, \frac{r}{R} \, ds
$$

$$
q_\varphi(\varphi) = \int\limits_A f_\varphi(r,\varphi,z) \, \frac{r}{R} \, dA + \int\limits_C T_\varphi(\mathbf{n}_s; r,\varphi,z) \, \frac{r}{R} \, ds
\tag{160}
$$

Distributed moments $m(\varphi)$ perform virtual power along the virtual rotation rates $\frac{\partial \dot{\tilde{u}}_a}{R\partial\varphi} - \frac{\dot{\tilde{v}}_a}{R}$

$$m(\varphi) = \int\limits_A f_\varphi(r,\varphi,z)(r-R)\,\frac{r}{R}\,dA + \int\limits_C T_\varphi(\mathbf{n}_s;r,\varphi,z)(r-R)\,\frac{r}{R}\,ds \tag{161}$$

Normal forces at the arch beginning $-N(\varphi_b)$ and at the arch end $N(\varphi_e)$, respectively, as well as shear forces at the arch beginning $-V(\varphi_b)$ and arch end $V(\varphi_e)$ perform virtual power along the virtual velocities $\dot{\tilde{v}}_a$ and $\dot{\tilde{u}}_a$

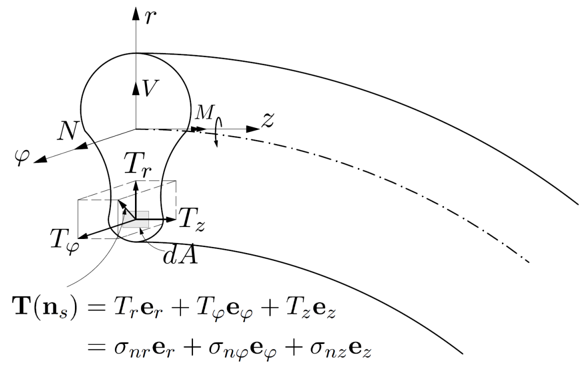

Figure 19: Positive normal force N, positive shear force V as well as positive bending moment M

$$N(\varphi) = \int\limits_A T_\varphi(\mathbf{e}_\varphi;r,\varphi,z)\,dA = \int\limits_A \sigma_{\varphi\varphi}(r,\varphi,z)\,dA$$

$$V(\varphi) = \int\limits_A T_r(\mathbf{e}_\varphi;r,\varphi,z)\,dA = \int\limits_A \sigma_{\varphi r}(r,\varphi,z)\,dA \tag{162}$$

Bending moments at the arch beginning $-M(\varphi_b)$ and at the arch end $M(\varphi_e)$ perform virtual power along the virtual rotation rates $\frac{\partial \dot{\tilde{u}}_a}{R\partial\varphi} - \frac{\dot{\tilde{v}}_a}{R}$

$$M(\varphi) = \int\limits_A T_\varphi(\mathbf{e}_\varphi;r,\varphi,z)(r-R)\,dA = \int\limits_A \sigma_{\varphi\varphi}(r,\varphi,z)(r-R)\,dA \tag{163}$$

B.2.4 Constitutive relations and relations between stresses and stress resultants

Since the real shear strains $\varepsilon_{r\varphi}$ and ε_{rz} are zero in the described constrained kinematic approach, we are not able to apply Hooke's law to determine the shear stresses $\sigma_{r\varphi}$ which are appearing in the shear forces $V(\varphi)$, see (162). As a remedy, the relation between shear forces and shear stresses can be determined through equilibrium equations in radial direction.

Normal stresses $\sigma_{\varphi\varphi}$ appearing in the normal forces $N(\varphi)$ and in the bending moments $M(\varphi)$ can be determined by applying Hooke's law

$$\sigma_{\varphi\varphi}(r,\varphi,z) = E\,\varepsilon_{\varphi\varphi}(r,\varphi,z) \tag{164}$$

Specifying Hooke's law (164) for strain component $\varepsilon_{\varphi\varphi}$ from (141) delivers

$$\sigma_{\varphi\varphi}(r,\varphi,z) = E\left[\frac{u_a(\varphi)}{r} + \frac{1}{r}\frac{\partial v_a(\varphi)}{\partial\varphi} - \frac{r-R}{r}\left(\frac{\partial^2 u_a(\varphi)}{R\partial\varphi^2} - \frac{\partial v_a(\varphi)}{R\partial\varphi}\right)\right] \tag{165}$$

Specifying normal forces (162) and bending moments (163) for normal stresses (165) delivers the following constitutive relations

$$\begin{aligned} N(\varphi) &= \int_A \sigma_{\varphi\varphi}(r,\varphi,z)\,dA \qquad (166)\\ &= \int_{r_b}^{r_e}\int_{z_b}^{z_e} E\left[\frac{u_a(\varphi)}{r} + \frac{1}{r}\frac{\partial v_a(\varphi)}{\partial\varphi} - \frac{r-R}{r}\left(\frac{\partial^2 u_a(\varphi)}{R\partial\varphi^2} - \frac{\partial v_a(\varphi)}{R\partial\varphi}\right)\right] dz\,dr \end{aligned}$$

and

$$\begin{aligned} M(\varphi) &= \int_A \sigma_{\varphi\varphi}(r,\varphi,z)(r-R)\,dA \qquad (167)\\ &= \int_{r_b}^{r_e}\int_{z_b}^{z_e} E\left[\frac{u_a(\varphi)}{r} + \frac{1}{r}\frac{\partial v_a(\varphi)}{\partial\varphi} - \frac{r-R}{r}\left(\frac{\partial^2 u_a(\varphi)}{R\partial\varphi^2} - \frac{\partial v_a(\varphi)}{R\partial\varphi}\right)\right](r-R)\,dz\,dr \end{aligned}$$

Normal force and bending moment expressions (166) and (167), respectively, contain four integrand terms, out of which only two are important. In order to identify these important terms, we consider first a very specific type of cross section; namely a trapezoidal cross section.

B.2.4.1 Isosceles trapezoidal cross-section Here, we consider a cross section in form of an isosceles trapezoid with constant height h, which is significantly smaller then the radius R

$$h \ll R \qquad \Rightarrow \qquad \frac{h}{R} \ll 1 \tag{168}$$

and variable width $b(r)$ (see Fig. 20)

$$b(r) = b_a \frac{r}{R} \tag{169}$$

Therefore, (166) takes the following form

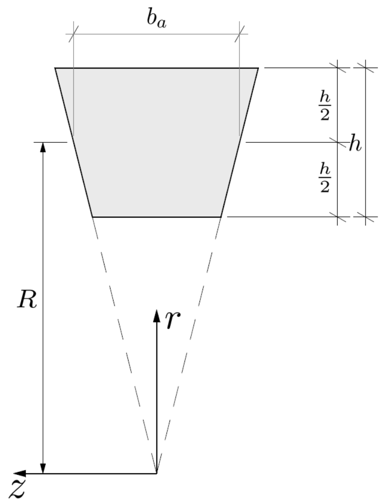

Figure 20: Isosceles trapezoidal cross section: constant height h; cross section width $b(r) = b_a \frac{r}{R}$; arch midsurface radius R

$$\begin{aligned} N(\varphi) &= \int_{R-\frac{h}{2}}^{R+\frac{h}{2}} E \left[\frac{u_a(\varphi)}{r} + \frac{1}{r}\frac{\partial v_a(\varphi)}{\partial \varphi} - \frac{r-R}{r}\left(\frac{\partial^2 u_a(\varphi)}{R\partial \varphi^2} - \frac{\partial v_a(\varphi)}{R\partial \varphi} \right) \right] b_a \frac{r}{R}\, dr \\ &= \frac{E b_a}{R} \int_{R-\frac{h}{2}}^{R+\frac{h}{2}} \left[u_a(\varphi) + \frac{\partial v_a(\varphi)}{\partial \varphi} - (r-R)\left(\frac{\partial^2 u_a(\varphi)}{R\partial \varphi^2} - \frac{\partial v_a(\varphi)}{R\partial \varphi} \right) \right] dr \end{aligned} \tag{170}$$

Eq.(170) contains the following two integrals over the cross section height

$$\int_{R-\frac{h}{2}}^{R+\frac{h}{2}} 1\, dr = h \qquad \int_{R-\frac{h}{2}}^{R+\frac{h}{2}} (r-R)\, dr = 0 \tag{171}$$

Specifying normal forces (170) for (171) delivers

$$N(\varphi) = E\, \frac{b_a h}{R} \left[u_a(\varphi) + \frac{\partial v_a(\varphi)}{\partial \varphi} \right] \tag{172}$$

i.e. the first two terms in the square brackets of (170) have turned out to be the governing terms, while the last two terms vanish.
Specifying bending moments (167) for (169) delivers

$$M(\varphi) = \int\limits_{R-\frac{h}{2}}^{R+\frac{h}{2}} E \left[\frac{u_a(\varphi)}{r} + \frac{1}{r}\frac{\partial v_a(\varphi)}{\partial \varphi} - \frac{r-R}{r}\left(\frac{\partial^2 u_a(\varphi)}{R\partial \varphi^2} - \frac{\partial v_a(\varphi)}{R\partial \varphi} \right) \right] (r-R)\, b_a \frac{r}{R}\, dr$$

$$= \frac{E b_a}{R} \int\limits_{R-\frac{h}{2}}^{R+\frac{h}{2}} \left[u_a(\varphi) + \frac{\partial v_a(\varphi)}{\partial \varphi} - (r-R)\left(\frac{\partial^2 u_a(\varphi)}{R\partial \varphi^2} - \frac{\partial v_a(\varphi)}{R\partial \varphi} \right) \right] (r-R)\, dr \quad (173)$$

Eq. (173) contains the second integral from (171) and the following integral over the cross section height

$$\int\limits_{R-\frac{h}{2}}^{R+\frac{h}{2}} (r-R)^2\, dr = \frac{h^3}{12} \tag{174}$$

Specifying bending moments (173) for (171) and (174), yields

$$M(\varphi) = -E \frac{b_a h^3}{12R} \left[\frac{\partial^2 u_a(\varphi)}{R\partial \varphi^2} - \frac{\partial v_a(\varphi)}{R\partial \varphi} \right] \tag{175}$$

i.e. the last two terms in the square brackets of (173) have turned out to be the governing terms, while the first two terms vanish.
Specifying normal stresses (165) for normal forces (172) and bending moments (175) delivers the relation between stresses and stress resultants

$$\sigma_{\varphi\varphi}(r,\varphi,z) = \left[\frac{N(\varphi)}{b_a h} + \frac{M(\varphi)}{b_a h^3/12}(r-R) \right] \frac{R}{r} \tag{176}$$

Considering a slender arch in the sense of $h \ll R$, the factor "$\frac{R}{r}$" is, in very good approximately, equal to 1. Hence, (176) takes the following form

$$\sigma_{\varphi\varphi}(r,\varphi,z) \approx \left[\frac{N(\varphi)}{b_a h} + \frac{M(\varphi)}{b_a h^3/12}(r-R) \right] \tag{177}$$

B.2.4.2 Rectangular cross section A rectangular cross section with height h and width b (Fig. 21) does not differ significantly from the aforementioned trapezoidal shape (Fig. 20), provided that the arch is slender, see slenderness conditions (168). Therefore, Eqs. (172), (175) to (177) apply in good approximation also for slender arches with rectangular cross section. This is shown next.

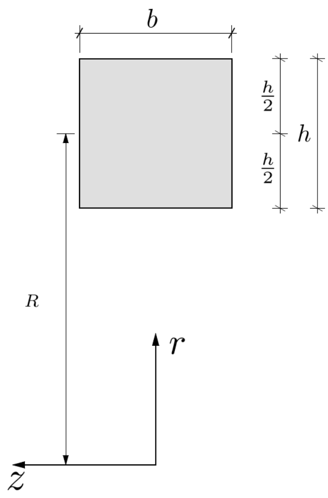

Figure 21: Rectangular cross section with height h and width b

Specifying normal force expression (166) for a constant cross-section width b, yields

$$N(\varphi) = Eb \int\limits_{R-\frac{h}{2}}^{R+\frac{h}{2}} \left[\frac{u_a(\varphi)}{r} + \frac{1}{r}\frac{\partial v_a(\varphi)}{\partial \varphi} - \frac{r-R}{r}\left(\frac{\partial^2 u_a(\varphi)}{R\partial \varphi^2} - \frac{\partial v_a(\varphi)}{R\partial \varphi} \right) \right] \, dr \tag{178}$$

The first integrand in the squared brackets of (178) results in the following expression

$$\begin{aligned} \int\limits_{R-\frac{h}{2}}^{R+\frac{h}{2}} \frac{1}{r}\, dr = \ln(r)\Big|_{R-\frac{h}{2}}^{R+\frac{h}{2}} &= \ln\left(R+\frac{h}{2}\right) - \ln\left(R-\frac{h}{2}\right) = \ln\left(\frac{R+\frac{h}{2}}{R-\frac{h}{2}}\right) \\ &= \frac{h}{R} + \frac{1}{12}\left(\frac{h}{R}\right)^3 + \frac{1}{80}\left(\frac{h}{R}\right)^5 + \ldots \end{aligned} \tag{179}$$

The last expression in (179) represents a Taylor series expansion which is developed around $\frac{h}{R} = 0$. Slenderness property (168) allows us to truncate the Taylor series (179) after the first term

$$\int\limits_{R-\frac{h}{2}}^{R+\frac{h}{2}} \frac{1}{r}\, dr \approx \frac{h}{R} \tag{180}$$

By analogy, the second type of integral showing up in (178) reads as

$$\int\limits_{R-\frac{h}{2}}^{R+\frac{h}{2}} \frac{r-R}{r}\, dr = -\frac{1}{12}\left(\frac{h^3}{R^2}\right) - \frac{1}{80}\left(\frac{h^5}{R^4}\right) - ... \approx -\frac{1}{12}\frac{h^3}{R^2} \tag{181}$$

Specifying (178) for (180) and (181), yields

$$\begin{aligned} N(\varphi) &= \frac{Ebh}{R}\left[u_a(\varphi) + \frac{\partial v_a(\varphi)}{\partial\varphi}\right] + \frac{Ebh^3}{12R^2}\left[\frac{\partial^2 u_a(\varphi)}{R\partial\varphi^2} - \frac{\partial v_a(\varphi)}{R\partial\varphi}\right] \\ &= Ebh\left\{\frac{u_a(\varphi)}{R} + \frac{\partial v_a(\varphi)}{R\partial\varphi} + \frac{1}{6}\left(\frac{h}{R}\right)\left[\left(\frac{h}{2R}\right)\frac{\partial^2 u_a(\varphi)}{R\partial\varphi^2} - \left(\frac{h}{2R}\right)\frac{\partial v_a(\varphi)}{R\partial\varphi}\right]\right\} \end{aligned} \tag{182}$$

Comparing terms inside the squared brackets in (182) with (16) we can conclude that the first two terms are by one order of magnitude larger than the last two terms

$$\underbrace{\left|\frac{u_a(\varphi)}{R}\right| \approx \left|\frac{\partial v_a(\varphi)}{R\partial\varphi}\right|}_{\text{1st order terms}} \gg \underbrace{\left|\frac{1}{6}\left(\frac{h}{R}\right)\left(\frac{h}{2R}\right)\frac{\partial^2 u_a(\varphi)}{R\partial\varphi^2}\right| \approx \left|\frac{1}{6}\left(\frac{h}{R}\right)\left(\frac{h}{2R}\right)\frac{\partial v_a(\varphi)}{R\partial\varphi}\right|}_{\text{2nd order terms}} \tag{183}$$

such that (182) can be approximated as

$$N(\varphi) \approx EA\left(\frac{u_a(\varphi)}{R} + \frac{\partial v_a(\varphi)}{R\partial\varphi}\right) \qquad \text{with} \qquad A = b\,h \tag{184}$$

Specifying bending moments (167) for a constant cross-section width, yields

$$M(\varphi) = Eb\int\limits_{R-\frac{h}{2}}^{R+\frac{h}{2}}\left[\frac{u_a(\varphi)}{r} + \frac{1}{r}\frac{\partial v_a(\varphi)}{\partial\varphi} - \frac{r-R}{r}\left(\frac{\partial^2 u_a(\varphi)}{R\partial\varphi^2} - \frac{\partial v_a(\varphi)}{R\partial\varphi}\right)\right](r-R)\, dr \tag{185}$$

Two integrals show up in (185)

$$\int\limits_{R-\frac{h}{2}}^{R+\frac{h}{2}} \frac{r-R}{r}\, dr = -R\left[\frac{1}{12}\left(\frac{h}{R}\right)^3 + \frac{1}{8}\left(\frac{h}{R}^5\right) + ...\right] \approx -\frac{1}{12}\frac{h^3}{R^2} \tag{186}$$

$$\int\limits_{R-\frac{h}{2}}^{R+\frac{h}{2}} \frac{(r-R)^2}{r}\, dr = -Rh + R^2\,\ln\left(\frac{R+\frac{h}{2}}{R-\frac{h}{2}}\right) = R^2\left[\frac{1}{12}\left(\frac{h}{R}\right)^3 + \frac{1}{80}\left(\frac{h}{R}\right)^5 + ...\right] \approx \frac{1}{12}\frac{h^3}{R}$$

Specifying bending moments (185) for (186) delivers

$$\begin{aligned} M(\varphi) &= -\frac{Ebh^3}{12R^2}\left[u_a(\varphi) + \frac{\partial u_a(\varphi)}{\partial\varphi}\right] - \frac{Ebh^3}{R}\left[\frac{\partial^2 u_a(\varphi)}{R\partial\varphi^2} - \frac{\partial v_a(\varphi)}{R\partial\varphi}\right] \\ &= -\frac{Ebh^3}{12R}\left[\frac{u_a(\varphi)}{R} + \frac{\partial u_a(\varphi)}{R\partial\varphi} + \frac{2R}{h}\left(\frac{h}{2R}\right)\frac{\partial^2 u_a(\varphi)}{R\partial\varphi^2} - \frac{2R}{h}\left(\frac{h}{2R}\right)\frac{\partial v_a(\varphi)}{R\partial\varphi}\right] \end{aligned} \tag{187}$$

Comparing terms inside squared brackets in (187) with (143) we can conclude that the last two terms are by one order of magnitude larger than the first two terms

$$\underbrace{\left|\frac{u_a(\varphi)}{R}\right| \approx \left|\frac{\partial v_a(\varphi)}{R\partial\varphi}\right|}_{\text{2nd order terms}} \ll \underbrace{\left|\frac{2R}{h}\left(\frac{h}{2R}\right)\frac{\partial^2 u_a(\varphi)}{R\partial\varphi^2}\right| \approx \left|\frac{2R}{h}\left(\frac{h}{2R}\right)\frac{\partial v_a(\varphi)}{R\partial\varphi}\right|}_{\text{1st order terms}} \tag{188}$$

such that (187) can be approximated as

$$M(\varphi) \approx -EI\left(\frac{\partial^2 u_a(\varphi)}{R^2\partial\varphi^2} - \frac{\partial v_a(\varphi)}{R^2\partial\varphi}\right) \tag{189}$$

Specifying normal stresses (164) for normal forces (184) and bending moments (189) delivers the relation between stresses and stress resultants

$$\sigma_{\varphi\varphi}(r,\varphi,z) = \left[\frac{N(\varphi)}{A} + \frac{M(\varphi)}{I}(r-R)\right]\frac{R}{r} \tag{190}$$

Considering a slender arch in the sense of $h \ll R$, the factor "$\frac{R}{r}$" is, in very good approximation, equal to 1. Hence, (190) takes the following form

$$\sigma_{\varphi\varphi}(r,\varphi,z) \approx \left[\frac{N(\varphi)}{A} + \frac{M(\varphi)}{I}(r-R)\right] \tag{191}$$

The most important thing that we learn from the above examples is that the calculation effort in the case of the rectangular cross section in comparison with the isosceles trapezoidal cross section is considerably higher, even though in the end we get approximately the same results.

B.3 Virtual power of internal forces

The virtual power of internal forces is defined as

$$\mathcal{L}^{int} = -\int_V \boldsymbol{\sigma} : \dot{\boldsymbol{\varepsilon}}\, dV \tag{192}$$

where membrane stresses $\boldsymbol{\sigma}$ perform power along the virtual strain rates $\dot{\boldsymbol{\varepsilon}}$.

B.3.1 Constraining virtual strain rates

The virtual strain rates are chosen by analogy to the real strains (141)

$$\dot{\check{\varepsilon}}_{\varphi\varphi}(r,\varphi,z;t) = \frac{\dot{\check{u}}_a(\varphi;t)}{r} + \frac{1}{r}\frac{\partial\dot{\check{v}}_a(\varphi;t)}{\partial\varphi} - \frac{r-R}{r}\left(\frac{\partial^2\dot{\check{u}}_a(\varphi;t)}{R\partial\varphi^2} - \frac{\partial\dot{\check{v}}_a(\varphi;t)}{R\partial\varphi}\right) \tag{193}$$

and

$$\dot{\check{\varepsilon}}_{rr}(r,\varphi,z;t) = \dot{\check{\varepsilon}}_{zz}(r,\varphi,z;t) = \dot{\check{\varepsilon}}_{\varphi r}(r,\varphi,z;t) = \dot{\check{\varepsilon}}_{\varphi z}(r,\varphi,z;t) = \dot{\check{\varepsilon}}_{rz}(r,\varphi,z;t) = 0 \tag{194}$$

B.3.2 Calculating virtual power of internal forces

According to (192), (193) and (194) only the normal stresses $\sigma_{\varphi\varphi}$ perform power along the virtual normal strain rates $\dot{\check{\varepsilon}}_{\varphi\varphi}$

$$\begin{aligned}
\mathcal{L}^{int} &= -\int\limits_V \boldsymbol{\sigma} : \dot{\check{\boldsymbol{\varepsilon}}}\, dV = -\int\limits_V \sigma_{\varphi\varphi}\, \dot{\check{\varepsilon}}_{\varphi\varphi}\, dV \\
&= -\int\limits_{\varphi_b}^{\varphi_e}\int\limits_A \sigma_{\varphi\varphi}\left[\frac{\dot{\check{u}}_a(\varphi;t)}{r} + \frac{1}{r}\frac{\partial\dot{\check{v}}_a(\varphi;t)}{\partial\varphi} - \frac{r-R}{r}\left(\frac{\partial^2\dot{\check{u}}_a(\varphi;t)}{R\partial\varphi^2} - \frac{\partial\dot{\check{v}}_a(\varphi;t)}{R\partial\varphi}\right)\right] r\, dA\, d\varphi \\
&= -\int\limits_{\varphi_b}^{\varphi_e}\int\limits_A \sigma_{\varphi\varphi}\left(\frac{\dot{\check{u}}_a(\varphi;t)}{R} + \frac{\partial\dot{\check{v}}_a(\varphi;t)}{R\partial\varphi}\right) dA\, Rd\varphi \\
&\quad + \int\limits_{\varphi_b}^{\varphi_e}\int\limits_A \sigma_{\varphi\varphi}\left(\frac{\partial^2\dot{\check{u}}_a(\varphi;t)}{R^2\partial\varphi^2} - \frac{\partial\dot{\check{v}}_a(\varphi;t)}{R^2\partial\varphi}\right)(r-R)\, dA\, Rd\varphi
\end{aligned} \tag{195}$$

Substituting normal forces (162) and bending moments (163) into (194), yields

$$\mathcal{L}^{int} = -\int\limits_{\varphi_b}^{\varphi_e} N(\varphi)\left(\frac{\dot{\check{u}}_a(\varphi;t)}{R} + \frac{\partial\dot{\check{v}}_a(\varphi;t)}{R\partial\varphi}\right) Rd\varphi + \int\limits_{\varphi_b}^{\varphi_e} M(\varphi)\left(\frac{\partial^2\dot{\check{u}}_a(\varphi;t)}{R^2\partial\varphi^2} - \frac{\partial\dot{\check{v}}_a(\varphi;t)}{R^2\partial\varphi}\right) Rd\varphi \tag{196}$$

Integrating (195) by parts and collecting terms multiplied with the same virtual velocity quantities, we obtain

$$
\begin{aligned}
\mathcal{L}^{int} = &- \int\limits_{\varphi_b}^{\varphi_e} \frac{N(\varphi)}{R} \; \dot{\check{u}}_a(\varphi;t) \; Rd\varphi - N(\varphi) \; \dot{\check{v}}_a(\varphi;t)\Big|_{\varphi_b}^{\varphi_e} + \int\limits_{\varphi_b}^{\varphi_e} \frac{\partial N(\varphi)}{R\partial\varphi} \; \dot{\check{v}}_a(\varphi;t) \; Rd\varphi \\
&- \frac{M(\varphi)}{R} \dot{\check{v}}_a(\varphi;t)\Big|_{\varphi_b}^{\varphi_e} + \int\limits_{\varphi_b}^{\varphi_e} \frac{\partial M(\varphi)}{R^2\partial\varphi} \; \dot{\check{v}}_a(\varphi;t) \; Rd\varphi + M(\varphi) \frac{\partial \dot{\check{u}}_a(\varphi;t)}{R\partial\varphi}\Big|_{\varphi_b}^{\varphi_e} \\
&- \frac{dM(\varphi)}{Rd\varphi} \; \dot{\check{u}}_a(\varphi;t)\Big|_{\varphi_b}^{\varphi_e} + \int\limits_{\varphi_b}^{\varphi_e} \frac{\partial^2 M(\varphi)}{R^2\partial\varphi^2} \; \dot{\check{u}}_a(\varphi;t) \; Rd\varphi = \\
= &\int\limits_{\varphi_b}^{\varphi_e} \left[-\frac{N(\varphi)}{R} + \frac{d^2 M(\varphi)}{R^2 d\varphi^2} \right] \; \dot{\check{u}}_a(\varphi;t) \; Rd\varphi + \int\limits_{\varphi_b}^{\varphi_e} \left[\frac{dN(\varphi)}{Rd\varphi} + \frac{\partial M(\varphi)}{R^2\partial\varphi} \right] \dot{\check{v}}_a(\varphi;t) \; Rd\varphi \\
&- N(\varphi) \; \dot{\check{v}}_a(\varphi;t)\Big|_{\varphi_b}^{\varphi_e} + M(\varphi) \left(\frac{\partial \dot{\check{u}}_a(\varphi;t)}{R\partial\varphi} - \frac{\dot{\check{v}}_a(\varphi;t)}{R} \right)\Big|_{\varphi_b}^{\varphi_e} - \frac{\partial M(\varphi)}{R\partial\varphi} \; \dot{\check{u}}_a(\varphi;t)\Big|_{\varphi_b}^{\varphi_e}
\end{aligned} \tag{197}
$$

B.4 Applying the principle of virtual power: identification of equilibrium conditions in stress resultants

Specifying the principle of virtual power (129) for the virtual power of external forces (159) as well as for the virtual power of internal forces (197), yields

$$
\begin{aligned}
&\mathcal{L}^{int} + \mathcal{L}^{ext} = \\
&\int\limits_{\varphi_b}^{\varphi_e} \left[-\frac{N(\varphi)}{R} + \frac{d^2 M(\varphi)}{R^2 d\varphi^2} \right] \dot{\tilde{u}}_a(\varphi;t)\ R d\varphi + \int\limits_{\varphi_b}^{\varphi_e} \left[\frac{dN(\varphi)}{R d\varphi} + \frac{\partial M(\varphi)}{R^2 \partial\varphi} \right] \dot{\tilde{v}}_a(\varphi;t)\ R d\varphi \\
&- N(\varphi)\ \dot{\tilde{v}}_a(\varphi;t) \Big|_{\varphi_b}^{\varphi_e} + M(\varphi) \left(\frac{\partial \dot{\tilde{u}}_a(\varphi;t)}{R\partial\varphi} - \frac{\dot{\tilde{v}}_a(\varphi;t)}{R} \right) \Bigg|_{\varphi_b}^{\varphi_e} - \frac{\partial M(\varphi)}{R\partial\varphi}\ \dot{\tilde{u}}_a(\varphi;t) \Big|_{\varphi_b}^{\varphi_e} \\
&+ \int\limits_{\varphi_b}^{\varphi_e} \left[q_r(\varphi) + \frac{\partial m(\varphi)}{R\partial\varphi} \right] \dot{\tilde{u}}_a(\varphi;t)\ R d\varphi + \int\limits_{\varphi_b}^{\varphi_e} \left[q_\varphi(\varphi) + \frac{m(\varphi)}{R} \right] \dot{\tilde{v}}_a(\varphi;t)\ R d\varphi \\
&+ [V(\varphi) - m(\varphi)]\ \dot{\tilde{u}}_a(\varphi;t) \Big|_{\varphi_b}^{\varphi_e} + N(\varphi)\ \dot{\tilde{v}}_a(\varphi;t) \Big|_{\varphi_b}^{\varphi_e} \\
&- M(\varphi) \left(\frac{\partial \dot{\tilde{u}}_a(\varphi;t)}{R\partial\varphi} - \frac{\dot{\tilde{v}}_a(\varphi;t)}{R} \right) \Bigg|_{\varphi_b}^{\varphi_e} = 0
\end{aligned}
\tag{198}
$$

After simplifying and collecting terms multiplied with the same virtual velocity quantities, (198) reduces to

$$
\begin{aligned}
\mathcal{L}^{ext} + \mathcal{L}^{int} = &\int\limits_{\varphi_b}^{\varphi_e} \left[-\frac{N(\varphi)}{R} + \frac{d^2 M(\varphi)}{R^2 d\varphi^2} + \frac{dm(\varphi)}{R d\varphi} + q_r(\varphi) \right] \dot{\tilde{u}}_a(\varphi;t)\ R d\varphi \\
&+ \int\limits_{\varphi_b}^{\varphi_e} \left[\frac{dN(\varphi)}{R d\varphi} + \frac{dM(\varphi)}{R^2 d\varphi} + \frac{m(\varphi)}{R} + q_\varphi(\varphi) \right] \dot{\tilde{v}}_a(\varphi;t)\ R d\varphi \\
&+ \left[V(\varphi) - m(\varphi) - \frac{dM(\varphi)}{R d\varphi} \right]\ \dot{\tilde{u}}_a(\varphi;t) \Big|_{\varphi_b}^{\varphi_e} = 0
\end{aligned}
\tag{199}
$$

From (199) we can identify the equilibrium equations for slender circular arches

$$
-\frac{N(\varphi)}{R} + \frac{d^2 M(\varphi)}{R^2 d\varphi^2} + \frac{dm(\varphi)}{R d\varphi} + q_r(\varphi) = 0 \tag{200}
$$

$$\frac{dN(\varphi)}{Rd\varphi} + \frac{dM(\varphi)}{R^2 d\varphi} + \frac{m(\varphi)}{R} + q_\varphi(\varphi) = 0 \tag{201}$$

$$V(\varphi) = \frac{dM(\varphi)}{Rd\varphi} + m(\varphi) \tag{202}$$

Specifying (200) and (201) for (202) delivers the more compact form

$$-\frac{N(\varphi)}{R} + \frac{dV(\varphi)}{Rd\varphi} + q_r(\varphi) = 0 \tag{203}$$

$$\frac{dN(\varphi)}{Rd\varphi} + \frac{V(\varphi)}{R} + q_\varphi(\varphi) = 0 \tag{204}$$

B.5 Conditions for arching thrust line behaviour

Arching thrust line behaviour implies that loads are carried exclusively by normal forces N, i.e. bending moments M and shear forces V vanish. We here analyse the derived equilibrium conditions (B.4) and (204), in order to identify a class of loading scenarios under which arching thrust line behaviour may develop.

The sought conditions for arching thrust line behaviour follow from specification of equilibrium conditions (B.4) and (204) for $M(\varphi) \equiv 0$ and $V(\varphi) \equiv 0$ as

$$m(\varphi) = 0 \tag{205}$$

$$-\frac{N(\varphi)}{R} + q_r(\varphi) = 0 \tag{206}$$

$$\frac{dN(\varphi)}{R\partial\varphi} + q_\varphi(\varphi) = 0 \tag{207}$$

The first condition (205) underlines that arching thrust line requires the absence of distributed bending moments. Combining the remaining two conditions (206) and (207) with the aim to eliminate the normal force $N(\varphi)$, i.e. deriving the equation (206) with respect to φ and adding the equation (207), delivers the following condition for the external loading functions $q_r(\varphi)$ and $q_\varphi(\varphi)$

$$\frac{\partial q_r(\varphi)}{\partial\varphi} = -q_\varphi(\varphi) \tag{208}$$

The corresponding solution of the normal force function $N(\varphi)$ follows from rearranging the Eq.(206), and the resulting equation in reminiscent of Barlows formula

$$N(\varphi) = R\, q_r(\varphi) \tag{209}$$

Eq.(208) represents a necessary condition for arching thrust line behaviour.

In the following, we consider three specific loading conditions, under which the arch will carry the external forces exclusively through normal forces. Eq.(209) together with Eq.(206) are necessary conditions for arching thrust behaviour. Infinitely many loading scenarios satisfy these conditions:

- constant radial line load $q_r(\varphi) = \mathit{const}$ (see Fig. 22): specifying (209) for $q_r(\varphi)$ delivers $q_\varphi(\varphi) = 0$;

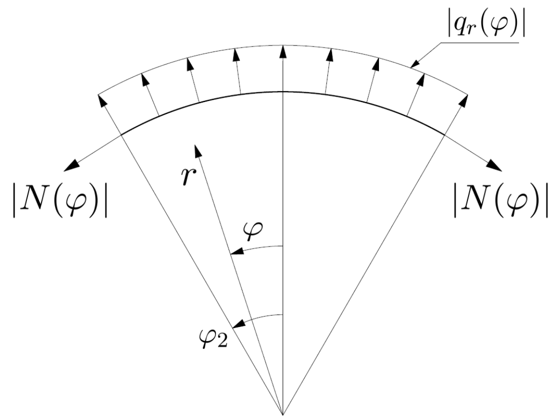

Figure 22: Symmetric loading for an arching thrust model: constant radial line load $q_r(\varphi)$(arrows point into physical directions)

- skew-symmetric distribution of $q_r(\varphi) = \max|q_r(\varphi)|\left(\frac{\varphi}{\varphi_2}\right)$ (see Fig. 23): specifying (209) for $q_r(\varphi)$ delivers $q_\varphi(\varphi) = -\frac{\max|q_r(\varphi)|}{\varphi_2}$;

- quadratic distribution of radial load $q_r(\varphi) = \max|q_r(\varphi)|\left[1 - \left(\frac{\varphi}{\varphi_2}\right)^2\right]$ (see Fig. 24): specifying (209) for $q_r(\varphi)$ delivers $q_\varphi(\varphi) = \frac{2\max|q_r(\varphi)|}{\varphi_2}\left(\frac{\varphi}{\varphi_2}\right)$.

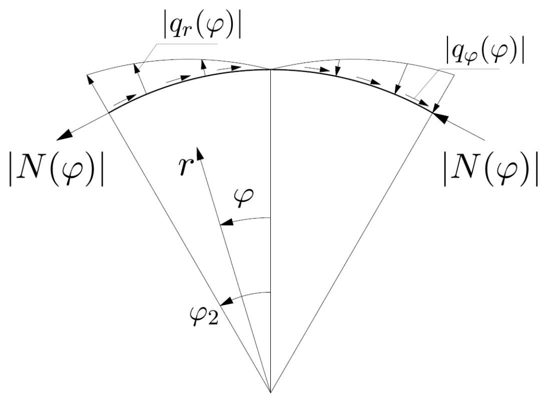

Figure 23: Symmetric loading for an arching thrust model: $q_r(\varphi)$ skew-symmetric; $q_\varphi(\varphi)$ constant (arrows point into physical directions)

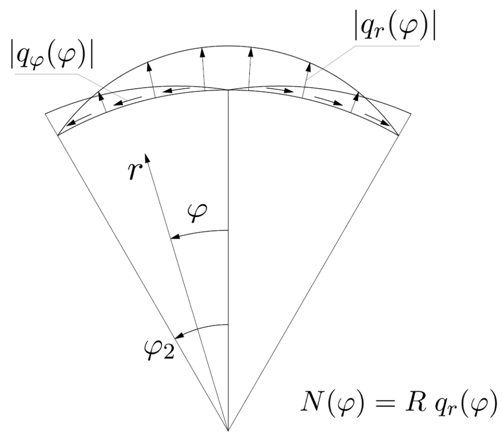

Figure 24: Symmetric loading for an arching thrust model: $q_r(\varphi)$ quadratic distribution; $q_\varphi(\varphi)$ skew-symmetric distribution (arrows point into physical directions)

However, necessary condition (208) is not limited to these three special cases, but it underlines that arching thrust line behaviour may develop for any loading type where the derivative of the radial loading $q_r(\varphi)$ with respect to φ is equal to the negative circumferential loading $q_\varphi(\varphi)$. The third special case was identified independently in tunnelling according to the New Austrian Tunnelling Method [**15**]. In more detail, the top heading of the cylindrical shotcrete tunnel shell of Sieberg Tunnel acted, one day after production, as an arching thrust. A virtually quadratic distribution of ground pressure and a virtually linear distribution of ground shear was obtained, see Fig. 25. Expressed in mathematical equations, they read as

$$q_r(\varphi) = -\max|q_r| \left[1 - \left(\frac{\varphi}{\varphi_2}\right)^2\right], \quad q_\varphi(\varphi) = -\max|q_\varphi| \left(\frac{\varphi}{\varphi_2}\right) \tag{210}$$

where the maximum intensities of ground pressure and ground shear are related via overall structural equilibrium as

$$\max|q_\varphi| = \frac{2\max|q_r|}{\varphi_2} \tag{211}$$

The shell exhibited a radius $R = 6.20$ m and a thickness $h = 0.3$ m. The opening angle φ_2 (see Fig. 25) amounted to $\varphi_2 = 1.46$ rad. The shell was loaded by symmetric ground pressure with a maximum $\max|q_r(\varphi)| = -0.83$ MN/m in the crown, as well as by symmetric ground shear with a maximum $\max|q_\varphi(\varphi)| = -1.137$ MN/m at the tunnel feet (see Fig. 25). Substituting the previous values in expressions (210) delivers

$$q_r(\varphi) = -0.83 \text{ MN/m} \left[1 - \left(\frac{\varphi}{1.46 \text{ rad}}\right)^2\right], \quad q_\varphi(\varphi) = -1.137 \text{ MN/m} \left(\frac{\varphi}{1.46 \text{ rad}}\right) \tag{212}$$

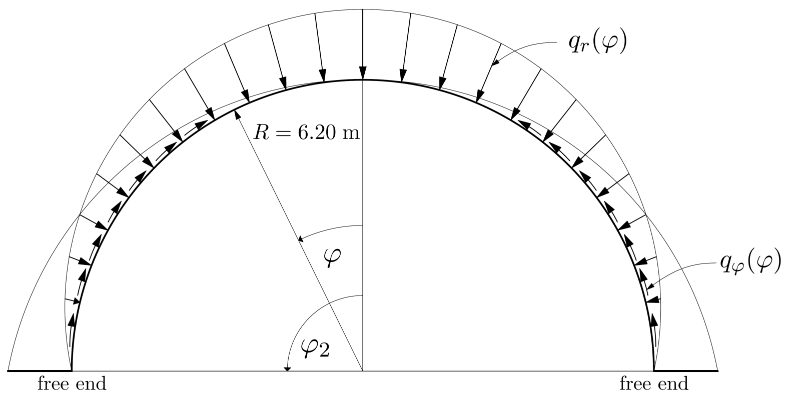

Figure 25: Load distribution due to ground pressure and shear

Specifying Eq.(209) for the first equation in (212) yields the normal force function $N(\varphi)$, see (Fig. 26)

$$N(\varphi) = -5.15 \text{ MN} \left[1 - \left(\frac{\varphi}{\varphi_2} \right)^2 \right] \tag{213}$$

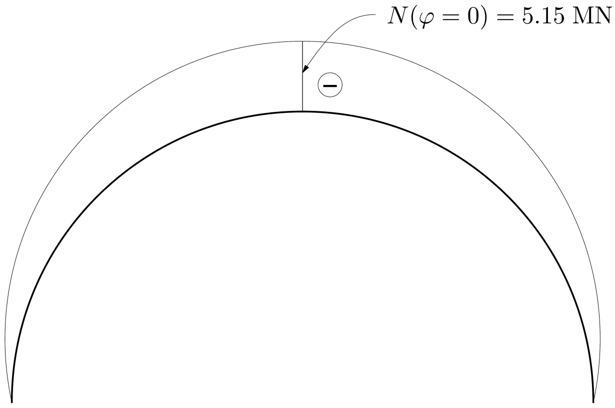

Figure 26: Normal force distribution due to ground pressure and shear

Expressions (210) indicate that the tunnel shell attracts significant vertical forces in the crown region, and that these are effectively back-transferred to the adjacent rock mass, via shear forces, in lateral parts of the top heading (Fig. 25). Notably, Eqs.(210) and (211) describe a loading scenario satisfying the necessary condition (208) for arching thrust line behaviour. Carrying of loads exclusively by normal forces (209) became actually possible because of the free ends of the tunnel feet (Fig. 25). The support conditions of an arch, namely, are decisive when it comes to the question whether or not arching thrust line behaviour will occur, provided that the necessary condition (208) is satisfied, which is the case only if the structure satisfies the additional necessary support condition stating that the reaction forces must be tangential to the axis of the arch.

B.6 Classical structural analysis interpretation of equilibrium conditions

In classical structural analysis the equilibrium equations are "identified" by formulating equilibrium conditions for a differential line element (see Fig. 27) loaded with radial load $q_r(\varphi)$, circumferential load $q_\varphi(\varphi)$ and linear distributed moments $m_\varphi(\varphi)$:

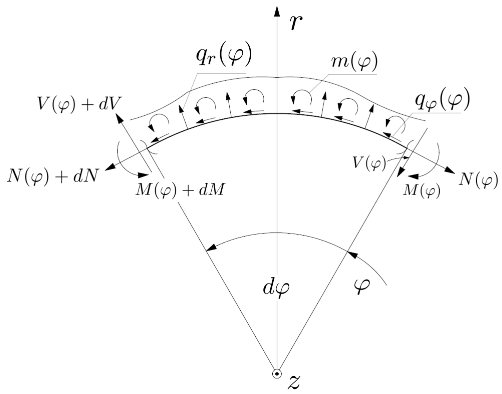

Figure 27: Arch differential line element in r, φ-plane

- Sum of forces in radial direction $\sum F_\varphi^{\uparrow +} = 0$

$$\begin{aligned} &- V(\varphi)\ \cos\frac{d\varphi}{2} + [V(\varphi) + dV]\ \cos\frac{d\varphi}{2} - N(\varphi)\ \sin\frac{d\varphi}{2} \\ &- [N(\varphi) + dN] \sin\frac{d\varphi}{2} + q_r(\varphi)\ Rd\varphi = 0 \end{aligned} \tag{214}$$

Furthermore we take into account the usual linearisation of small-angles (small-angle approximation)

$$\begin{cases} \cos\alpha & = 1 \qquad \alpha \ll 1 \\ \sin\alpha & = \alpha \qquad \alpha \ll 1 \end{cases} \tag{215}$$

Specifying (214) for the small-angle approximation (215) yields

$$dV(\varphi) - N(\varphi)\ d\varphi + dN(\varphi)\ \frac{d\varphi}{2} + q_r(\varphi)\ Rd\varphi = 0 \tag{216}$$

Neglecting, in (216), terms containing two differentials with respect to terms containing one differential, and dividing the resulting expression by $Rd\varphi$ yields

$$-\frac{N(\varphi)}{R} + \frac{dV(\varphi)}{Rd\varphi} + q_r(\varphi) = 0 \tag{217}$$

- Sum of forces in circumferential direction $\sum F_{\varphi}^{\overrightarrow{+}} = 0$

$$
\begin{aligned}
&+ N(\varphi)\ \cos\frac{d\varphi}{2} - V(\varphi)\ \frac{d\varphi}{2} - [V(\varphi) + dV(\varphi)]\ \frac{d\varphi}{2} \\
&- [N(\varphi) + dN(\varphi)]\ \cos\frac{d\varphi}{2} - q_{\varphi}(\varphi)\ Rd\varphi = 0
\end{aligned} \tag{218}
$$

Specifying (218) for small-angle approximation (215) delivers

$$
-dN(\varphi) - V(\varphi)\ d\varphi - q_{\varphi}(\varphi)\ Rd\varphi = 0 \tag{219}
$$

Dividing (219) by $\frac{1}{-Rd\varphi}$ we get

$$
\frac{dN(\varphi)}{Rd\varphi} + \frac{V(\varphi)}{R} + q_{\varphi}(\varphi) = 0 \tag{220}
$$

- Sum of moments $(\sum M)_{\varphi}^{\frown +} = 0$

$$
\begin{aligned}
&- M(\varphi) + [M(\varphi) + dM(\varphi)] - [V(\varphi) + dV(\varphi)]\ Rd\varphi + [N(\varphi) + dN(\varphi)]\ \frac{d\varphi}{2}\ Rd\varphi \\
&+ m(\varphi)\ Rd\varphi - q_r(\varphi)\ Rd\varphi\ R\frac{d\varphi}{2} = 0
\end{aligned} \tag{221}
$$

Specifying (221) for small-angle approximation (215) delivers

$$
dM(\varphi) - V(\varphi)\ Rd\varphi + m(\varphi)\ Rd\varphi = 0 \tag{222}
$$

Dividing (222) by $Rd\varphi$ we get

$$
V(\varphi) = \frac{dM(\varphi)}{Rd\varphi} + m(\varphi) \tag{223}
$$

Eqs. (217), (220) and (223) represent the arch equilibrium equations

$$
-\frac{N(\varphi)}{R} + \frac{dV(\varphi)}{Rd\varphi} + q_r(\varphi) = 0 \tag{224}
$$

$$
\frac{dN(\varphi)}{Rd\varphi} + \frac{V(\varphi)}{R} + q_{\varphi}(\varphi) = 0 \tag{225}
$$

$$
V(\varphi) = \frac{dM(\varphi)}{Rd\varphi} + m(\varphi) \tag{226}
$$

References

[1] Ventsel, E., Krauthammer, T. and Ventsel, V. Thin plates and shells: Theory, Analysis, and applications. New York: Taylor and Francis (2001)

[2] C. Hellmich und B. Pichler: Studienblätter zur Vorlesung aus Flächentragwerke: Das Prinzip der virtuellen Leistungen und seine Anwendung zur Herleitung der Theorie der Zylinderschale. Institut für Mechanik der Werkstoffe und Strukturen, Technische Universität Wien, Wien (2012).

[3] P. Germain, The method of virtual power in continuum mechanics. Part 2: Microstructure, SIAM Journal on Applied Mathematics 25 (3) (1973) 556-575.

[4] M. Frémond, B. Nedjar, Damage, gradient of damage and principle of virtual power, International Journal of Solids and Structures 33 (3) (1996) 1083-1103.

[5] J. Salaçon, Handbook of Continuum Mechanics: General Concepts-Thermoelasticity, Springer Science & Business Media, 2001.

[6] VCH. Der Ingenieurbau - Grundwissen. Edition. Wiley-VCH Verlag GmbH (1995), (Kapitel 4, Mang, H.) 110-125.

[7] Girkmann, K., Flächentragwerke, 6. Auflage, Springer, Wien (1963).

[8] Timoshenko, S., Woinowsky-Krieger, S., Timoshenko, S.P. and Woinowsky-Kreiger, S. Theory of plates and shells (McGraw-Hill classic textbook reissue series). 2nd edn. Auckland: McGraw Hill Higher Education (1964).

[9] Zoelly, R., *Über ein Knickungsproblem an der Kugelschale*, Diss, Zrich, 1915.

[10] Volmir, A.S., Stability of Elastic Systems, Gos. Izd-vo Fiz.-Mat. Lit., Moscow, 1963.

[11] Kollar, L. and Dulacska, E., Buckling of Shells for Engineers, John Wiley and Sons, New York, 1948.

[12] Mang, H. and Hofstetter, G., Festigkeitslehre, Springer Verlag Wien GmbH, Wien (2000).

[13] Del Piero, G. (2009) On the method of virtual power in continuum mechanics, Journal of Mechanics of Materials and Structures, 4(2), pp. 281292. doi: 10.2140/jomms.2009.4.281.

[14] Obrecht, H., Baumechanik - Statik VII - Gekrümmte Flčhentragwerke, Lehrstuhl für Baumechanik-Statik, Dortmund (2007).

[15] S. Ullah, B. Pichler, and C. Hellmich. Ground-shell forces in NATM tunnelling: quantification from 3D displacement measurements. *Journal of Geotechnical and Geoenvironmental Engineering (ASCE)*, 139(3):444-457, 2013.